



POLLUTION REDUCTION TECHNOLOGY PROGRAM, TURBOPROP ENGINES - PHASE I

by

R. D. Anderson, A. S. Herman, J. G. Tomlinson
J. M. Vaught, A. J. Verdouw

**DETROIT DIESEL ALLISON
DIVISION OF GENERAL MOTORS CORPORATION**

(NASA-CR-135040) POLLUTION REDUCTION
TECHNOLOGY PROGRAM, TURBOPROP ENGINES, PHASE
1 (Detroit Diesel Allison, Indianapolis,
Ind.) 134 p HC \$6.00

CSSL 21E

N76-28237

Unclas
G3/07 46793

Prepared for

NATIONAL AERONAUTICS AND SPACE ADMINISTRATION

NASA Lewis Research Center
Contract NAS3-18561



1. Report No. NASA CR-135040		2. Government Accession No.		3. Recipient's Catalog No.	
4. Title and Subtitle POLLUTION REDUCTION TECHNOLOGY PROGRAM, TURBOPROP ENGINES - PHASE I				5. Report Date March, 1976	
				6. Performing Organization Code	
7. Author(s) R. D. Anderson, A. S. Herman, J. G. Tomlinson, J. M. Vaught, A. J. Verdouw				8. Performing Organization Report No. EDR 8708	
9. Performing Organization Name and Address Detroit Diesel Allison Division of General Motors Corporation, P.O. Box 894, Indianapolis, In. 46206				10. Work Unit No.	
				11. Contract or Grant No. NAS3-18561	
12. Sponsoring Agency Name and Address National Aeronautics and Space Administration Washington, D.C. 20546				13. Type of Report and Period Covered Contractor Report	
				14. Sponsoring Agency Code	
15. Supplementary Notes Program Manager, Edward J. Mularz, Air Breathing Engines Division, NASA-Lewis Research Center, Cleveland, Ohio					
16. Abstract Exhaust pollutant emissions were measured from a 501-D22A turboprop engine combustor and three low emission combustor types; reverse flow, prechamber and staged fuel, operating over a fuel-air ratio range of .0096 to .020. EPAP LTO cycle data were obtained for a total of nineteen configurations. Hydrocarbon emissions were reduced from 15.0 to .3 lb/1000 Hp-Hr/cycle, CO from 31.5 to 4.6 lb/1000 Hp-Hr/cycle with an increase in NO _x of 17 percent, which is still 25% below the program goal. The smoke number was reduced from 59 to 17. Emissions given here are for the reverse flow Mod. IV combustor which is the best candidate for further development into eventual use with the 501-D22A turboprop engine. Even lower emissions were obtained with the advanced technology combustors reported herein.					
17. Key Words (Suggested by Author(s)) Reverse Flow Combustor Prechamber Combustor Staged Fuel Combustor Exhaust Emissions			18. Distribution Statement Unclassified - Unlimited		
19. Security Classif. (of this report) Unclassified		20. Security Classif. (of this page) Unclassified		21. No. of Pages	
				22. Price*	

FOREWORD

The work described herein was conducted by the Combustion Research and Development Department of Detroit Diesel Allison Division of General Motors Corporation under the direction of Mr. F. J. Verkamp. Funding was provided under contract NAS3-18561 sponsored by NASA-Lewis Research Center and by General Motors Corporation.

The NASA Program Manager was Dr. E. J. Mularz. Mr. J. G. Tomlinson was the Detroit Diesel Allison (DDA) Program Manager and Mr. R. D. Anderson the technical director. Messrs. J. M. Vaught, A. S. Herman, and A. J. Verdouw were responsible for all aspects of the reverse flow, prechamber, and staged fuel combustor concepts, respectively.

TABLE OF CONTENTS

<u>Section</u>	<u>Title</u>	<u>Page</u>
I	Summary	1-1
II	Introduction	2-1
III	Description of Combustor Designs	3-1
IV	Test Equipment	4-1
V	Test Procedure	5-1
VI	Test Results	6-1
VII	Discussion of Results	7-1
VIII	Conclusions	8-1
IX	References	9-1

LIST OF ILLUSTRATIONS

<u>Figure</u>	<u>Title</u>	<u>Page</u>
3-1	501-D22A combustion system	3-1
3-2	501-D22A combustion liner currently in production	3-2
3-3	Airflow distribution in the production liner	3-4
3-4	Production liner instrumented for skin temperature measurement	3-4
3-5	Dual-orifice fuel nozzle used in the 501-D22A combustion system	3-5
3-6	Dual-orifice fuel nozzle schematic	3-5
3-7	Model 501 combustors	3-6
3-8	Model 501 industrial engine airblast fuel nozzle (partial view)	3-7
3-9	Combustion inefficiency, 501-K industrial engine reverse flow airblast combustion system	3-11
3-10	Changes to 501-K production combustor airflow distribution	3-11
3-11	Thermal analysis of the reverse flow combustor	3-14
3-12	Flow visualization, short-prechamber combustor	3-15
3-13	Flow visualization, long-prechamber combustor	3-16
3-14	Short-prechamber combustor design	3-17
3-15	Reduced width radial swirler, prechamber Mod IV & V	3-18
3-16	Long-prechamber combustor design	3-18
3-17	Original staged fuel combustor design	3-20
3-18	Original design main prechamber	3-22
3-19	Original design combustion zone equivalence ratio	3-25
3-20	Original design staged fuel combustor	3-25
3-21	Staged fuel combustor pilot fuel injectors	3-26
3-22	Mod V, VI staged fuel combustor design	3-28
3-23	Mod V, VI design main prechamber	3-29
3-24	Mod V, VI design combustion zone equivalence ratio	3-31
3-25	Mod V, VI staged fuel combustor	3-32
4-1	Combustor test rig	4-2
4-2	Airflow diagram for 501 Model D test rig	4-3
4-3	Rig test section	4-4
4-4	Emission probe	4-4
4-5	Gas path view of emission probes	4-5
4-6	Emission sample line arrangement	4-5
4-7	Exhaust gas rake	4-6
4-8	Exhaust gas temperature and pressure measurement locations	4-6

<u>Figure</u>	<u>Title</u>	<u>Page</u>
4-9	Smoke sampling system	4-7
4-10	Emission instrumentation system	4-8
6-1	Results of combustion rig tests of baseline design reverse flow system	6-5
6-2	Results of combustion rig tests of Mod I design reverse flow system	6-6
6-3	Results of combustion rig tests of Mod II design reverse flow system	6-8
6-4	Results of combustion rig tests of Mod III design reverse flow system	6-9
6-5	Effect of air assist fuel nozzle air pressure on Mod III idle emissions	6-10
6-6	Results of combustion rig tests of Mod IV design reverse flow system	6-11
6-7	Mod II parametric test, effect of liner velocity on emissions	6-12
6-8	Mod II parametric test, effect of inlet temperature on emissions	6-13
6-9	Thermal paint markings, Mod IV combustor	6-14
6-10	Reverse flow Mod IV combustor lean-blowout results . . .	6-16
6-11	Short prechamber combustors—CO emissions at idle . . .	6-19
6-12	Short prechamber combustors—HC emissions at idle . . .	6-19
6-13	Short prechamber combustors—NO _x emissions at idle . .	6-20
6-14	Short prechamber combustors—smoke emissions at idle .	6-20
6-15	Short prechamber combustors—CO emissions at takeoff. .	6-21
6-16	Short prechamber combustors—HC emissions at takeoff. .	6-21
6-17	Short prechamber combustors—NO _x emissions at takeoff.	6-22
6-18	Short prechamber combustors—smoke emissions at takeoff.	6-22
6-19	Prechamber Mod I—CO emissions at idle	6-23
6-20	Prechamber Mod II—CO emissions at idle	6-23
6-21	Prechamber Mod I—HC emissions at idle	6-24
6-22	Prechamber Mod II—HC emissions at idle	6-24
6-23	Prechamber Mod I—NO _x emissions at idle.	6-25
6-24	Prechamber Mod II—NO _x emissions at idle	6-25
6-25	Prechamber Mod I—smoke emissions at idle	6-26
6-26	Prechamber Mod II—smoke emissions at idle	6-26
6-27	Prechamber Mod I—CO emissions at takeoff.	6-27
6-28	Prechamber Mod II—CO emissions at takeoff	6-27
6-29	Prechamber Mod I—HC emissions at takeoff.	6-28

<u>Figure</u>	<u>Title</u>	<u>Page</u>
6-30	Prechamber Mod II—HC emissions at takeoff	6-28
6-31	Prechamber Mod I—NO _x emissions at takeoff	6-29
6-32	Prechamber Mod II—NO _x emissions at takeoff	6-29
6-33	Prechamber Mod I—smoke emissions at takeoff	6-30
6-34	Prechamber Mod II—smoke emissions at takeoff	6-30
6-35	Baseline Prechamber combustor—hot spot thermocouple location	6-31
6-36	Baseline Prechamber combustor	6-32
6-37	Prechamber Mod III combustor	6-32
6-38	Prechamber Mod V—thermal paint results (left side) . . .	6-32
6-39	Prechamber Mod V—thermal paint results (right side) . .	6-33
6-40	Prechamber combustor low-pressure blowout results . . .	6-34
6-41	Staged fuel EPAP results	6-37
6-42	Effect of fuel/air ratio on idle emissions	6-40
6-43	Effect of variable geometry setting on idle emissions . . .	6-41
6-44	Effect of fuel staging on idle emissions	6-41
6-45	Effect of reference velocity on idle emissions	6-42
6-46	Effect of pilot fuel injector on idle HC emission	6-43
6-47	Effect of pilot fuel injector on idle CO emissions	6-44
6-48	Effect of pilot fuel injector on idle smoke emission	6-44
6-49	Effect of pilot fuel injector on takeoff smoke emission . . .	6-45
6-50	Effect of pilot fuel injector on idle NO _x emissions	6-46
6-51	Effect of fuel/air ratio on takeoff emissions (100% pilot fuel)	6-46
6-52	Effect of fuel/air ratio on takeoff emissions (0% pilot fuel)	6-47
6-53	Effect of fuel staging on takeoff emissions (Build 3)	6-48
6-54	Effect of variable geometry setting on takeoff emissions . .	6-49
6-55	NO _x characteristics for Build three (takeoff)	6-49
6-56	Effect of fuel/air ratio on takeoff emissions (100% pilot fuel)	6-50
6-57	Effect of fuel staging on takeoff emissions (Build 4)	6-51
6-58	Effect of variable geometry setting on takeoff emissions, Build 4	6-51
6-59	NO _x characteristics for Build four	6-52
6-60	Staged fuel combustor pattern factor	6-53
6-61	Staged fuel combustor pressure loss	6-53
6-62	Staged fuel combustor low pressure blow out results	6-54
6-63	Typical staged fuel combustor temperature pattern	6-55
7-1	Hydrocarbon emissions at idle conditions	7-2
7-2	Improvement in combustion efficiency from redesign of primary zone to increase equivalent ratio	7-3

<u>Figure</u>	<u>Title</u>	<u>Page</u>
7-3	Comparison of emissions at idle showing effect of pilot fuel flow and increased airflow into second reversing baffle	7-4
7-4	Effect of air assist fuel nozzle air pressure on Mod III idle emissions.	7-6
7-5	Flow visualization, short-prechamber combustor	7-9
7-6	EPA parameter—CO emissions—prechamber combustors	7-12
7-7	EPA parameter—HC emissions—prechamber combustors	7-12
7-8	EPA parameter—NO _x emissions—prechamber combustors	7-13
7-9	Max smoke number for LTO cycle—prechamber combustors	7-14
7-10	Flow visualization, long-prechamber combustor.	7-15
7-11	Prechamber Mod I—CO emissions at idle	7-17
7-12	Prechamber Mod II—CO emissions at idle	7-17
7-13	Prechamber Mod I—HC emissions at idle	7-18
7-14	Prechamber Mod II—HC emissions at idle	7-18
7-15	Prechamber Mod I—smoke emissions at idle.	7-20
7-16	Prechamber Mod II—smoke emissions at idle	7-20
8-1	Emissions from final design (Mod IV) reverse flow system	8-1

LIST OF TABLES

<u>Table</u>	<u>Title</u>	<u>Page</u>
3-I	501-D22A Production Liner Air Flow Passages	3-3
3-II	501-D22A Combustor Inlet Conditions	3-3
3-III	Emission Reduction Required for Reverse Flow Design .	3-8
3-IV	Major Design Features of the Baseline Reverse Flow Combustion System	3-10
3-V	Air Flow Area Distribution for Baseline Reverse Flow Design	3-10
3-VI	Reverse Flow Combustion System Emissions Predicted by Reaction Kinetics Analysis.	3-12
3-VII	Variable Geometry Range for Short Prechamber Combustor.	3-17
3-VIII	Short Prechamber Configurations Tested Over LTO Cycles	3-17
3-IX	Staged Fuel Baseline Air Flow Distribution	3-23
3-X	Original Design Functional Airflow Distribution	3-23
3-XI	Mod V/VI Design Airflow Distribution.	3-30
3-XII	Mod V/VI Functional Airflow Distribution.	3-31
4-I	Emission Instruments	4-8
6-I	Emissions of Production Liner at EPAP LTO Cycle Conditions	6-1
6-II	Emission Reduction Required	6-2
6-III	Comparison of EPA Emission Parameters—Reverse Flow Designs	6-3
6-IV	Summary of Reverse Flow Configuration Emissions Data	6-4
6-V	Reverse Flow Combustion System, Takeoff Design Point Performance Summary	6-15
6-VI	Prechamber Combustor Emission Results	6-17
6-VII	Prechamber Combustor Pressure Loss (%)	6-17
6-VIII	Measured Prechamber Combustion Efficiency (%)	6-18
6-IX	Prechamber Combustors Measured Pattern Factor	6-18
6-X	Staged Fuel Combustor Configurations	6-35
6-XI	Fixed Geometry Definitions	6-36
6-XII	Fuel Staging Schedule	6-36
6-XIII	EPAP Results	6-38
6-XIV	Staged Fuel Combustor Emission Index Summary	6-39
7-I	Effect of Air Assist Fuel Nozzle Performance on Mod III Emissions.	7-7
7-II	Combustion Liner Wall Temperatures	7-8
7-III	Duty Cycle Emissions for Test 1—Low NO _x Operating Mode.	7-22

I. SUMMARY

The Pollution Reduction Technology Program, Turboprop Engines-Phase I is directed toward the generation of emission reduction technology for EPA Class P2 turboprop engines. The objective of this effort was to establish combustion system concepts which would operate over the EPA LTO cycle within the EPA Exhaust Emission Standards published in the Federal Register, Volume 38, Number 136, July 17, 1973, applicable to commercial turboprop engines effective January 1, 1979. The Allison 501-D22A turboprop engine was selected as the vehicle for this program since it represents a large portion of the applied power in the EPA P2 class engine category.

Emission reduction requirements for this program were based initially on values obtained under EPA Contract 68-04-0029 for Model 501-D22A turboprop engines and directly from component rig test values obtained on a baseline combustion system in this program. Goals were established at 25% below the EPA regulation requirements to provide margin for engine development and production variations as follows:

	<u>EPA LTO Cycle</u> (lb/1000 hp-hr/cycle)		<u>Emission Index</u> g pollutant/kg fuel	
	<u>Requirements</u>	<u>Goals</u>	<u>Conditions</u>	<u>EI Goals</u>
Total hydrocarbons	4.9	3.7	Idle	5.4
Carbon monoxide	26.8	20.1	Idle	27.9
Oxides of nitrogen	12.9	9.7	Takeoff	18.8
Exhaust smoke	29.2	21.9		

Three basic alternate combustor designs were tested then modified and retested to achieve the goals of the program. These designs were designated 1) the reverse flow combustor, 2) the prechamber combustor and 3) the staged fuel combustor listed in order of complexity difference from the baseline combustor. All configurations were designed for adequate cooling and structural integrity to provide satisfactory durability and minimal performance goals as follows:

- Combustion efficiency greater than 99% at all operating conditions
- Combustor exit temperature pattern factor equal to or less than 0.25 at the takeoff power conditions
- Combustor pressure drop of 5% or less at takeoff power conditions

The total program was conducted on the DDA single combustor rig operating in the DDA Combustion Development Facility. This combustor rig exactly simulates a one-sixth segment of the flow path inside the six-burner turboprop engine. Test conditions were controlled to the exact values of flow, pressure, and temperature for the Model 501-D22A engine, and the inlet temperature was obtained with direct-fired heaters which provided nonvitiated inlet air to the component combustor test rig. Emission measurements were obtained from 11 four-port sampling probes mounted in the combustor exit, and pressures, flows, and temperatures were measured with appropriate total and static pressure probes, thermocouples, and flow measurement orifices. Combustors were operated to conditions corresponding to the power settings for the EPA LTO cycle and variations of fuel/air ratio and reference velocity were evaluated at takeoff and idle conditions to obtain further emission definition at these limiting operation conditions.

Emission measurements made on the baseline combustor configuration established that significant reductions of carbon monoxide (CO), unburned hydrocarbons (HC) and exhaust smoke would be necessary to meet EPA regulations (CO, 14.9%; HC, 67.3%; and smoke, 47.3%) considering no margin for development and production variations. There was 52% margin in NO_x emissions to meet the standards which provided some tradeoff room for the CO and HC reductions required.

Development variations of all three combustor design concepts met the projected EPA requirements with varying degrees of margin tabulated as follows:

	Emission Regulation Margin (%)							
	CO		HC		NO _x		Smoke	
	% Margin	EPAP value	% Margin	EPAP value	% Margin	EPAP value	% Margin	Value
Production liner	-17.5	31.5	-206	15.0	51.9	6.2	-89.7	59.0
Reverse flow Mod IV	82.2	4.6	93.9	0.3	43.4	7.3	41.4	17.0
Prechamber Mod III	92.4	2.1	92.0	0.4	34.1	8.5	96.3	1.0
Staged fuel Mod V	78.7	5.7	87.8	0.6	44.2	7.2	72.4	8.0

At this stage of development, margin exists beyond the desired 25% on all three low emission combustor configurations and barring any undue compromises in development to meet engine operational requirements, it should be possible to meet the EPA emission regulations in production. Although these initial component development results indicated no significant compromises in steady-state performance, further component rig development is required before engine testing can proceed with assurance.

II. INTRODUCTION

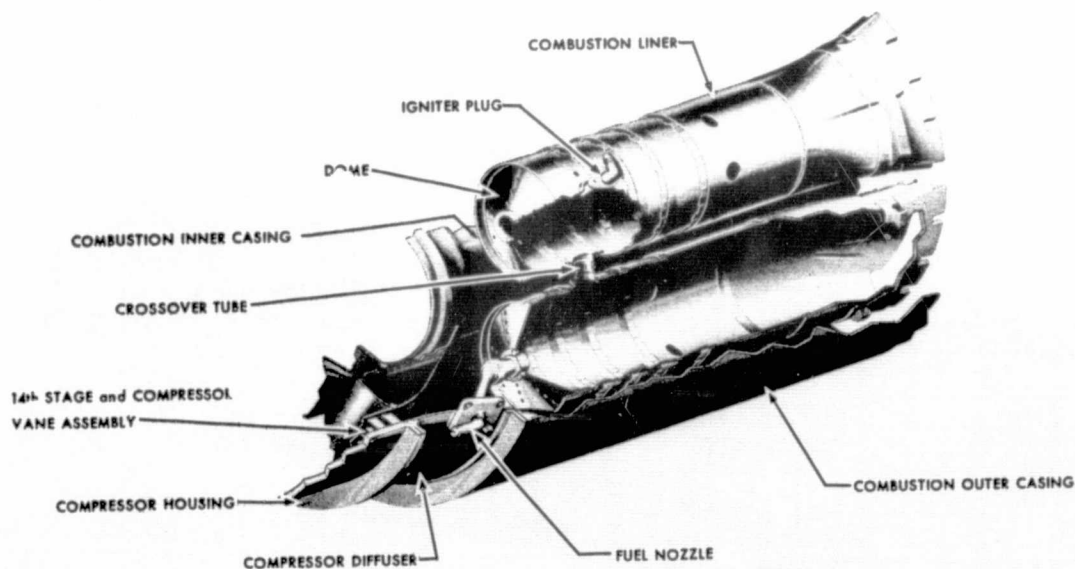
The Clean Air Act of 1970 charged the EPA with the responsibility to establish acceptable exhaust emission levels of carbon monoxide (CO), total unburned hydrocarbons (HC), oxides of nitrogen (NO_x), and smoke for all types of aircraft engines. In response to this charge, the EPA promulgated the Exhaust Emission Standards published in the Federal Register, Volume 38, Number 136, July 17, 1973. Prior to the release of these standards, the aircraft engine industry, various independent research laboratories and universities, and the government were involved in the research and development of low emission gas turbine engine combustors. Some of this research was used as a guide to set the levels of the EPA standards.

The levels established in the standards and the first compliance date, January 1, 1979, have acted as a catalyst for the timely development of advanced technology combustors. Two major NASA sponsored low emissions technology development programs, the Experimental Clean Combustor Program (ECCP) implemented six months prior to the issuance of the standards and the Pollution Reduction Technology Program (PRTTP) implemented within one year after the issuance date, have emission level goals consistent with the EPA standards. Most independent research and development (IR&D) programs in the industry are also using the EPA standards as goals for advanced technology developments. The Pollution Reduction Technology Program, Turboprop Engines - Phase I covered by this report is the joint effort between NASA and Detroit Diesel Allison directed toward the EPA Class P2 engine category in the overall NASA Pollution Reduction Technology Program. The principal goal in this program was to reduce CO, HC, and smoke emissions while maintaining acceptable NO_x emissions without affecting fuel consumption, durability, maintainability and safety. This Phase I program covers component combustor concept screening directed toward the demonstration of advanced combustor technology required to meet the EPA exhaust emission standards for Class P2 turboprop engines. The combustion system for the Allison 501-D22A engine was used as the basis for this program and descriptions of the engine, combustor design concepts, component combustor program and results are presented in this report. Three combustor design concepts; reverse flow, prechamber, and staged fuel were evaluated in the program and results indicated that all three design concepts have the potential for meeting the applicable EPA emission standards.

III. DESCRIPTION OF COMBUSTOR DESIGNS

The combustion system of the 501-D22A engine consists of six can type combustion liners located in the annulus formed by the outer and inner casings as shown in Figure 3-1. Radial position of each can is set, at the inlet end, by a fuel nozzle centered within a flared fitting in the dome and in the exhaust end by the combustor transition engaging the turbine inlet vane assemblies. Axial positioning is accomplished by igniter plugs in two cans and dummy igniter plugs in the remaining four cans. Six crossover tubes interconnect the cans and provide flame transfer for starting. The six fuel nozzles are connected to a fuel manifold attached to the external surface of the outer case.

Details of the 501-D22A production combustion system and the three low emission combustion systems developed in this program are described in the remainder of this section.



8708-71

Figure 3-1. 501-D22A combustion system.

PRODUCTION LINER

The combustion liner currently in production in the 501-D22A engine, part number 6876880, is shown in Figure 3-2. Conventional design features of this combustor are:

1. Dome air entry holes backed by baffles to induce a circular flow pattern across the hot face of the dome
2. Film cooling slots formed by overlapped wall segments
3. Dome-center-mounted fuel nozzle
4. Primary zone trim holes
5. Nonuniform dilution hole spacing for gas temperature-pattern control

The flow areas available for air entry into the combustor are presented in Table 3-I. Estimated discharge coefficients are also shown for each air entry location. With this information and the combustor inlet conditions shown in Table 3-II, it is possible to calculate the air flow distribution. These data and flow splits in percent are indicated for each location in Table 3-I and shown in Figure 3-3.

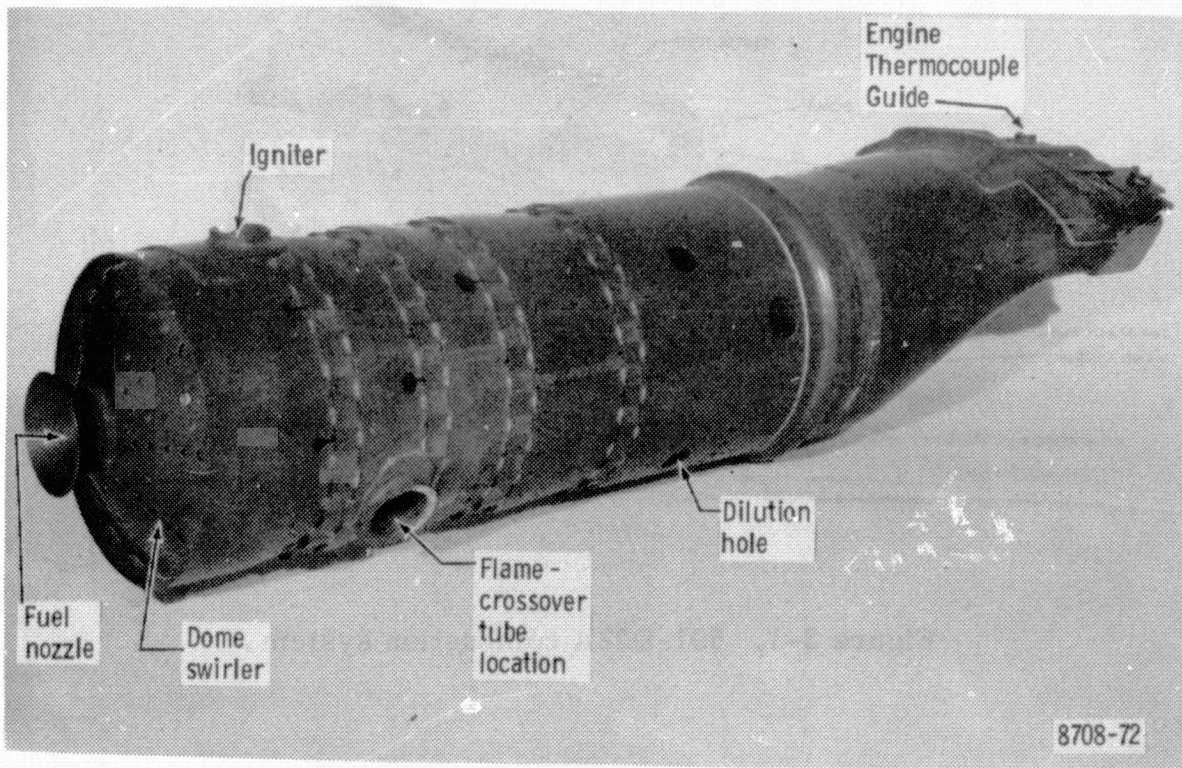


Figure 3-2. 501-D22A combustion liner currently in production.

TABLE 3-I. 501-D22A PRODUCTION LINER AIR FLOW PASSAGES

Location	Air Flow Area (cm ²)	Discharge Coefficient, Cd	Flow Split (%)
Dome	5.19	.6	7.90
First corrugation	7.28	.8	14.81
Primary holes	2.21	.6	3.38
Second corrugation	5.05	.8	10.26
Second primary holes	1.77	.6	2.68
Baffle	0.77	.6	1.10
Third corrugation	5.05	.8	10.26
Intermediate holes	3.88	.6	5.92
Baffles	1.43	.6	2.18
Fourth corrugation	3.88	.8	9.12
Fifth corrugation	3.88	.8	9.12
Dilution holes	7.92	.6	12.07
Baffles	1.43	.6	2.18
Second dilution holes	5.19	.6	7.92
Baffle	<u>0.72</u>	.6	<u>1.10</u>
TOTAL	55.6 cm ²		100.00%

TABLE 3-II. 501-D22A COMBUSTOR INLET CONDITIONS

Mode	Engine Shaft Power (kW)	Burner Inlet Temp K	Burner Outlet Temp K	Fuel/Air Ratio	Burner Inlet Pressure (kPa)	Burner* Airflow (kg/s)
Taxi/idle	116	441.5	899.8	.0113	369.6	1.134
Takeoff	3256	610.4	1322.0	.0200	983.2	2.495
Climbout	2931	605.9	1269.3	.0185	957.7	2.502
Approach	977	588.2	963.7	.0096	841.2	2.527
*For one combustor						

For rig test purposes three thermocouples were welded to the combustor outer surface at the locations shown in Figure 3-4. Thermocouple leads were fastened to the combustor to minimize heat loss and stress at the junction.

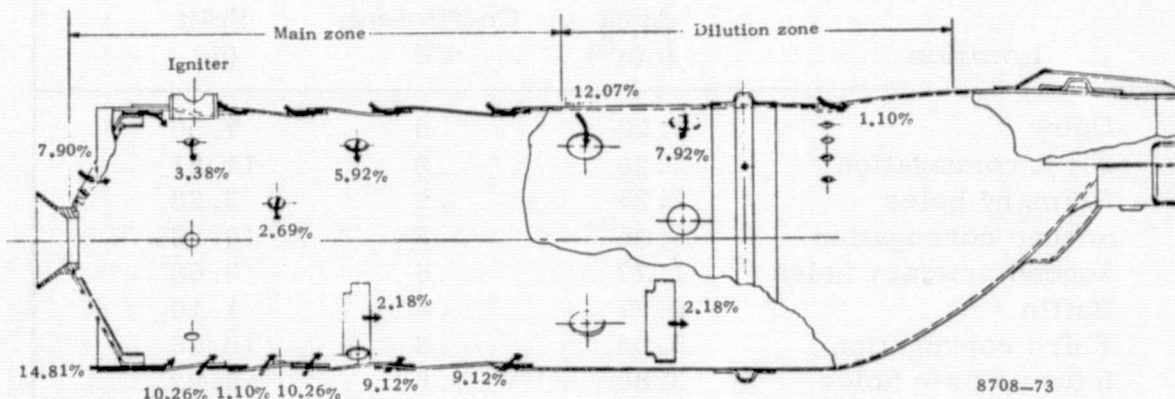


Figure 3-3. Airflow distribution in the production liner.

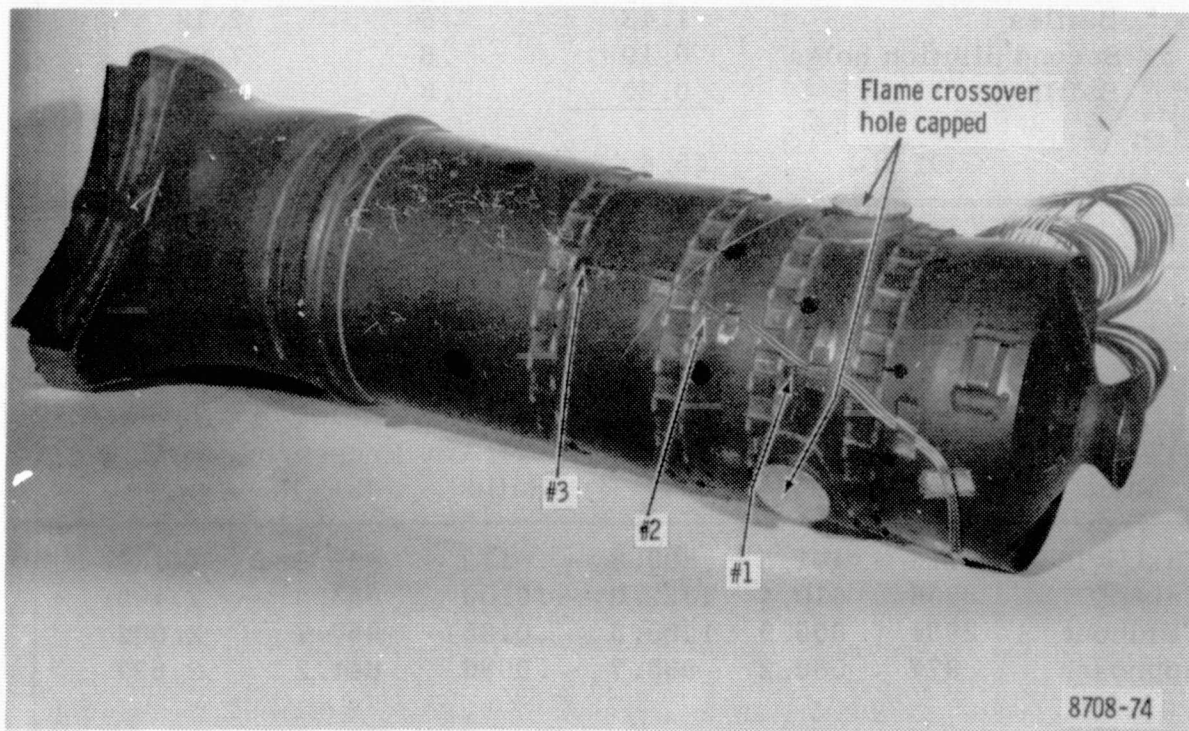


Figure 3-4. Production liner instrumented for skin temperature measurement.

The fuel injector used with the production liner is a dual-orifice, pressure atomizing type identified as Part Number 6809618 and shown in Figure 3-5. An internal switching valve of this nozzle opens only the small pilot orifice for low fuel flows so that a high quality spray pattern is obtained. For high flows the main section of the nozzle is operational in addition to the pilot. This valving arrangement is shown in Figure 3-6.

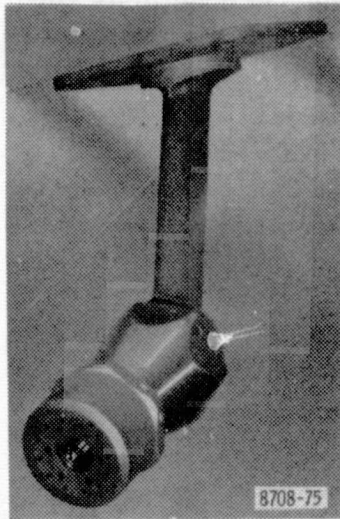


Figure 3-5. Dual-orifice fuel nozzle used in the 501-D22A combustion system.

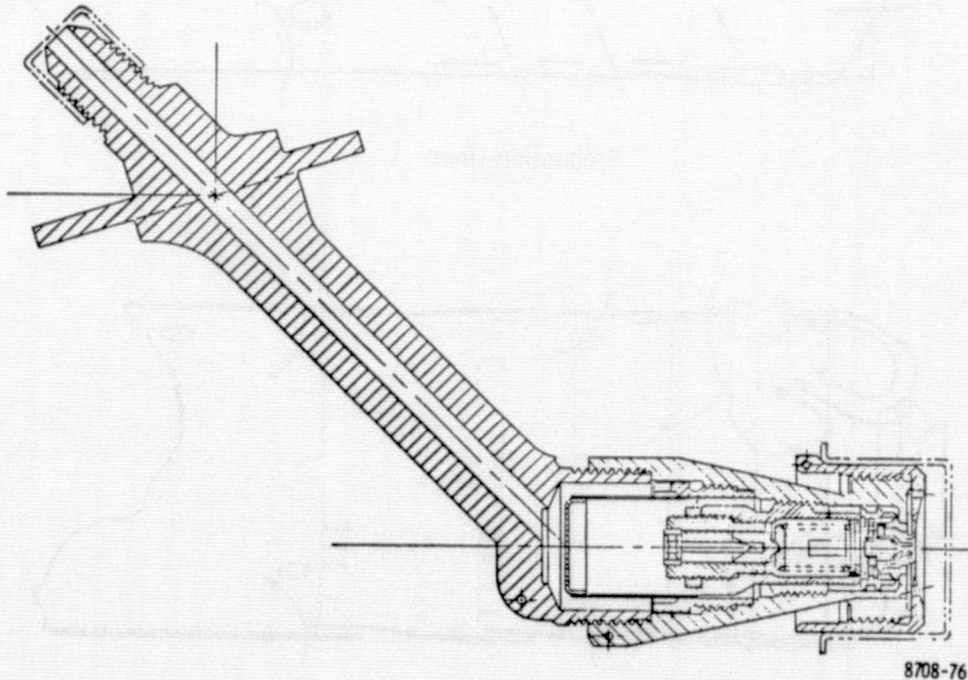
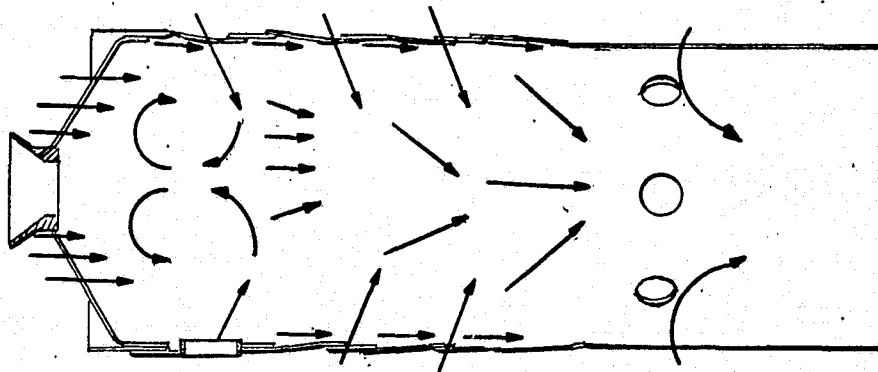


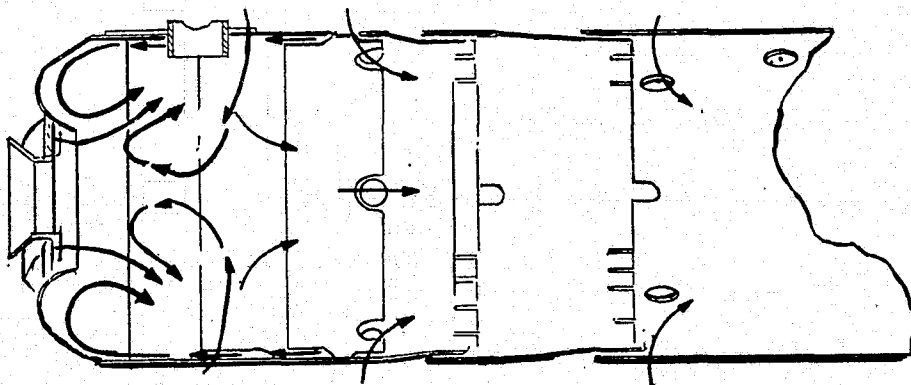
Figure 3-6. Dual-orifice fuel nozzle schematic.

REVERSE FLOW DESIGN

The low emissions combustion system currently in production in the Allison Model 501-K industrial engine formed the basis of the reverse flow combustor-airblast fuel injector system used in this program. The reverse flow concept is compared with the standard design in Figure 3-7. It incorporates a unique primary zone flow system which increases the amount of recirculating products, improves the fuel and air mixing, and returns the partially burned products, which become trapped in the primary zone cooling film, back into the reaction. This design operates with great stability over the fuel/air ratio range of 0.004 to 0.022, which is typical of single shaft industrial applications. Other features of the combustor were kept simple and conventional so that the low cost and durability of the original system were retained.



Production liner



Reverse flow design

8708-11

Figure 3-7. Model 501 combustors

The airblast fuel nozzle design uses the combustion liner differential air pressure to atomize the fuel. This is done by accelerating the air through a row of vanes and using its high velocity for atomization. With this device, the fuel droplet diameters are reduced approximately threefold and a modest degree of fuel/air premixing also occurs with the atomizing air. An important feature of this injector design is that droplet size remains small over the entire engine operating range. A pressure atomizing pilot is used to retain good engine starting. A diagram of the 501-K airblast injector is shown in Figure 3-8.

In this program, the 501-K industrial engine combustion system was redesigned so that its exhaust emissions would comply with the program emissions goals (75% of the EPA turboprop Standard).

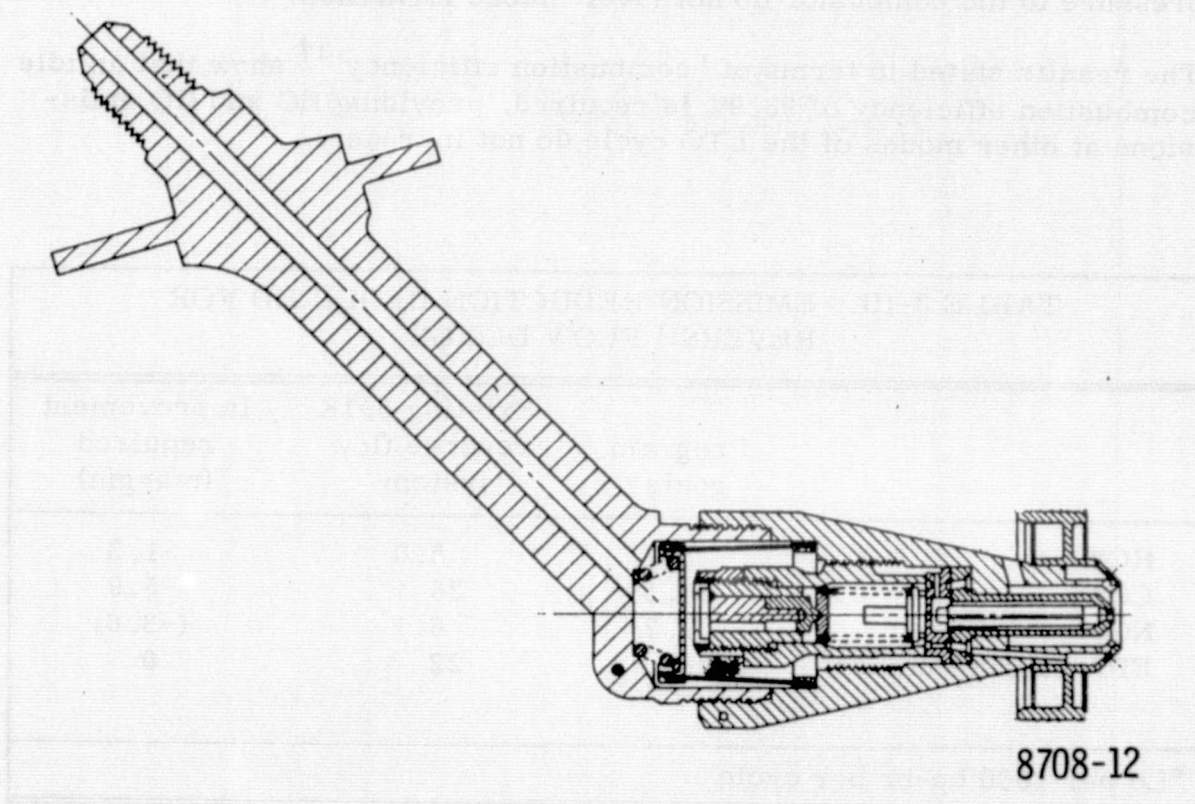


Figure 3-8. Model 501 industrial engine airblast fuel nozzle (partial view).

The emission reduction required for the reverse flow airblast combustion system is given in Table 3-III. Reductions in carbon monoxide and unburned hydrocarbons are required, while margin exists in oxides of nitrogen.

Since about 95% of the mass of CO and HC are created in the taxi-idle mode, a tradeoff study was made to determine the reduction in idle emissions required to meet program goals.

- CO must be decreased 10%
- HC must be decreased 70%

Oxides of nitrogen on the other hand could be allowed to increase 162%. Smoke at idle was not considered because the low inlet temperature and pressure to the combustor do not favor smoke formation.

The results stated in terms of "combustion efficiency"[†] show that an idle combustion efficiency of 98.9% is required, providing HC and CO emissions at other modes of the LTO cycle do not increase.

TABLE 3-III. EMISSION REDUCTION REQUIRED FOR REVERSE FLOW DESIGN			
	Program goals	Existing 501K reverse flow system	Improvement required (margin)
HC*	3.7	5.0	-1.3
CO*	20.1	26	-5.9
NO _x *	9.7	6.1	(+3.6)
EPA Smoke Number	22	22	0
*Lb per 1000 hp-hr per cycle			

[†]Superscript numbers correspond to the references listed in Section IX.

Design Considerations

The reduction of CO and HC emissions at idle is discussed by Lefebvre² who, in summarizing the state of art, lists the following major methods:

1. Improved fuel atomization
2. Redistribution of airflow to bring the primary zone equivalence ratio to 0.85 at design
3. Increased primary zone volume or residence time
4. Reduction of film cooling air
5. Compressor air bleed
6. Fuel staging

Each of these methods was reviewed for its applicability to the reverse flow system. Knowledge of the reverse flow design characteristics and development experience with this system led to the conclusion that the initial (baseline) design need depart only slightly from the production reverse flow, airblast system used on 501-K industrial engines. Subsequent designs could then incorporate more novel features as required to meet the program goals.

Design Analysis of Baseline System

Air Distribution

The baseline design is a modification of the industrial engine combustion liner and uses the same fuel nozzle. Its major features are given in Table 3-IV. The axial air distribution and equivalence ratios are given in Table 3-V.

The modification to redistribute the primary-dilution zone airflow was determined from an analysis of combustion efficiency test results made over a wide range of equivalence ratios. Both engine operating lines were used: 10,000 rpm (idle speed) and 13,280 rpm (flight speed). This data, a plot of combustion inefficiency ($100 - \eta_p$) and primary zone equivalence ratio is given in Figure 3-9. This shows that to achieve a taxi-idle combustion efficiency of 98.9% (program emission goal) the primary zone equivalence ratio at idle should be increased from $\phi = 0.395$ to $\phi 0.47$. This was confirmed by the analysis of other combustor designs tested during the industrial engine development. In these, a two to threefold reduction in idle emissions was obtained from the production liner by the use of primary zone equivalence ratios of 0.42 through 0.50.

TABLE 3-IV. MAJOR DESIGN FEATURES OF THE BASELINE
REVERSE FLOW COMBUSTION SYSTEM

Type: Turbo Annular - 6 liners	
Fuel Nozzle: Airblast main, pressure atomizing pilot - 6 nozzles	
Annulus area	110.3 cm ²
Liner area	154.8 cm ²
Liner hole area	66.1 cm ²
Length	63.0 cm
Diameter	14.0 cm
L/D	4.49
$\Delta P/P$, % calc	3.3 (Liner)
$\Delta P/q$, factors	37.
Design temp	1322 + 56 K
Hot gas velocity	60.7 m/s
Airflow	2.49 kg/s
Vol flow	7.5×10^{-3} m ³ /s
Inlet press.	95.2 N/cm ²
Inlet temp	594 K

TABLE 3-V. AIR FLOW AREA DISTRIBUTION FOR BASELINE
REVERSE FLOW DESIGN

Feature	Calculated area (cm ²)	C_D^*	Effective area (cm ²)	ϕ Station (at idle)	ϕ Station (at max power)
Fuel nozzle	1.61	0.86	1.39	4.65	
Swirler	2.25	0.86	1.94	1.94	
1st reversal	4.43	0.45	1.99	1.21	
2nd reversal	8.54	0.45	3.86	0.702	
Primary holes	6.24	0.60	3.74	0.499	0.998
1st cooling	4.65	0.45	2.09	0.429	
Secondary	7.60	0.60	4.56	0.329	0.655
Corrugations	8.39	0.83	6.97	0.242	
Tertiary	13.61	0.60	8.17	0.186	
Tertiary	5.20	0.60	3.12	0.170	
Baffle	1.42	0.50	0.71	0.167	
Baffle	2.13	0.50	1.06	0.163	
	66.10	0.599	39.60	0.163	0.325
*From DDA flow tests.		$\phi = (F/A_{\text{station}})/(F/A_{\text{stoichiometric}})$			

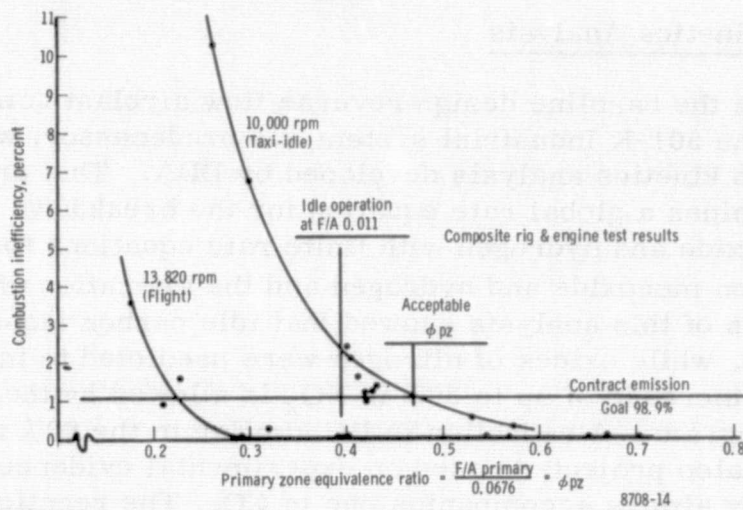


Figure 3-9. Combustion inefficiency, 501-K industrial engine reverse flow airblast combustion system.

Because of this analytical and experimental evidence, the primary zone equivalence ratio at idle was increased to a value of $\phi = 0.50$ by primary zone area reductions of 6.245 cm^2 , which is 9% of the total liner area. The value $\phi = 0.50$ includes a small margin above the $\phi = 0.46$ which was indicated by the experimental data shown in Figure 3-9. In addition, the primary zone area change was made principally in the first air entry stages (swirler and first reversal). This was done to enrichen the initial reaction. Figure 3-10 illustrates these changes.

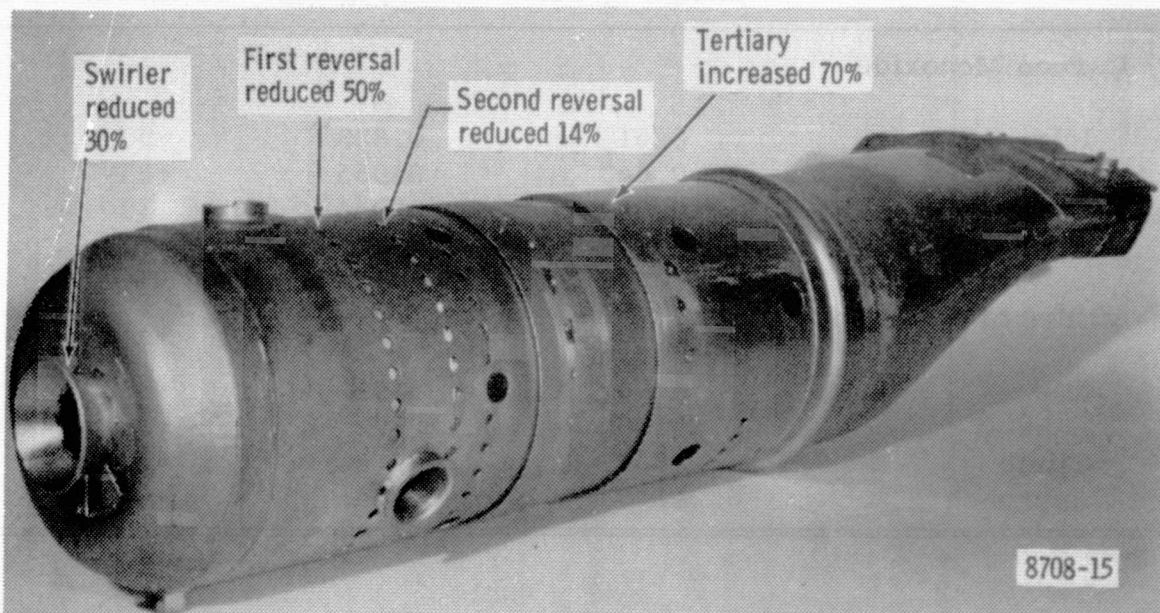


Figure 3-10. Changes to 501-K production combustor airflow distribution.

Reaction Kinetics Analysis

Emissions from the baseline design reverse flow airblast combustion system and from the 501-K industrial system, its predecessor, were predicted using a reaction kinetics analysis developed by DDA. This analytical procedure combines a global rate equation for the breakdown of hydrocarbons to carbon monoxide and hydrogen with finite rate equations for the combustion of carbon monoxide and hydrogen and the formation of nitrogen oxides. Results of this analysis showed that idle carbon monoxide would be reduced 90%, while oxides of nitrogen were predicted to increase 34% at takeoff. An increase of up to 80% in NO_x is allowed by the emission goals of the program. A reduction in HC similar to the 90% reduction of CO at idle was also projected based on experimental evidence that a HC reduction nearly always accompanies one in CO. The reaction kinetics analysis confirmed the changes in air distribution computed for the baseline design. Table 3-VI summarizes the results of the reaction kinetics analysis.

TABLE 3-VI. REVERSE FLOW COMBUSTION SYSTEM EMISSIONS
PREDICTED BY REACTION KINETICS ANALYSIS

	501-K Industrial design (g/kg)	501-D22A Reverse flow baseline design (g/kg)	Change Predicted Percent
Carbon Monoxide			
Idle	8.51	0.833	-90
Takeoff	0.043	0.055	+28
Climb	0.032	0.044	+38
Approach	4.17	0.41	-90
Oxides of Nitrogen			
Idle	4.94	5.91	+20
Takeoff	21.0	28.2	+34
Climb	18.7	24.0	+28
Approach	15.3	17.4	+14

Heat Transfer

A heat transfer analysis was made to verify the adequacy of combustor cooling and aid in locating the skin temperature thermocouples used in the experimental tests. For the analysis, a simple heat balance was used and conduction in the combustor skin was neglected except at the double acting baffle where axial conduction was considered. The predicted skin temperatures are shown in Figure 3-11. The highest of these was 1037 K which is well below the design skin temperature for the 501-D22A aircraft liner of 1089 K. The maximum temperature predicted for the double acting baffle was 1374 K at the upstream tip. This is within 100 K of the oxidation temperature of the baffle material, Hastelloy X. However, since the hot area was localized at the edge, which is not a critical part of the baffle, no further design action was required.

Designs Tested

In addition to the baseline, design modifications I through IV were tested. These consisted of a minor change in the combustor primary zone and major changes in fuel injection mode. The test configurations are listed below:

Baseline - Reverse flow combustor with rich primary zone (ϕ at takeoff = 1.00); airblast fuel nozzle with pressure atomizing pilot and air atomizing main.

Mod I - Reverse flow combustor same as Baseline; airblast fuel nozzle operated on airblast main only.

Mod II - Reverse flow combustor with rich primary zone modified to increase flow 19% in second reversing baffle (ϕ at takeoff = 0.96); airblast fuel nozzle with pressure atomizing pilot and airblast main.

Mod III - Reverse flow combustor, same as Mod II; air assist (outside air pressure) fuel nozzle no pilot.

Mod IV - Reverse flow combustor, same as Mod II; airblast fuel nozzle operated on airblast main only.

PRECHAMBER DESIGN

Two basic prechamber designs were tested:

- A short prechamber where fuel and air mix but do not have time to burn in the prechamber
- The longer prechamber which serves as a small combustor

Zone	Gas flow rate kg/s	Local gas temp K	Flame temp K	Fuel/air	Luminosity factor
A	0.749	2311	2514	0.073	1.7
B	1.201	1894	2068	0.046	1.3
C	1.201	1894	2068	0.046	1.3
D	2.280	1408	1444	0.024	1.0

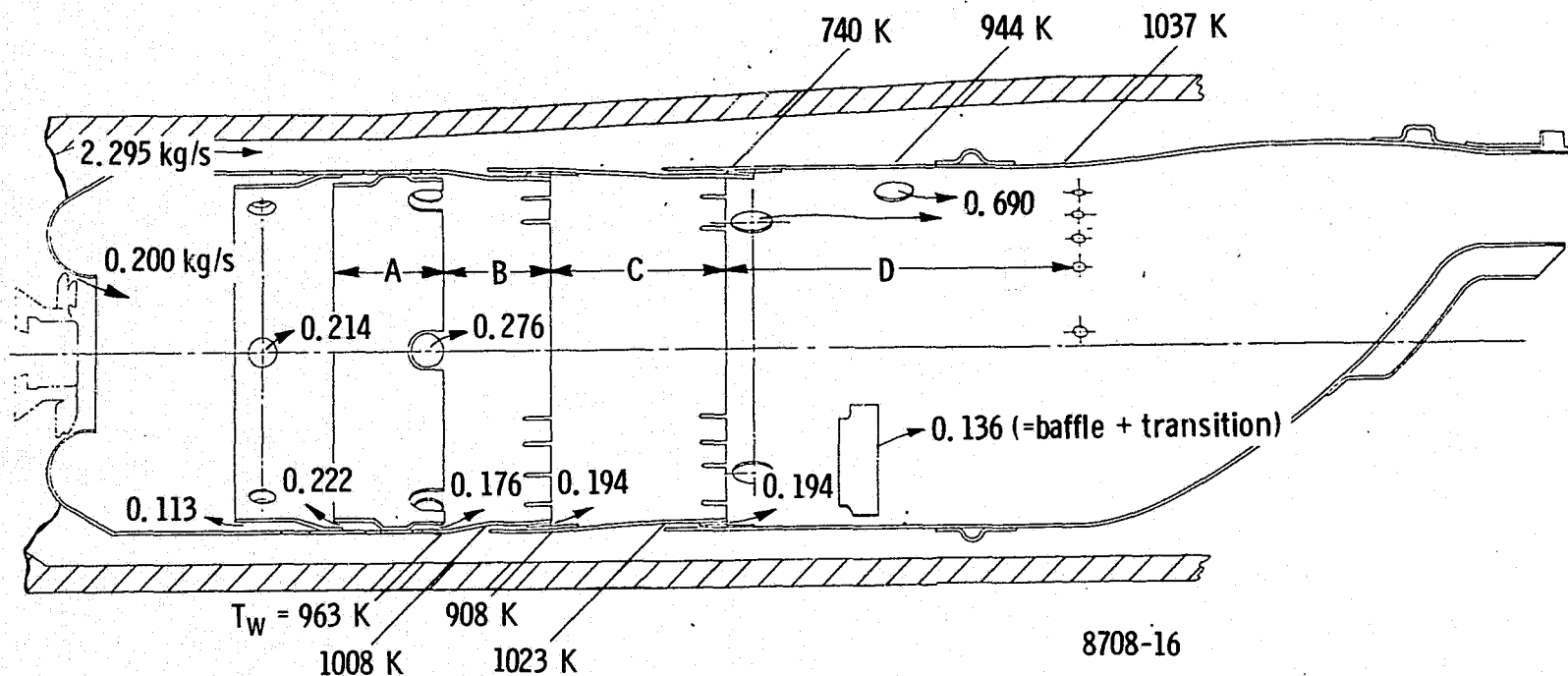


Figure 3-11. Thermal analysis of the reverse flow combustor.

In both cases, the prechambers are attached to main combustion sections having primary zone trim holes and dilution holes. Details of the prechamber combustor designs and their modifications are described below.

The features common to all the prechamber combustors are as follows:

1. An airblast fuel nozzle (under certain conditions a pressure atomizer pilot was used in conjunction with the airblast system). See Figure 3-8.
2. A prechamber, employing an axial swirler at the inlet and a center mounted fuel nozzle.
3. A radial swirler at the end of the prechamber, with the same swirl direction as the axial swirler and fuel nozzle airblast swirl.
4. A trip between the radial swirler at the end of the prechamber, and the main chamber. This trip, in conjunction with the swirler caused two distinct recirculation zones. These are shown in Figures 3-12 and 3-13.
5. A secondary fuel system which placed fuel on the wall of the prechamber just upstream of the radial swirler, denoted as wall-film fuel injection.
6. The combustor exit transition section.
7. A variable geometry band used to open and close the dilution holes.

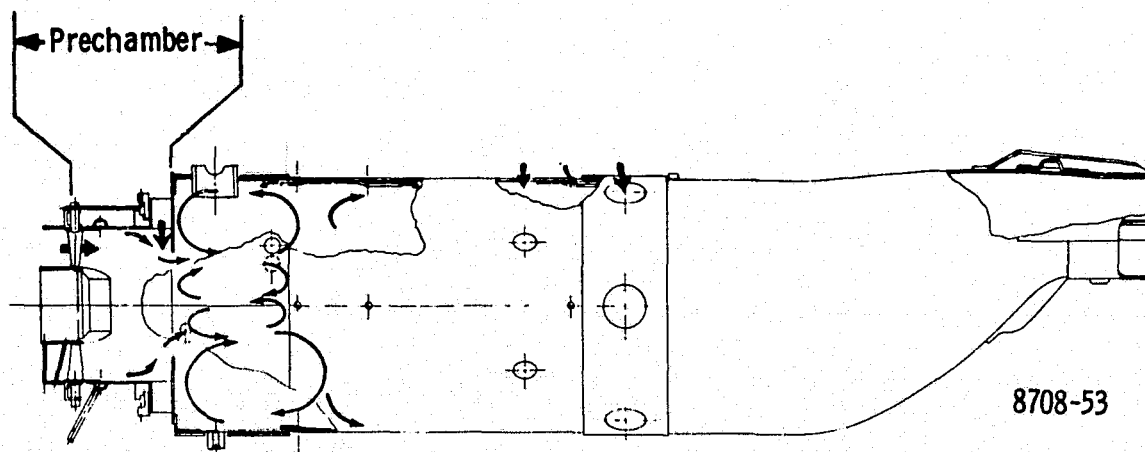


Figure 3-12. Flow visualization, short-prechamber combustor.

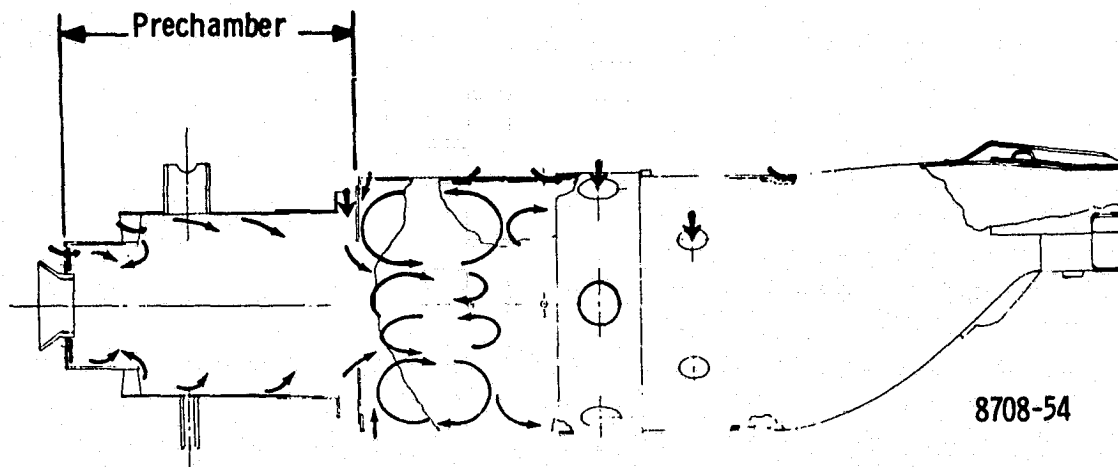


Figure 3-13. Flow visualization, long-prechamber combustor.

Short Prechamber Design

Specific details of the short prechamber design are shown in Figure 3-14. Variable geometry is installed in three locations; the axial swirler at the front end of the prechamber is variable relative to vane turning angle, the small holes in the primary zone can be uncovered fore or aft, and the dilution holes can be partly or fully covered. These variable geometry systems are operational during the test and can be separately positioned by remote control while the combustor is on point.

The range of positions possible with the variable geometry systems is indicated in Table 3-VII.

A total of four configurations of the short prechamber combustor were tested. These are identified in Table 3-VIII.

The Baseline and Mod. III designs have two differences:

1. 240 0.89-mm-diameter holes were added to the Mod. III configuration in an area in which high skin temperatures were measured on the baseline design. The total area of these holes is 1.5 cm^2 , or the equivalent of one hole 1.38 cm diameter.
2. The fuel nozzle used in the Prechamber Baseline was an airblast type with a pressure atomizer pilot. This pilot was capped off in the Mod. III configuration.

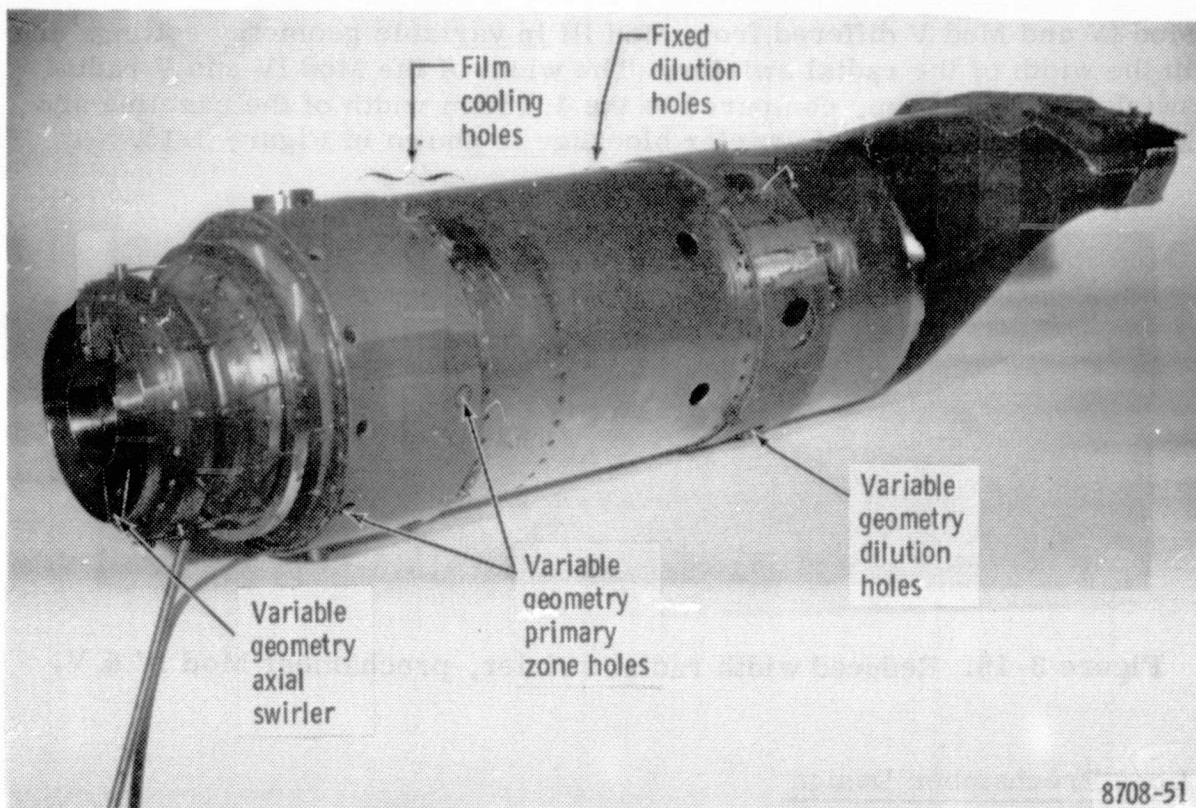


Figure 3-14. Short-prechamber combustor design.

TABLE 3-VII. VARIABLE GEOMETRY RANGE FOR SHORT PRECHAMBER COMBUSTOR

Axial swirler angle, radians	0.17 to 0.52
Primary hole location distance from aerodynamic tip, cm	0.64 and 5.69
Dilution hole area, cm ²	0 to 26.6

TABLE 3-VIII. SHORT PRECHAMBER CONFIGURATIONS TESTED OVER LTO CYCLE

Configuration	Axial Swirler setting (radians)	Position of primary zone holes (cm)	Dilution area (cm ²)
Baseline	0.17	5.69	14.2
Mod III	0.17	5.69	14.2
Mod IV	0.35	5.69	14.2
Mod V	0.17	5.69	6.5

Mod IV and Mod V differed from Mod III in variable geometry settings and in the width of the radial swirler. The width of the Mod IV and V radial swirler was 0.84 cm, compared to the 1.15 cm width of the baseline and Mod III designs. Radial swirler blockage is shown in Figure 3-15.

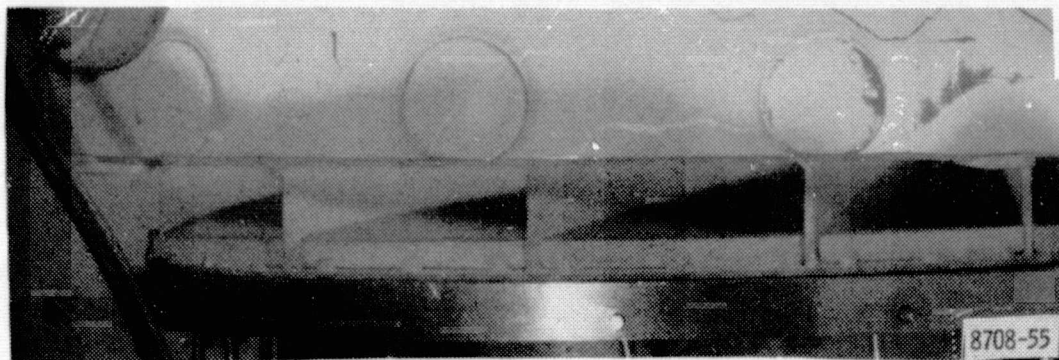


Figure 3-15. Reduced width radial swirler, prechamber Mod IV & V.

Long Prechamber Design

The long prechamber design is shown in Figure 3-16. In this combustor variable geometry is installed in the dilution section to regulate dilution airflow. Primary zone holes are located in the forwardmost position.

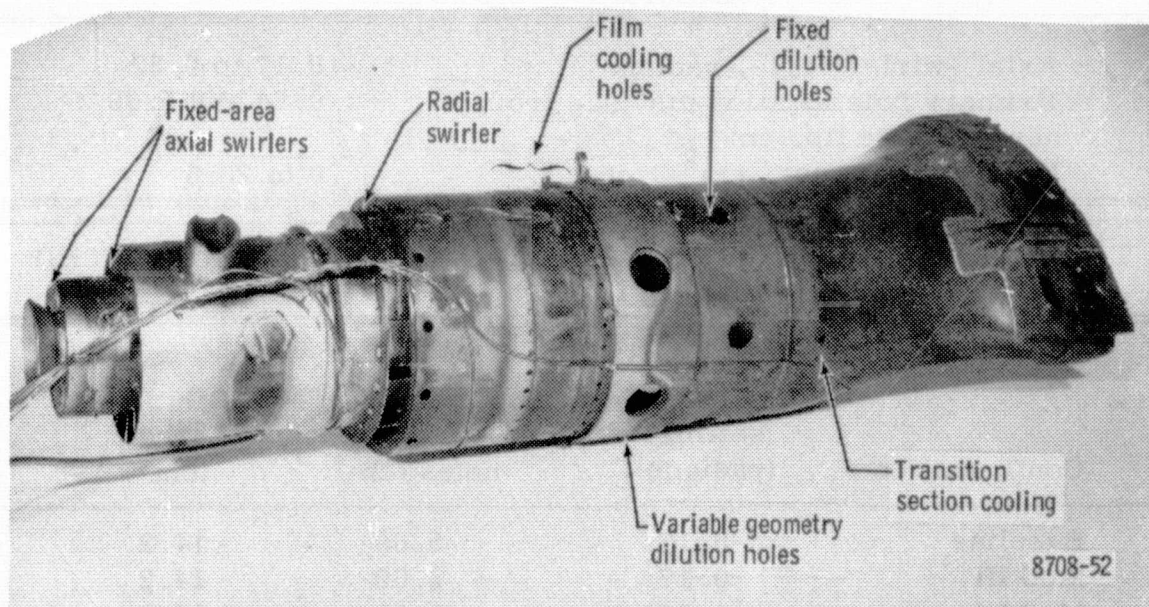


Figure 3-16. Long-prechamber combustor design.

Other fixed-area air flow orifices are the two sets of axial swirler vanes at the inlet to the prechamber and fuel nozzle chamber, a radial swirler at the forward end of the primary combustion zone, film cooling holes in the primary zone and transition section and fixed dilution holes. The area of the variable dilution holes fully open is 26.6 cm^2 , the same as for the short prechamber design. The fixed position axial swirler is set at .35 radians.

The long prechamber design was tested over the LTO cycle at two variable geometry settings:

- Mod I - dilution area 26.6 cm^2 (full open)
- Mod II - dilution area 12.9 cm^2

STAGED FUEL

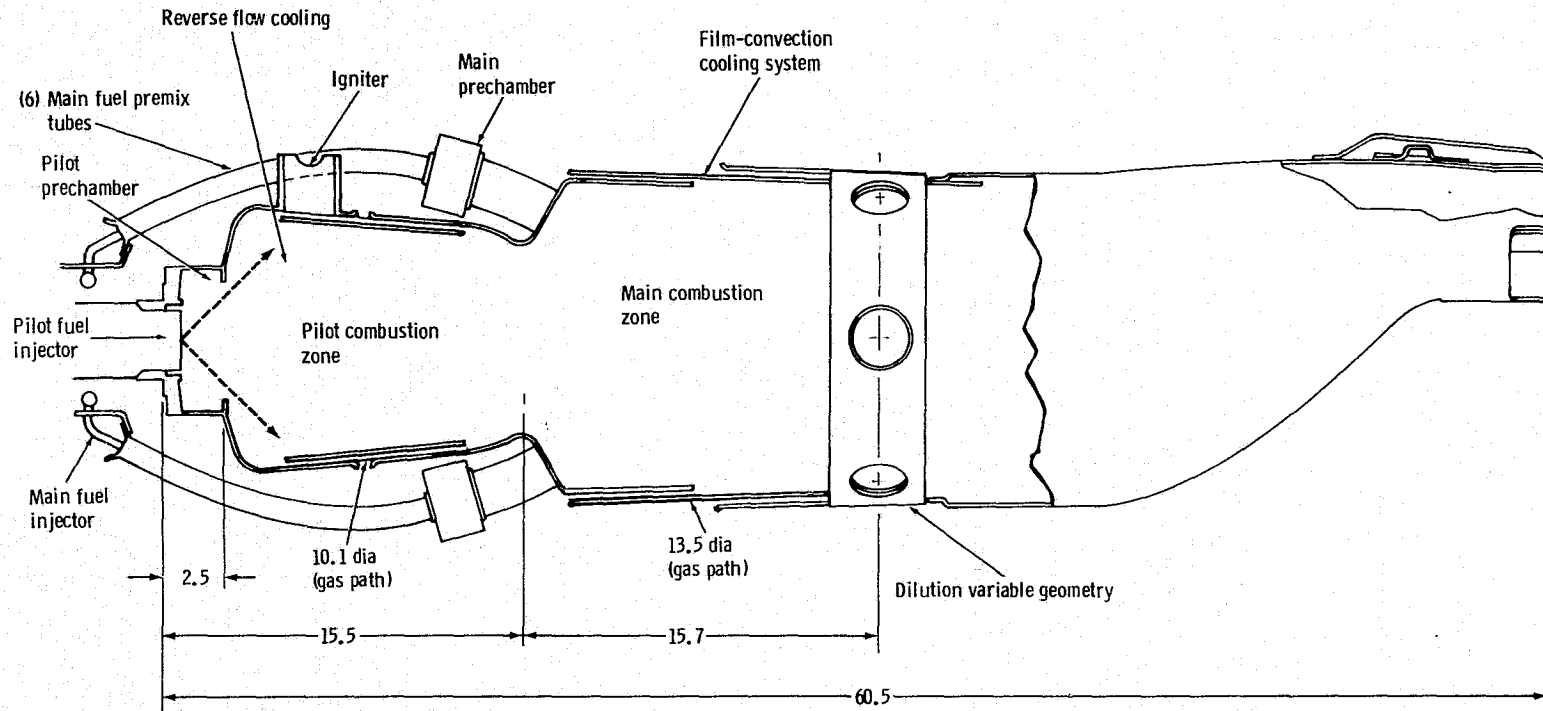
Two basic combustor designs "original design," and "Mod V, VI design," and three pilot fuel injectors were tested for a total of four basic configurations as listed below:

- Original design with dual orifice pressure atomizing pilot nozzle
- Original design with air assist pilot nozzle
- Original design with airblast pilot nozzle
- Mod V, VI design with airblast pilot nozzle

The basic combustor and fuel injector designs are described in the following paragraphs.

Original Staged Fuel Combustor Design

To meet the program goals and EPA proposed emission limits,³ large HC, and smoke reduction, and a moderate CO reduction are required. No NO_x improvement is required. In fact, a considerable NO_x increase is allowed. The original staged fuel design was, therefore, designed to provide maximum CO, HC, and smoke reduction with no attempt to reduce or control NO_x . Analysis of the 501-D22A production liner emissions over the LTO cycle shows that approximately 95% of the total CO and HC is emitted in the idle mode. Improvements must be made at the idle condition if program goals are to be met. The staged fuel combustor as originally designed is shown in Figure 3-17. The following design features were incorporated in the pilot combustion zone specifically to reduce idle CO and HC:



Note: All dimensions are in centimeters.

8708-31

Figure 3-17. Original staged fuel combustor design.

- Slightly lean pilot zone for high reaction rates
- Low pilot zone airflow loading. About 50% of the combustion air is admitted into a separate, main combustion zone.
- Low wall-quenching. A film-convection wall cooling system was employed. This provides excellent cooling performance with approximately 50% cooling flow reduction relative to conventional film cooling systems.
- Initial cooling step flow reversal. This feature is also used on the reverse flow combustor to "recycle" CO and HC trapped in the cooling air close to the dome.
- Swirl prechamber. The fuel is introduced into a short axial swirl prechamber to provide good initial fuel/air mixing, and good stabilization and mixing patterns in the combustion region. The prechamber fuel/air mixing quality, and the limited operating range required from the pilot zone allowed the use of the standard dual-orifice, pressure atomizing fuel injector to obtain the required smoke reduction. The arrangement of two combustion chambers in series, the upstream chamber being the pilot zone and the downstream chamber the main zone, provides for extended residence time and combustor volume for emission reduction at the critical idle and approach conditions. Flame stabilization was accomplished by aerodynamic means, employing recirculation associated with geometric expansions to maintain pilot and main zone flames. In the main combustion chamber, flame stabilization was augmented by the hot pilot zone gas mixing with the main-zone fuel-air mixture.

The fueling system was a key main zone design feature. The main zone fuel manifold was located in close proximity to the pilot zone fuel nozzle to demonstrate the feasibility of obtaining pilot and main zone fuel from a single line. This capability would allow incorporation of a staged fuel combustor into the 501-D22A engine with only minor engine modifications, and with no "buried" main fuel injectors or manifolds. As shown in Figure 3-17, the main fuel is injected from the main manifold into six fuel premix tubes. Airflow in these tubes transports the fuel from the fuel manifold at the pilot zone front end to the main combustion zone. Some fuel prevaporization occurs during transport. The degree of fuel prevaporization obtained is a function of many variables (fuel properties, pressure, temperature, residence time, etc.), and is probably small at the relatively low inlet temperature conditions of the 501-D22A (605.4 K at takeoff). Higher inlet temperature cycles would have increased main fuel prevaporization. Six main prechambers were incorporated in the fuel-air premix tubes at the inlet to the main combustion zone. Radial inflow swirl air was introduced into these prechambers to centrifuge the remaining liquid fuel onto

the tube walls to obtain good main fuel distribution and reduced preignition or flashback potential. An airblast atomization rim was provided at the main prechamber exit to airblast atomize the main fuel. The fuel-air mixture exiting each prechamber was directed in a swirling pattern to aid in main zone stabilization and assist mixing. The original main zone prechamber design is shown in Figure 3-18. The exit swirl angle is computed to be 0.873 radians.

A dilution zone variable geometry (DZ VG) band was incorporated to readily accomplish airflow distribution changes during hot testing. This band allowed the dilution hole area to be adjusted from fully open to fully closed. The program objective, however, was to demonstrate low emissions and stable operation over the engine operating range in a fixed geometry mode.

The airflow distribution for the original design is listed in Table 3-IX for fully open and fully closed dilution zone variable geometry (DZ VG) positions. Many intermediate flow distributions are, of course, possible. The functional airflow distribution is shown in Table 3-X.

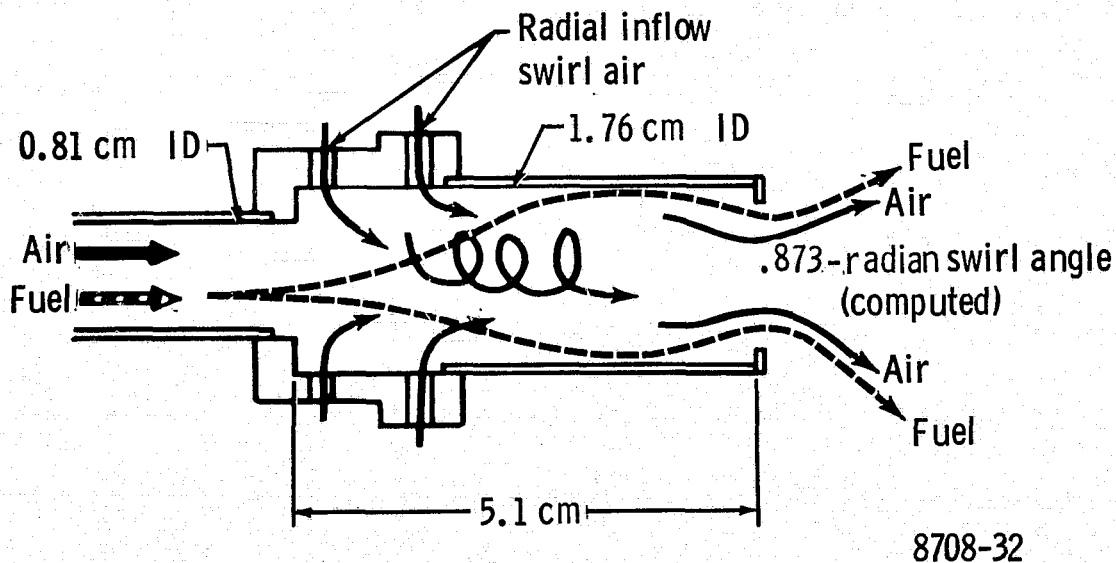


Figure 3-18. Original design main prechamber.

TABLE 3-IX. STAGED FUEL BASELINE AIR FLOW DISTRIBUTION

Flow station	Dilution holes open			Dilution holes closed		
	Area (cm ²)	C _D	Air Flow (%)	Area (cm ²)	C _D	Air Flow (%)
Swirler	3.95	.70	6.83	3.95	.70	11.67
Cooling No. 1	2.41	.70	4.17	2.41	.70	7.12
Primary holes	4.28	.60	6.35	4.28	.60	10.85
Cooling No. 2	2.41	.70	4.17	2.41	.70	7.12
Baffles	1.61	.60	2.39	1.61	.60	4.09
Main prechamber	6.34 (1)	.85	13.35	6.34	.85	22.79
Cooling No. 3	3.19	.70	5.52	3.19	.70	9.43
Cooling No. 4	3.19	.70	5.52	3.19	.70	9.43
Dilution holes	29.72	.60	44.13	1.81 (2)	.60	4.58
Cooling No. 5	2.22	.60	3.29	2.22	.60	5.62
Transition baffle	2.87	.60	4.28	2.87	.60	7.31
Total	62.21		100.00	34.28		100.00
(1) Swirl angle = 0.873 radians						
(2) VG band leakage						

TABLE 3-X. ORIGINAL DESIGN FUNCTIONAL AIRFLOW DISTRIBUTION

	Air Flow Distribution (%)	
	Dilution holes open	Dilution holes closed
Pilot combustion air	17.35	29.64
Main combustion air	19.91	34.00
Total combustion air	37.26	63.64
Wall cooling air (1)	25.17	43.00
(1) Reverse Flow Air Not Included		

Combustion zone equivalence ratios for the staged fuel combustor design are a function of the selected fuel flow split, and DZ VG setting. The zonal equivalence ratios are summarized in Figure 3-19 for "open" and "closed" DZ VG settings, respectively. This shows that the pilot zone equivalence ratio is proportional to the percent pilot fuel selected, and the overall fuel/air ratio. The main zone overall fuel/air ratio depends on the overall combustor fuel/air ratio only, assuming rapid pilot and main zone mixing. Figure 3-19 shows that with an "open" DZ VG setting, the design pilot zone equivalence ratio is 0.96, (slightly lean) at idle for rapid combustion and low CO, and HC. As the engine fuel/air ratio and engine power are increased, the pilot zone becomes rich, increasing the potential for smoke and high CO and HC formation. This can be alleviated by scheduling fuel to the main combustion zone, or by closing the DZ VG as indicated in Figure 3-19. The pilot and main zone design equivalence ratios at takeoff are 0.80 (DZ VG open) at the design fueling split of ~50% pilot. High NO_x emission would be expected in this fueling mode. Figure 3-19 shows that lower equivalence ratios can be obtained by closing the DZ VG.

The original staged fuel combustor design shown in Figure 3-20 was tested with the three different pilot zone fuel injectors as shown in Figure 3-21. The first build employed the production 501-D22A dual orifice pressure atomizing nozzle. The pilot and main orifices had 0.000216 and 0.00106 flow number (FN) respectively ($FN = W_{fuel}/\sqrt{\Delta P}$). The main spray angle was 1.57-1.745 radians.

The second test employed an air assist fuel nozzle having an external air source for fuel atomization. The nozzle air pressure was variable from 0 to 135 kPa (40 in. Hg) differential pressure.

A pilot zone airblast fuel injector was used in the third test. This nozzle (Figure 3-21) was operated on combustor airflow and pressure drop. Fuel was injected through 16 orifices 0.58 mm diameter and airblast atomized by nozzle-swirl air. The nozzle swirler effective area was 1.23 cm² (A_xCd), giving a typical nozzle air/fuel ratio of 2.9 at takeoff, with 50% pilot fuel, and 3% combustor pressure loss. No pressure atomizing pilot tips were used with the air assist or airblast nozzles. As discussed in Section VI, the original staged fuel design met all emission objectives.

Mod V, VI Staged Fuel Combustor Design

Following the successful testing of the original design, the staged fuel combustor was extensively modified to achieve the following objectives:

- Further CO reduction
- NO_x reduction

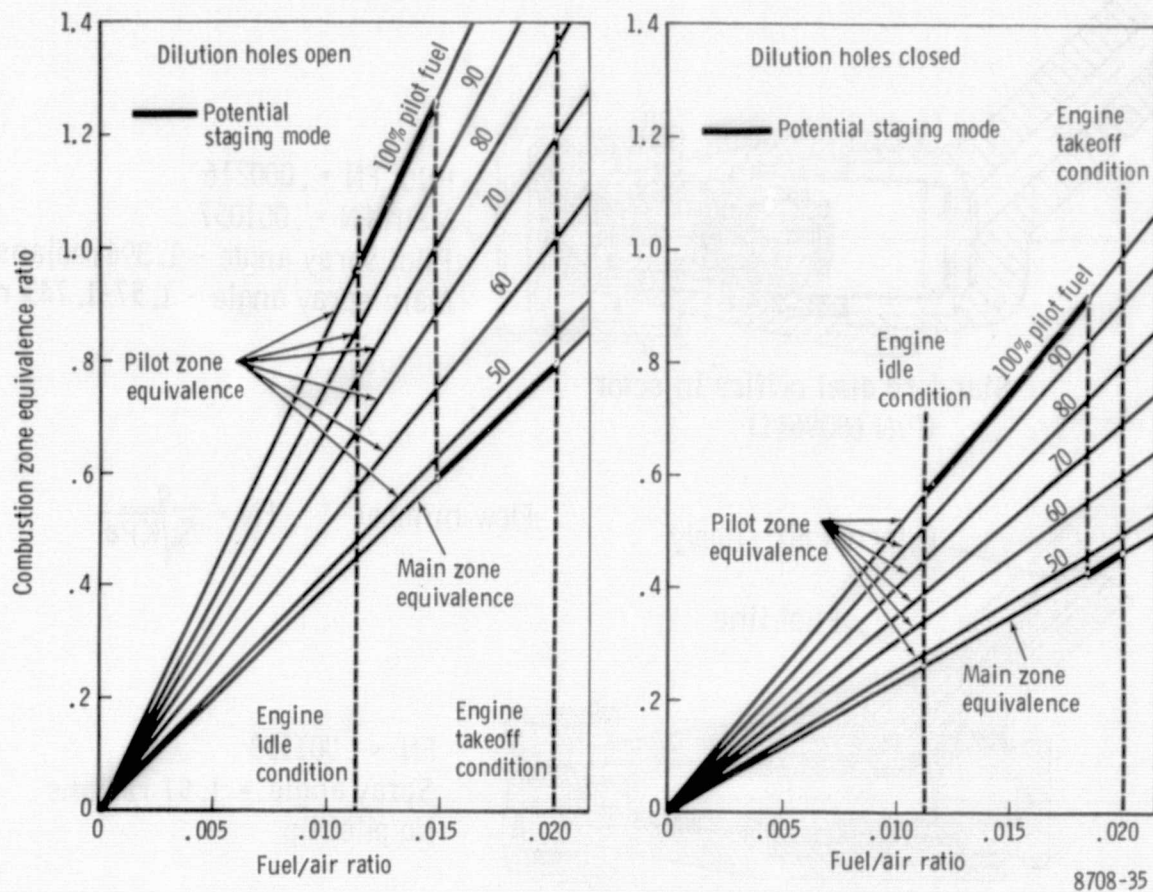


Figure 3-19. Original design combustion zone equivalence ratio.

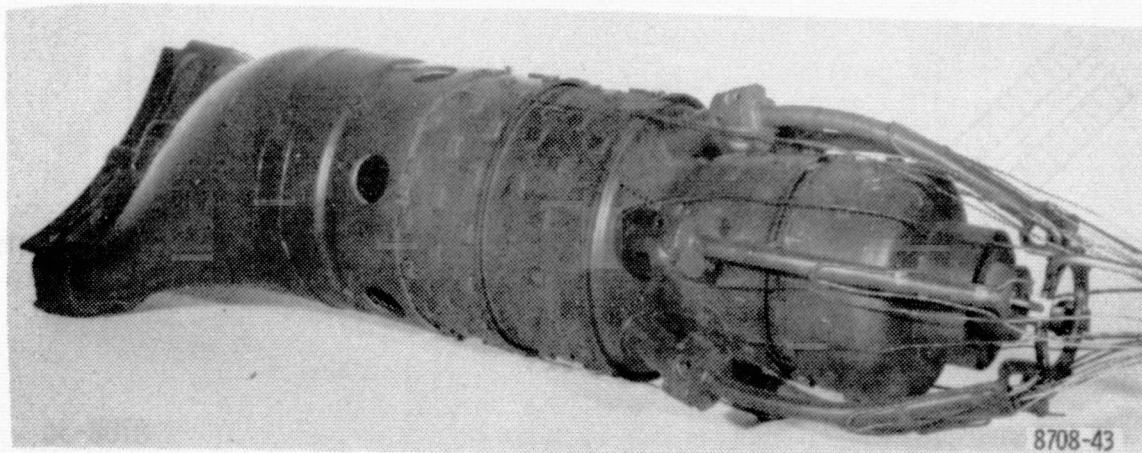
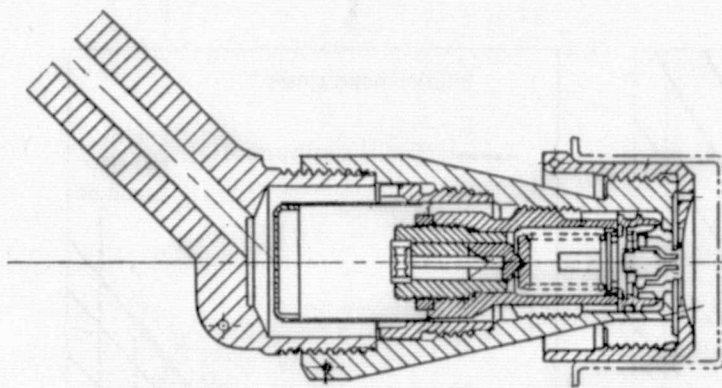
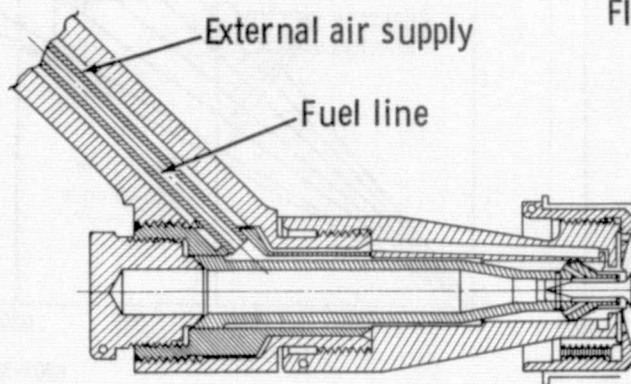


Figure 3-20. Original design staged fuel combustor.



Standard dual orifice injector
(P/N 6809611)

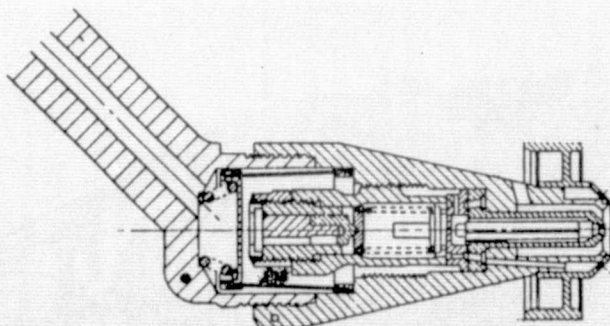
Pilot FN = .000216
Main FN = .001057
Pilot spray angle - 1.396 radians
Main spray angle - 1.57-1.745 radians



Air assist injector
(EX 118902)

Flow number $FN = \frac{q}{S\sqrt{KPa}}$

FN = .001153
Spray angle = 1.57 radians
No pilot tip



Airblast injector
(EX 115875)

Main FN = .001537
Main spray angle = 1.57 radians
No pilot tip used

8708-36

Figure 3-21. Staged fuel combustor pilot fuel injectors.

The following design changes were made:

1. Increased pilot zone volume to reduce idle CO
2. Reduced pilot zone equivalence ratio to reduce idle CO and high power NO_x .

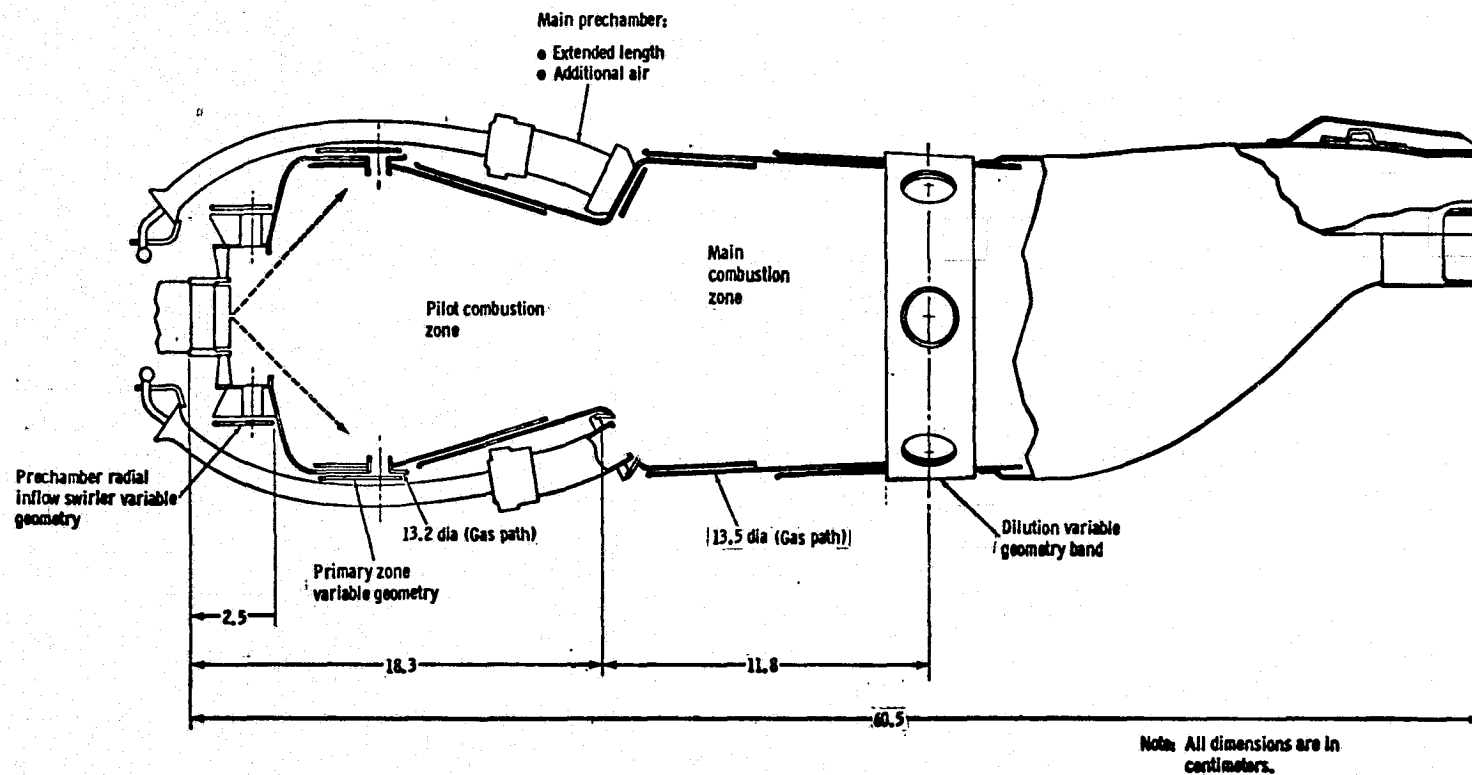
Equivalence ratio reductions were achieved operationally by further closing the dilution holes. At high exhaust temperatures the DZ VG settings are limited by the combustor exit-temperature pattern factor which tends to increase as the dilution holes are closed. Dilution hole closure increases the cooling air percentage and this reduces the dilution jet penetration and mixing. Cooling air was, therefore, minimized in Mods. V and VI by increasing pilot and main combustion airflow, and minimizing combustor wall cooling air, particularly in the transition section. VG systems were also added to regulate airflow in the new pilot zone prechamber (PC) radial inflow swirler, and the primary zone (PZ) air jets.

The Mod. V/VI design is shown in Figure 3-22. The differences between this design and the baseline staged fuel combustor are as follows:

- Increased pilot zone axial swirler area
- Pilot prechamber radial inflow swirler with VG system
- Increased pilot zone diameter
- Increased pilot zone length
- Primary zone variable geometry system
- Modified pilot zone cooling system mechanical construction
- Altered main fuel premix tube profile
- Increased main zone prechamber length to improve main fuel preparation
- Increased main prechamber swirl angle
- Increased main zone airflow delivered through auxiliary swirlers
- Reduced transition cooling flow

The overall combustor length remained the same.

The main zone prechamber details are shown in Figure 3-23. The length was increased from 5.1 to 6.3 cm to improve fuel distribution. Additional prechamber radial inflow swirl air increased the exit swirl angle from 0.873 to 0.960 radians and increased main zone mixing rates. Additional main zone air was injected through an auxiliary axial swirler at the prechamber exit. This provided air on both sides of the fuel for improved mixing.



3708-37

Figure 3-22. Mod V, VI staged fuel combustor design.

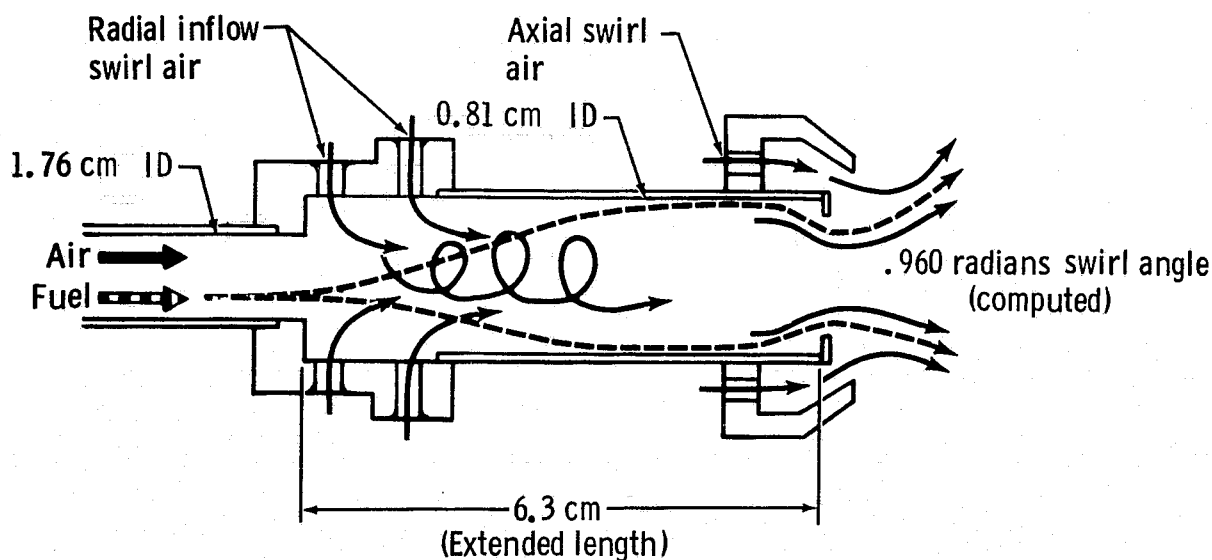


Figure 3-23. Mod V, VI design main prechamber.

The air flow distribution depends entirely on the variable geometry (VG) settings selected. The most influential VG system is the dilution hole system. Table 3-XI shows the air flow distribution for open and closed dilution hole settings. The functional airflow distribution is shown in Table 3-XII for pilot prechamber swirler and primary zone VG open and closed respectively.

The combustion zone equivalence ratios are shown in Figure 3-24 as a function of overall fuel/air ratio, and pilot to main fuel flow split for open and closed DZ VG settings. The system was leaned to a pilot zone equivalence ratio of 0.60 at idle, and a main zone equivalence ratio of 0.50 at takeoff (at ~ 50% pilot-to-main fuel split) for an open dilution hole setting. Additional leaning, to a main zone equivalence ratio of 0.38, was obtainable by dilution hole closure. A small amount of additional leaning is obtainable by opening the pilot radial inflow swirler.

The Mod. V, VI staged fuel design was tested with an airblast pilot zone fuel injector. Figure 3-25 is a photograph of the combustor.

TABLE 3-XI. MOD V/VI DESIGN AIRFLOW DISTRIBUTION

Flow station	Dilution holes open			Dilution holes closed		
	Flow area (cm ²)	C _D	Flow (%)	Flow area (cm ²)	C _D	Flow (%)
Airblast nozzle	1.54	.80	2.85	1.54	.80	4.68
Axial swirler	5.74	.70	9.36	5.74	.70	15.34
Radial swirler	---	---	---	---	---	---
Cooling No. 1	2.96	.70	4.82	2.96	.70	7.90
Primary holes	4.27	.60	5.97	4.27	.60	9.80
Cooling No. 2	2.37	.70	3.88	2.37	.70	6.35
Cooling baffles	1.61	.60	2.25	1.61	.60	3.69
Main prechamber ⁽¹⁾	5.51	.85	10.91	5.51	.85	17.88
Auxiliary swirler	4.29	.60	5.99	4.29	.60	9.83
Cooling No. 3	3.19	.70	5.20	3.19	.70	8.52
Cooling No. 4	3.19	.70	5.20	3.19	.70	8.52
Dilution holes	29.72	.60	41.52	1.81 ⁽²⁾	.60	4.14
Cooling No. 5	.74	.60	1.04	.74	.60	1.70
Transition baffle	.72	.60	1.01	.72	.60	1.60
Total	65.84		100.00	37.94		100.00
(1) Swirl angle = 0.960 radians						
(2) VG band leakage						
Pilot prechamber swirler closed						
Primary holes open						

TABLE 3-XII. MOD. V/VI FUNCTIONAL AIRFLOW DISTRIBUTION

	Airflow distribution ⁽¹⁾ (%)	
	Dilution holes open	Dilution holes closed
Pilot combustion air	27.36	43.28
Main combustion air	21.73	34.38
Total combustion air	49.09	77.66
Wall cooling air ⁽²⁾	15.39	24.36

(1) Pilot prechamber swirler closed, primary holes open

(2) Reverse flow air not included

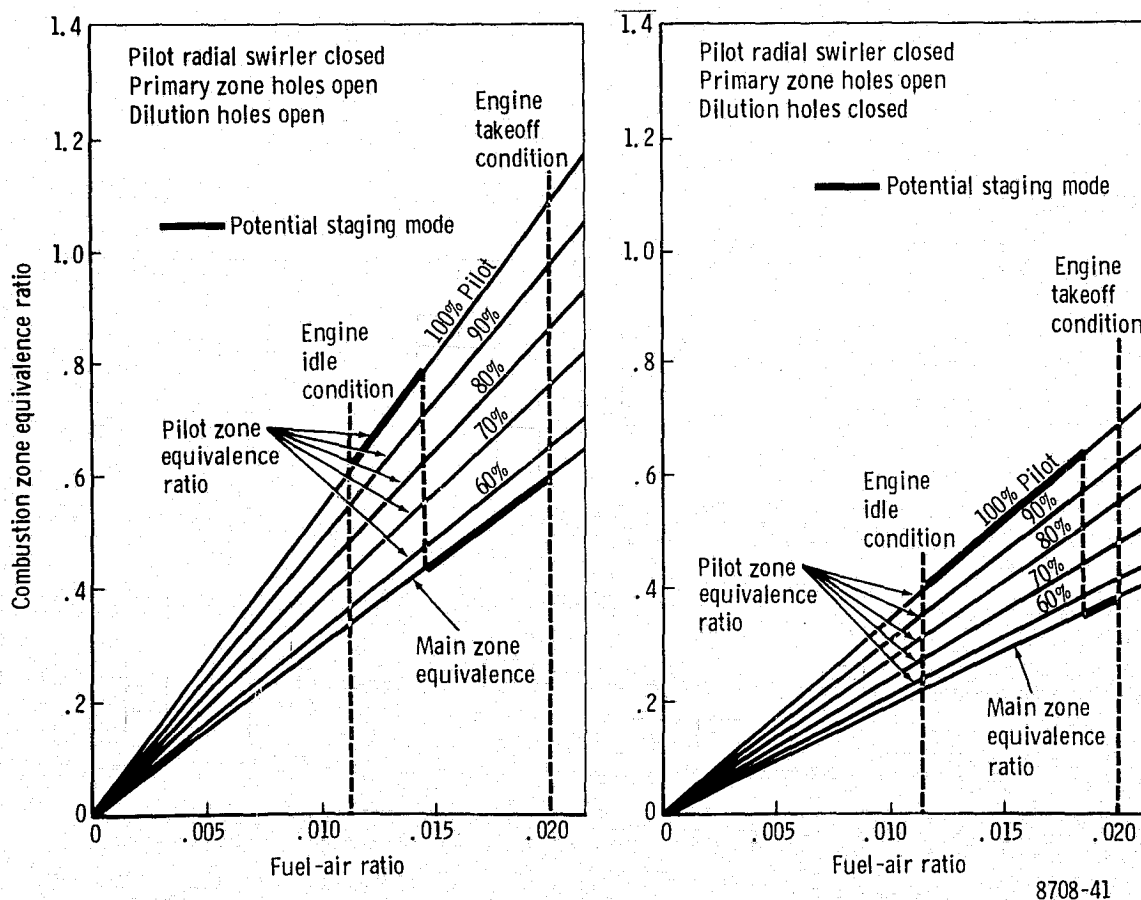


Figure 3-24. Mod V, VI design combustion zone equivalence ratio.

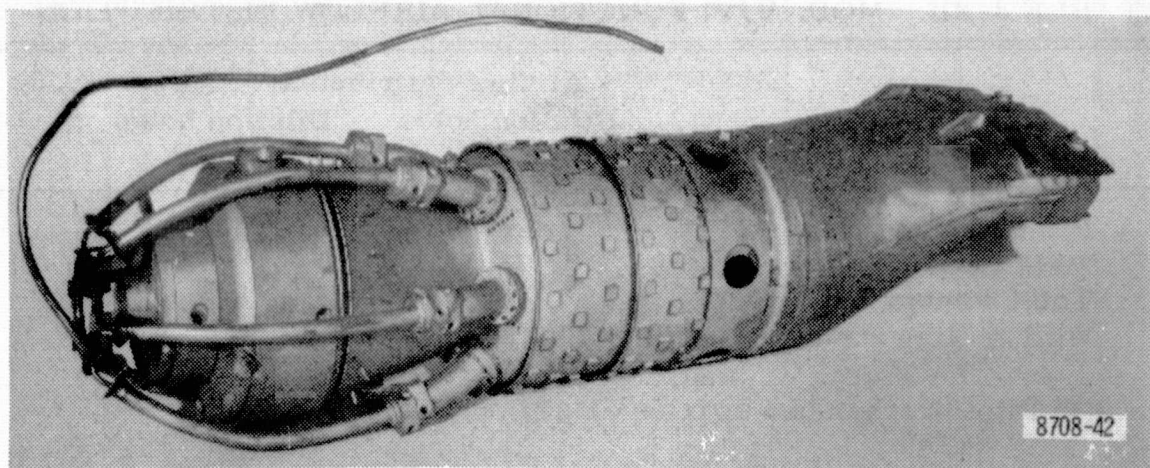


Figure 3-25. Mod V, VI staged fuel combustor.

IV. TEST EQUIPMENT

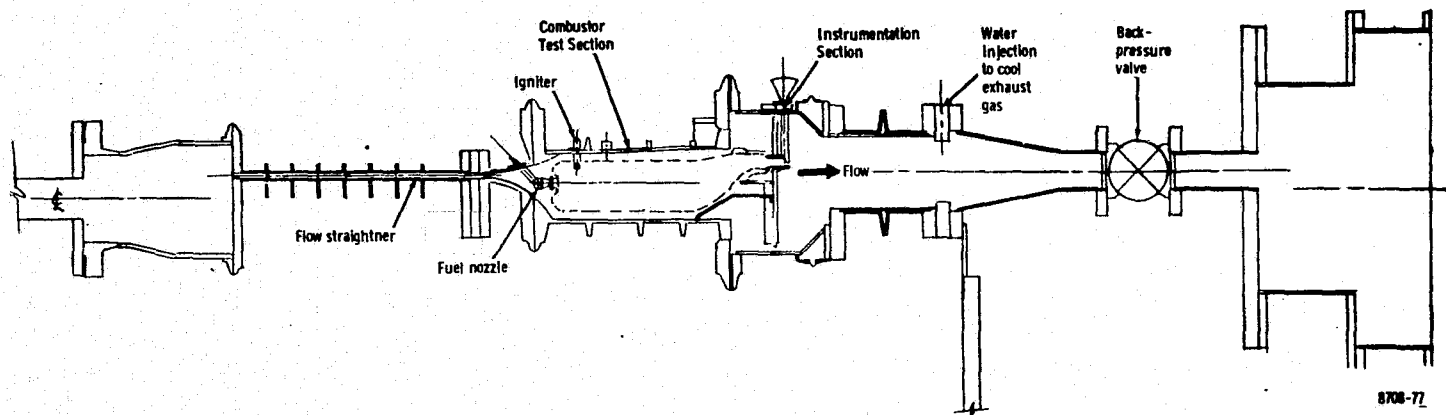
The test equipment used in the performance of this contract consisted of (1) a test rig with instrumentation and read-out equipment and (2) a support facility supplying conditioned nonvitiated (neat) air at 501-D22A inlet conditions.

An existing 501 Model D Combustion rig was modified and used to test the production and low emission combustors. This rig is a single-burner configuration that simulates one-sixth of the 501D turboannular combustion system.

The air flow path of the 501-D rig simulates the engine in that the axial-station cross sections at all locations are defined to the dimensions of a 60 degree segment of the engine combustion system. Flow path simulation also includes the compressor discharge passage and extends through the diffuser combustion section and into the turbine inlet.

An overall view of the rig is shown in Figure 4-1. Figure 4-2 is a flow diagram of the rig and air supply equipment. Flow and pressure level in the rig test section are regulated by an upstream control valve and a downstream, back pressure valve with final temperature trimmed with oil fired heaters at the rig inlet. Flow is measured upstream near the test section, pressure and temperature in the diffuser and exhaust gas pressure, temperature and emissions are measured just downstream of the test section.

The test section of this rig was modified by mounting three variable-geometry rod attachments and operators to the housing. The rig test section is shown in Figure 4-3. A second rig modification was the addition of eleven emission probes of the type shown in Figure 4-4. As noted in the photograph there are five tubes; one sample-out, two water, and two steam system lines. The objective of the probe design is to obtain a representative sample, four holes per probe and eleven probes, and maintain suitable probe tip temperatures for durability and suitable sample temperatures for accuracy of measurement. The emission probes installed in the gas path are shown in Figure 4-5. Outside the rig conditioning and sample lines are attached so that the sample temperature is maintained between the rig and sample manifold. Electric heaters are used to regulate sample line temperature from the manifold to the instruments. The steam traced sample lines are shown in Figure 4-6 prior to insulating.



8708-77

Figure 4-1. Combustor test rig.

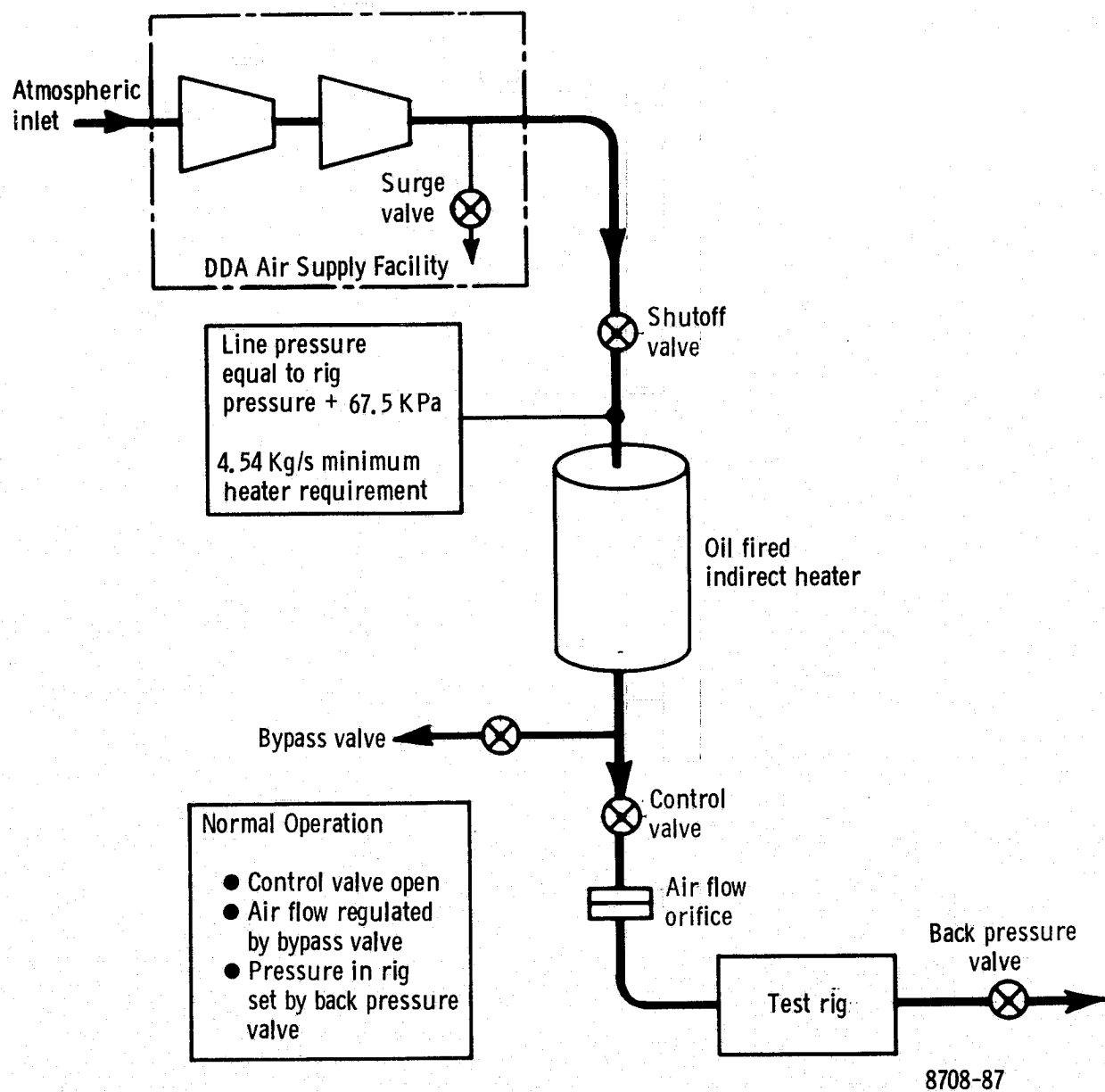


Figure 4-2. Airflow diagram for 501 Model D test rig.

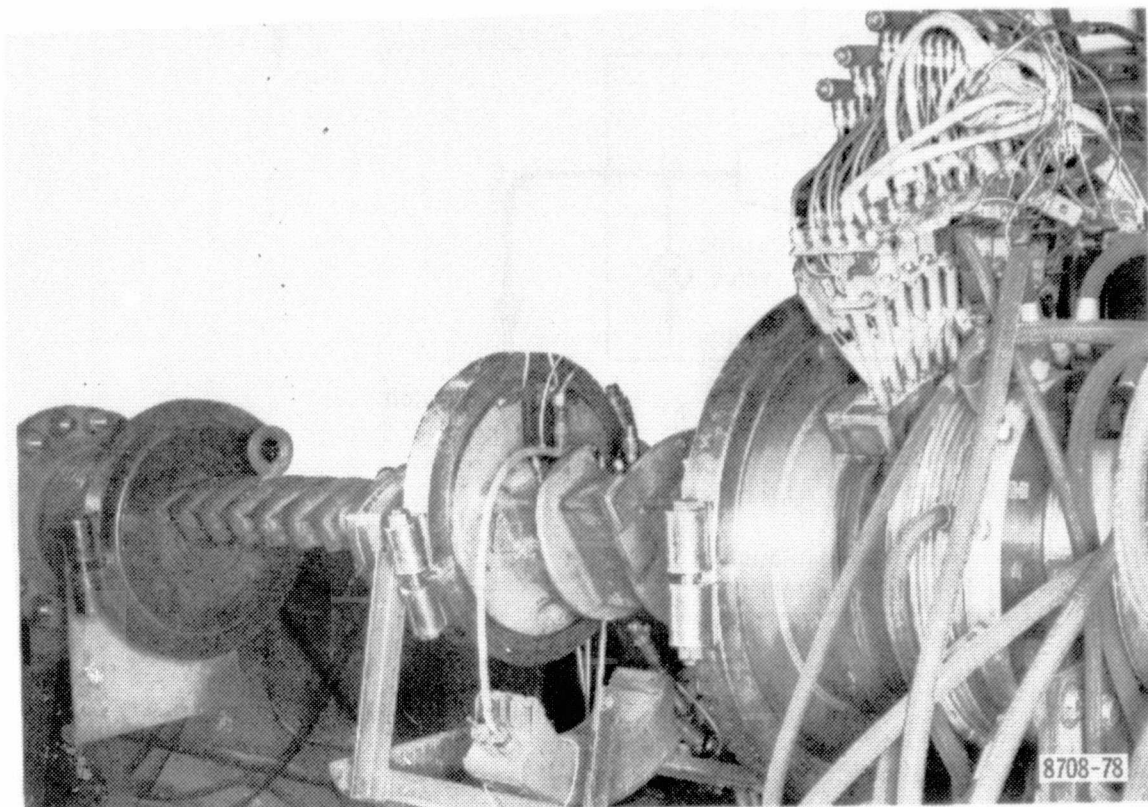


Figure 4-3. Rig test section.

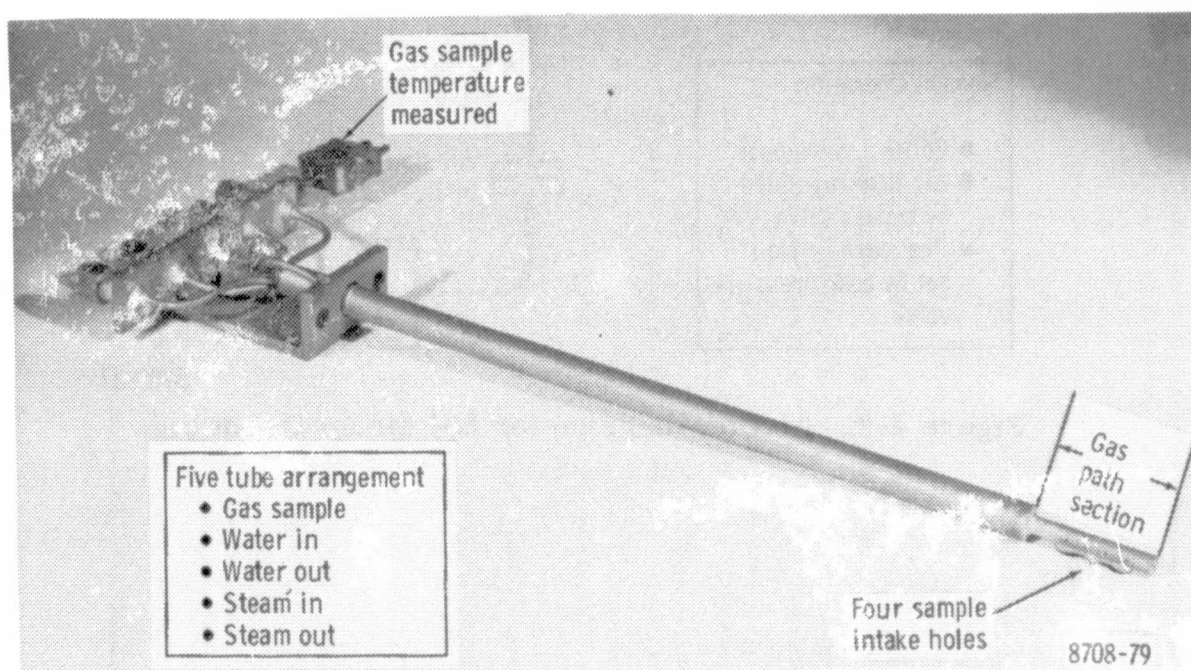


Figure 4-4. Emission probe.

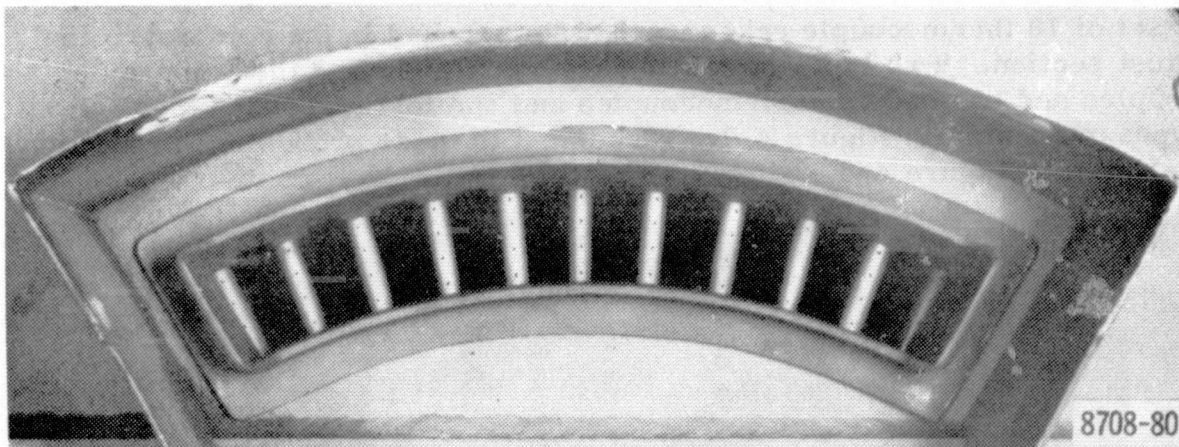


Figure 4-5. Gas path view of emission probes.

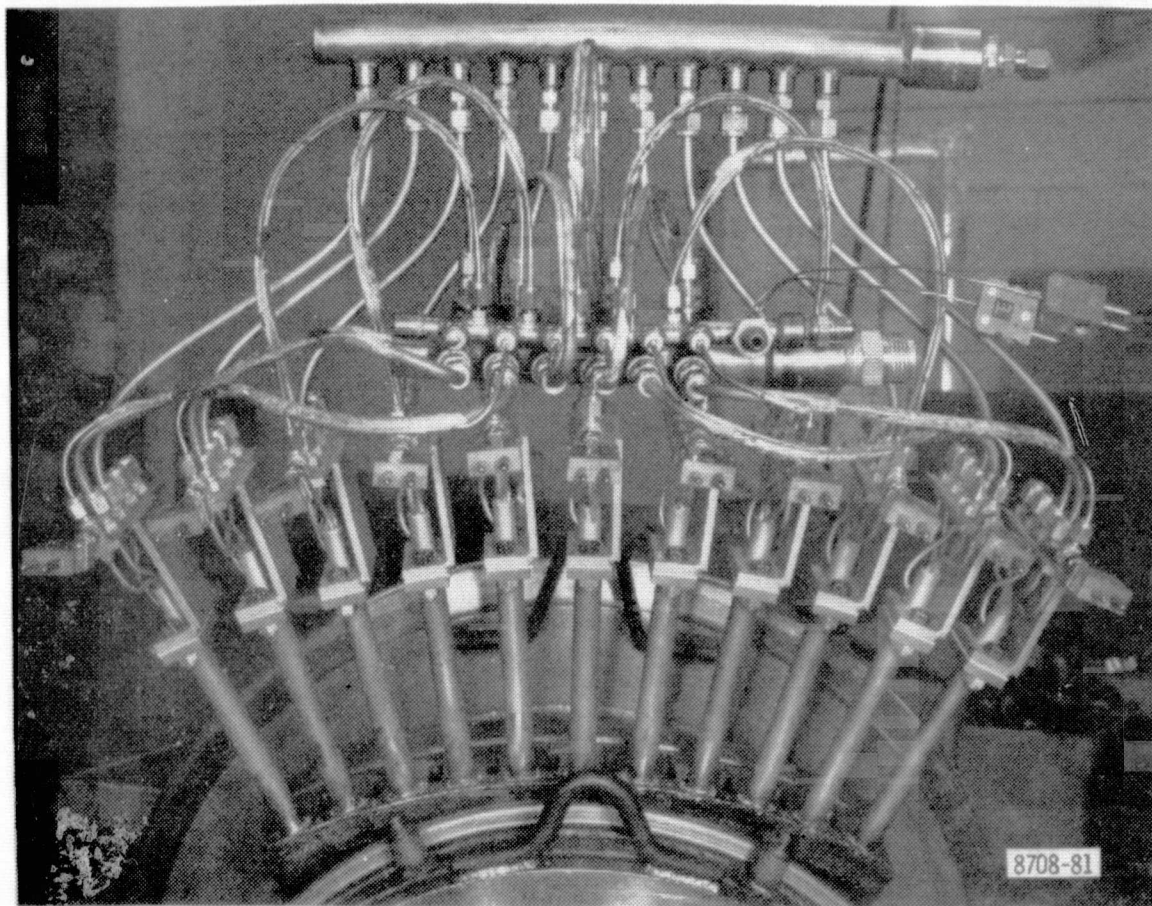


Figure 4-6. Emission sample line arrangement.

A set of 10 thermocouple rakes were also installed in the combustor exhaust section. Two types of rakes were used; eight had three thermocouples and two had two thermocouples and one total pressure tube. Both types are shown in Figure 4-7. Placement of these probes in the gas path is shown in Figure 4-8.

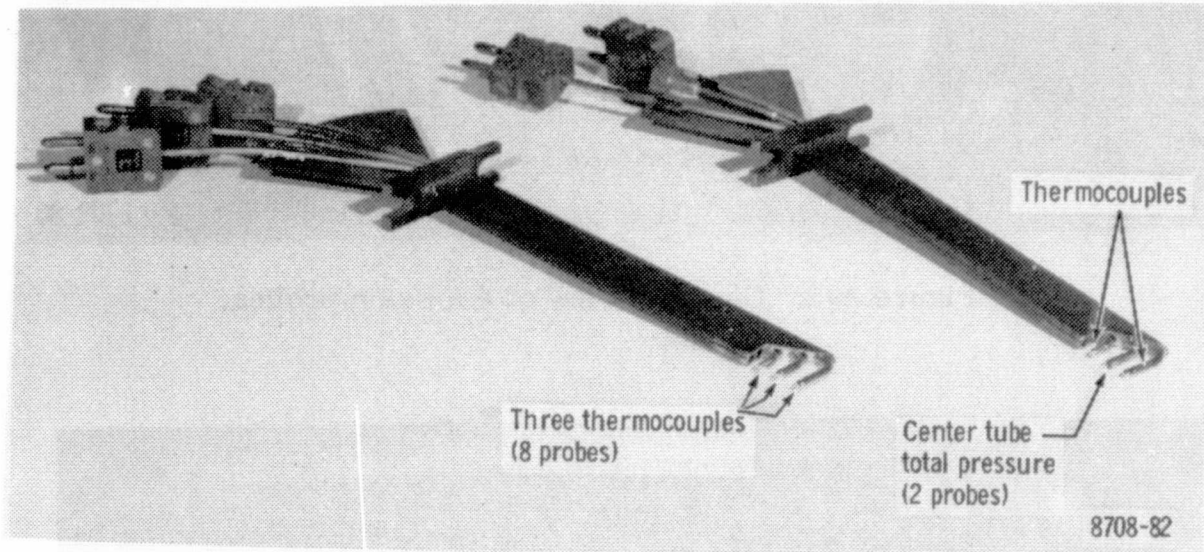


Figure 4-7. Exhaust gas rake.

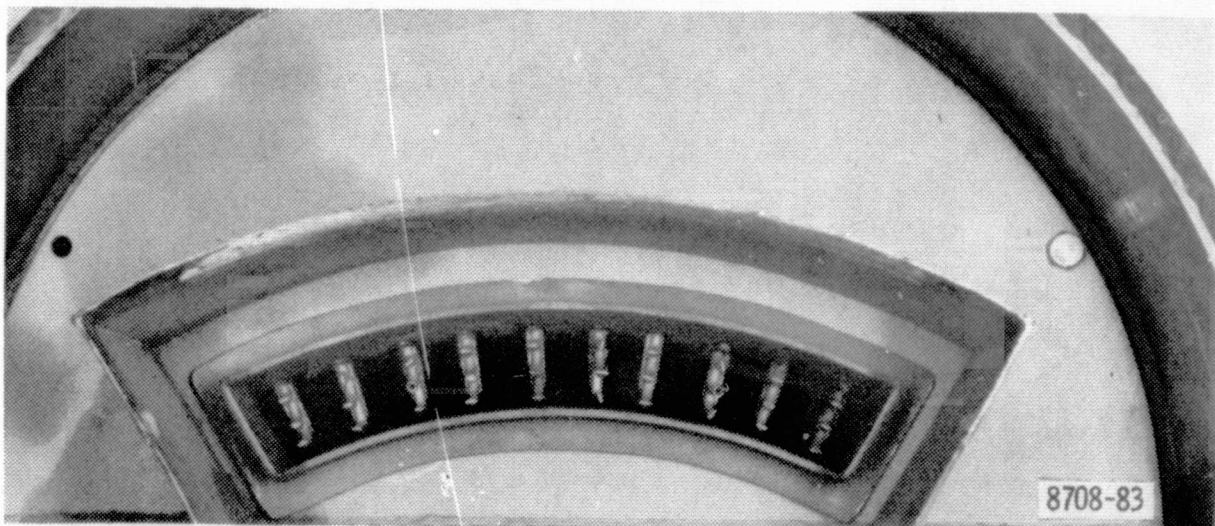


Figure 4-8. Exhaust gas temperature and pressure measurement locations.

The on-line instruments used to measure emissions are listed in Table 4-1. A set of secondary standards previously crosschecked with GM Proving Ground master gases are used to check vendor supplied span gases. These secondary master gases are reverified twice each year. Analyzers used in this program were calibrated prior to starting and at the completion of the test program. The oxides of nitrogen converter was checked weekly for efficiency with a Model 100 Thermo Electron NO_x generator.

The smoke measurement system is shown schematically in Figure 4-9.

The emission measurement system is shown in Figure 4-10. An on-line verification of emission measurement is employed whereby the fuel-air ratio from the measured exhaust gas composition is compared to the metered value. These values should be same, within $\pm 5\%$. Combustion efficiency is also calculated from the exhaust gas composition, using the following equation:

$$\% \eta_b = \left[1 - \frac{\text{fr}_{\text{CO}}(-121,745) + \text{fr}_{\text{HC}}(\text{A}) - \text{fr}_{\text{NO}}(38,880) - \text{fr}_{\text{NO}_2}(12,654)}{(\text{fr}_{\text{CO}_2} + \text{fr}_{\text{CO}} + \text{fr}_{\text{HC}})(\text{A})} \right] \times 100$$

where: A is a constant depending upon the fuel used;
 -263,070 for JP-4, -258,843 for JP-5, etc
 fr is the fraction defining volume.

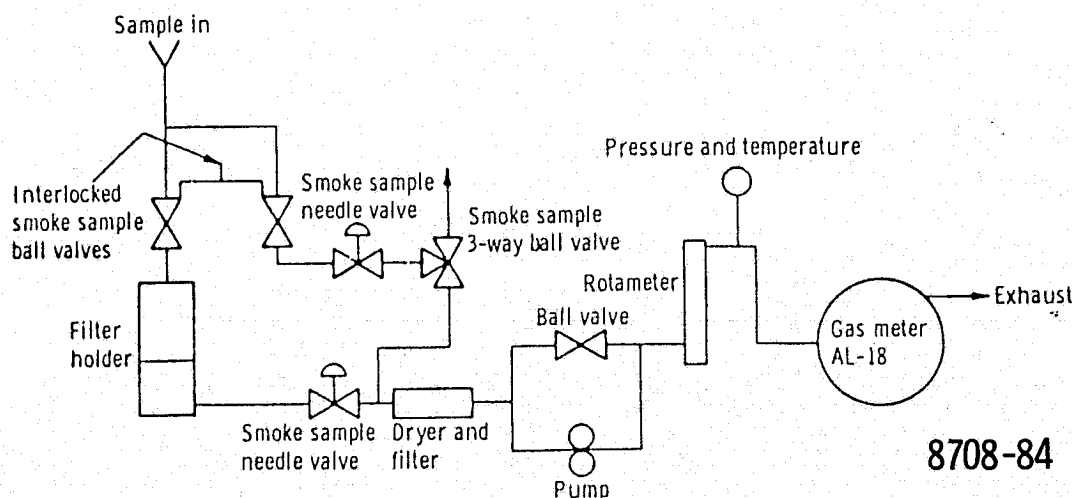
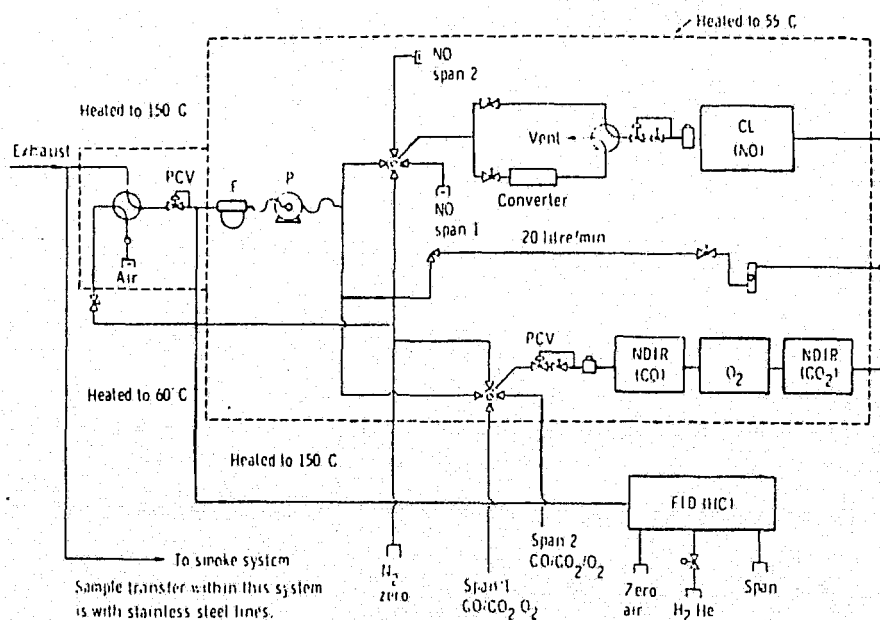


Figure 4-9. Smoke sampling system.

TABLE 4-I. EMISSIONS INSTRUMENTS			
Emission	Method	Instrument	Accuracy
Oxides of Nitrogen	Chemiluminescence	Thermo Electron (Model 10A with converter)	$\pm 1\%$
Carbon monoxide + water vapor	Nondispersive infrared	Beckman (Model 865)	$\pm 2\%$
Carbon dioxide	Nondispersive infrared	Beckman (Model 864)	$\pm 1\%$
Unburned hydrocarbons	Flame ionization detector	Beckman (Model 402)	$\pm 1\%$



8708-85

Figure 4-10. Emission instrumentation system.

ORIGINAL PAGE IS
OF POOR QUALITY

V. TEST PROCEDURE

Tests were conducted by establishing the desired test conditions, lighting the combustor with a spark igniter and gradually increasing fuel flow to the required fuel-air ratio while carefully noting combustor skin thermocouple readings for excessive temperature in the combustor primary zone. After establishing steady operation, data were recorded by the computer center and log entries were made of key readings. The test conditions were the four EPAP LTO cycle points; idle, approach, climbout, and takeoff for the 501-D22A engine.

Parametric tests were conducted on selected configurations to determine the effect of off-design-point operation and variations in fuel and air schedules. The parameters evaluated and the test procedure are as follows:

<u>Parameter</u>	<u>Rig Test Procedure</u>
(1) Combustor inlet pressure	- Reset back pressure and control valves
(2) Combustor inlet temperature	- Reset heater
(3) Combustor loading (gas velocity)	- Change air flow rate
(4) Primary zone equivalence ratio	- Combustor fuel staging - Change combustor air flow distribution with variable geometry - Change overall fuel flow rate
(5) Fuel atomization	- Change nozzle air assist pressure - Change pilot to main split in air blast nozzle - Use wall-film fuel injection together with the fuel nozzle

The test time was significantly reduced in evaluating the primary zone equivalence-ratio parameter by utilizing variable geometry dilution holes, a movable axial swirler, a variable area radial swirler and primary zone variable-area holes in selected combustors. With the variable geometry techniques primary zone equivalence ratio was changed while the test was in progress. Other provisions for reducing test time were separate pilot and main fuel lines to the airblast nozzle which allowed pilot to main fuel split control during the test, and separate fuel lines for the pilot and main combustion zones in the staged fuel combustor to permit optimization of fuel splits at each EPAP LTO cycle condition.

Data acquisition was accomplished through a computerized system for both combustor performance and emissions.

A second type of test was performed to determine the stability characteristics of the final configurations of each combustor type. The procedure was to reduce fuel flow gradually and note the fuel air ratio at blow-out. Altitude operation was simulated by reducing inlet pressure and combustor air loading.

VI. TEST RESULTS

The test results are described for the production liner and the three low emission combustors. A total of nineteen configurations were tested:

- One production liner
- Five reverse flow configurations
- Six prechamber configurations
- Seven staged fuel configurations

PRODUCTION LINER

The 501-D22A production liner was tested at eight conditions, the four EPA LTO cycle points and two off design fuel air points at both idle and takeoff conditions. The results computed for the EPA-LTO cycle are shown in Table 6-I. These data, expressed as EPA Index values are compared with the program goals in Table 6-II.

TABLE 6-I. EMISSIONS OF THE PRODUCTION LINER AT EPAP LTO CYCLE CONDITIONS							
Mode	Time in mode (min)	Hydrocarbon emissions		Carbon monoxide emissions		Oxides of nitrogen emissions	
		EI*	EPAP	EI*	EPAP	EI*	EPAP
Taxi/Idle (Out)	19.0	19.94	78.5	41.15	162.0	2.94	11.6
Takeoff	0.5	0.31	0.2	1.97	1.1	8.51	4.6
Climbout	2.5	0.39	0.2	1.97	1.1	8.72	4.9
Approach	4.5	2.14	1.9	4.74	4.1	6.28	5.5
Taxi/Idle (In)	7.0	19.94	78.5	41.15	162.0	2.94	11.6
Cycle Total	33.5		15.0		31.5		6.2
*g/kg fuel.		lb/1000 hp-hr/cycle.					

As indicated in Table 6-II considerable reduction of hydrocarbons, carbon monoxide and smoke are required. Oxides of nitrogen are below the program goal.

TABLE 6-II. EMISSION REDUCTION REQUIRED

	Total hydrocarbons lb/1000 hp- hr/cycle	Carbon monoxide lb/1000 hp- hr/cycle	Oxides of nitrogen lb/1000 hp- hr/cycle	Maximum SAE smoke No.
EPA limits				
Class P2	4.9	26.8	12.9	29
Program goals				
75% of Class P2	3.7	20.1	9.7	22
Production liner	15.0	31.5	6.2	59
Reduction required, percent based on program goals	75.5	36.1	0	62.7

Performance data for the production liner is summarized as follows:

	Combustor pressure loss, %	Combustion efficiency %	Pattern factor $\frac{T_{avg}-T_{max}}{T_{avg}-T_{in}}$
Idle	4.91	97.4	0.15
Approach	6.49	99.7	0.16
Climbout	5.76	99.8	0.20
Takeoff	5.12	99.9	0.18

REVERSE FLOW

Five configurations of the reverse flow combustion system were tested for emissions and combustion system operating parameters. Operation of the combustion system and of the rig, stand and test equipment was satisfactory throughout these tests.

Emissions

Exhaust emissions from all five of the reverse flow designs were beneath the required contract goals except smoke from Mod III, which was excessive at approach, climb and takeoff. This is shown in Table 6-III which

compares the EPA emissions parameters (EPAP) of each design Mod tested. Emission indices for each design are given in Table 6-IV. The results of the emissions tests of each design modification are presented in the following text.

TABLE 6-III. COMPARISON OF EPA EMISSIONS PARAMETERS—REVERSE FLOW DESIGNS				
Configuration	EPA parameter ($\frac{\text{lb pollutant}}{1000 \text{ hp-hr/cycle}}$)			Maximum smoke
	HC	CO	NO _x	
Conventional design				
501-D22A production	15.0	31.5	6.2	59
Reverse flow - air blast				
Baseline	2.5	5.0	7.8	9
Mod I	0.7	3.5	7.7	8
Mod II	1.3	9.2	6.8	15
Mod III	1.0	5.6	7.4	29
Mod IV	0.3	4.6	7.3	17
Mod II (Repeat)	0.8	6.7	7.2	21
Program goal	3.7	20.1	9.7	22
<div style="border: 1px solid black; display: inline-block; width: 15px; height: 10px; vertical-align: middle;"></div> Exceeds program goal				

Baseline

The baseline was a modified version of the reverse flow industrial engine combustor. The modification enriched the primary zone (equivalence ratio of 0.98). The fuel nozzle was the same airblast type used in the industrial engine. Both the pressure atomizing pilot and the airblast main operate when the combustor is run at the EPA LTO cycle points. The emissions from the baseline design are presented in Table 6-IV, which shows the exhaust emission indices generated at each nodal point in the LTO cycle. Results of the test are also expressed in EPAP and given in Figure 6-1 for comparison with the P2 standard and with the uncontrolled emissions. All emissions were below the program goals which are represented in the figure by a horizontal line.

TABLE 6-IV. SUMMARY OF REVERSE FLOW CONFIGURATION EMISSIONS DATA*

Configuration	Mode	Emissions Index (g/kg fuel)			Smoke
		HC	CO	NO _x	
Baseline	Taxi/idle	2.30	5.51	3.84	3
	Approach	2.09	1.78	6.64	9
	Climbout	0.66	1.00	9.99	9
	Takeoff	0.39	0.95	9.64	9
Mod I	Taxi/idle	0.57	3.65	3.82	5
	Approach	0.52	1.72	6.10	8
	Climbout	0.49	0.95	9.96	7
	Takeoff	0.72	0.90	10.00	8
Mod II	Taxi/idle	1.48	11.50	3.68	7
	Approach	0.46	2.46	5.39	11
	Climbout	0.33	1.11	9.35	14
	Takeoff	0.15	1.12	10.51	12
Mod III	Taxi/idle	0.85	6.16	3.92	3
	Approach	1.07	3.19	5.99	29
	Climbout	0.43	1.14	10.32	25
	Takeoff	0.34	1.11	9.95	26
Mod IV	Taxi/idle	0.18	5.04	3.86	3
	Approach	0.37	2.54	5.70	16
	Climbout	0.26	1.11	10.40	13
	Takeoff	0.14	1.02	10.49	17
Mod II (Repeat)	Taxi/idle	0.91	7.95	3.58	3
	Approach	0.58	2.54	6.26	12
	Climbout	0.13	1.16	10.28	19
	Takeoff	0.15	1.14	10.81	21
*Corrected for sampling error using carbon balance.					

Mod I

In the Mod I tests, the baseline combustor was run with the same baseline industrial airblast fuel nozzle but with no pressure atomizing pilot. The emissions results, shown in Figure 6-2, show an even further reduction in all four pollutants, than that obtained by the baseline design. As in the baseline tests, all emissions were below the program goals.

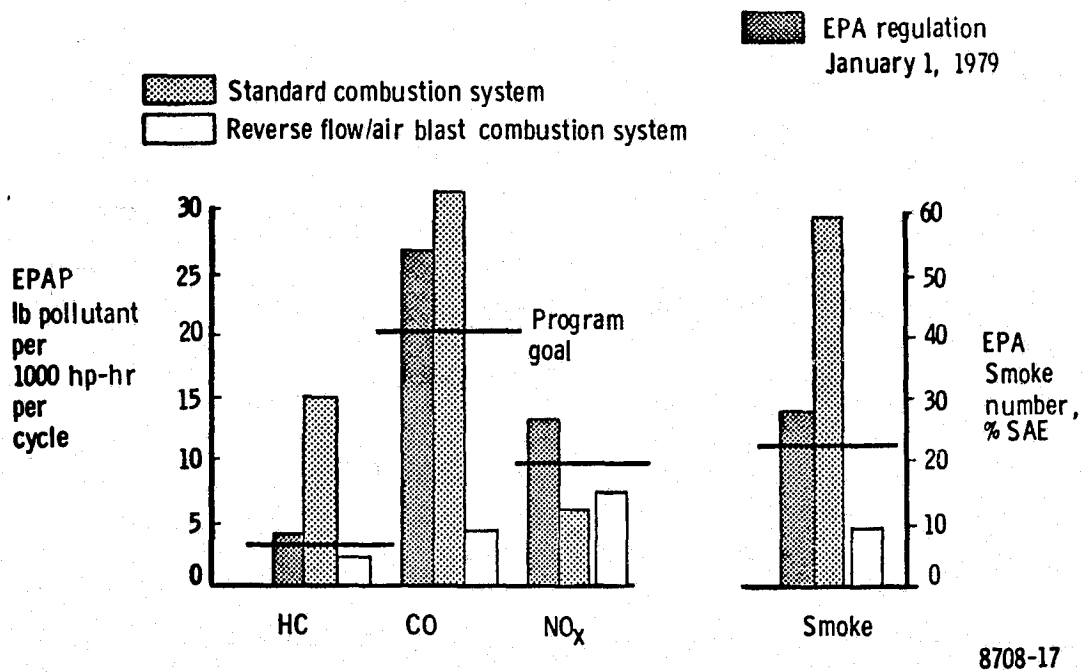


Figure 6-1. Results of combustion rig tests of baseline design reverse flow system.

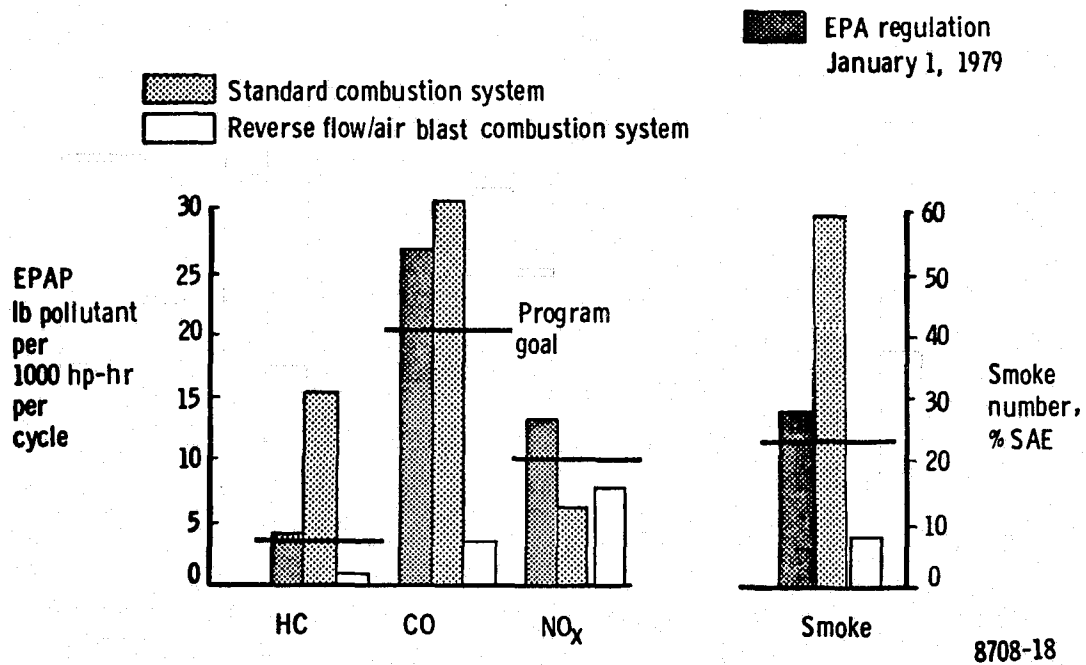


Figure 6-2. Results of combustion rig tests of Mod I design reverse flow system.

Mod II

For Mod II tests, the combustor was changed to increase the air flow in the second reversing baffle by 19%. This reduced the design primary zone equivalence ratio from 0.98 to 0.96. A production model airblast fuel nozzle (industrial engine part with both pilot and main sprays operating) was used for this test. The gaseous emissions were well below the program goals, but not as low as Mod I or the baseline. The smoke number was 15, the same as the baseline and slightly higher than Mod I smoke. The emissions from the Mod II configuration are shown in Figure 6-3.

Mod III

In the Mod III tests the combustor was left the same as Mod II but the fuel nozzle was changed to an air assist design. In this design external air under pressure is fed into the cavity in the nozzle. The air assists in atomizing the fuel by forcing it out of the orifice. At low nozzle pressures (idle operation) the effects are pronounced because the air supplies an appreciable amount of the energy used in atomizing the fuel. At high nozzle pressures (and flows) the fuel breakup is already good and the atomization effects of air assist are much less pronounced. Based on flow bench visual observations simulating idle, air assist pressures of zero, 6.75, 10.1, and 13.5 N/cm² were used for the testing. Without air assist, the fuel spray is a 1.571 radian hollow cone. The nozzle flow number is .00115.

Emissions from Mod III are shown in Figure 6-4. The lowest values of EI and EPAP were obtained at highest fuel nozzle air pressure (13.5 N/cm²) and these lowest values are the ones shown in Figure 6-4. The effect of various fuel nozzle air assist pressures on idle emissions is shown in Figure 6-5. During the tests idle combustor inlet conditions were maintained and fuel flow and nozzle air pressure were varied. The Mod III configuration passed all program goals except smoke which was excessive at approach, climbout and takeoff.

Mod IV

In the Mod IV series of tests the combustor was again left unmodified but the fuel nozzle was changed to the industrial design airblast without a pilot. This is the same fuel nozzle as was tested in Mod I.

The emissions from the tests of the Mod IV configuration are shown in Figure 6-6. All emissions were below the program goals.

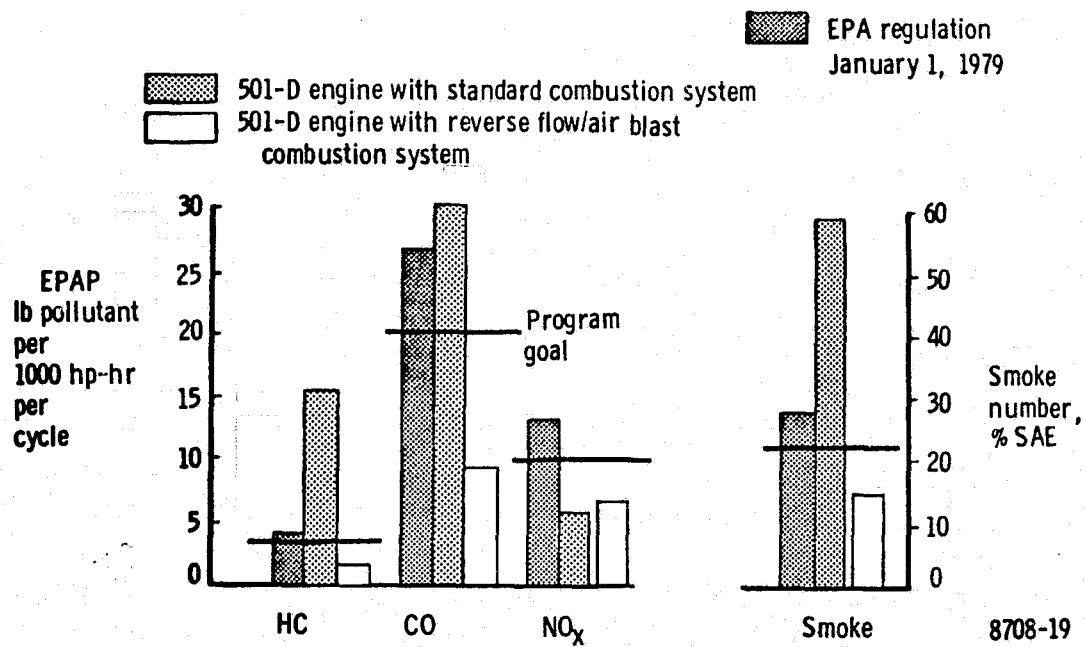
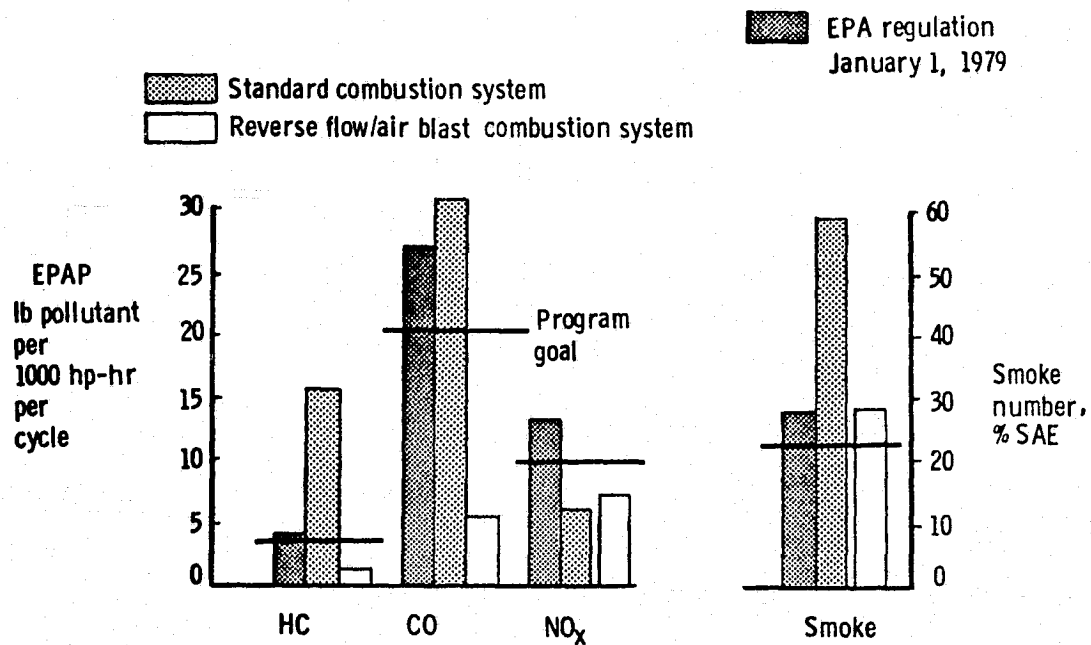


Figure 6-3. Results of combustion rig tests of Mod II design reverse flow system.



8708-20

Figure 6-4. Results of combustion rig tests of Mod III design reverse flow system.

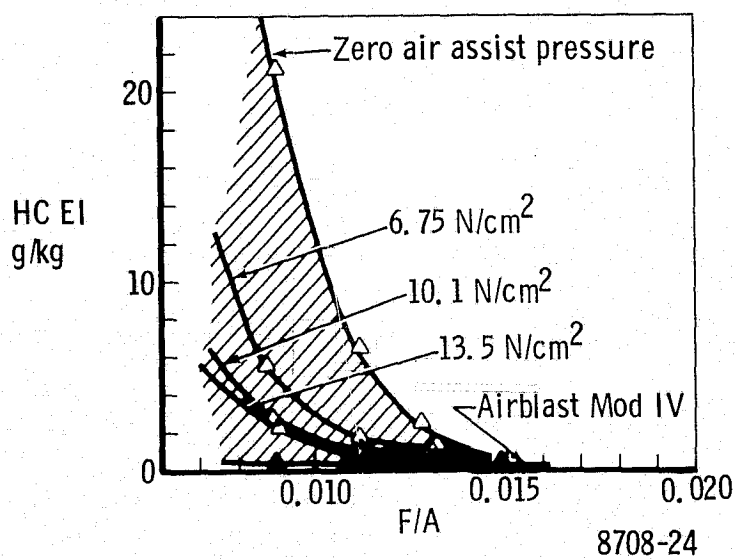
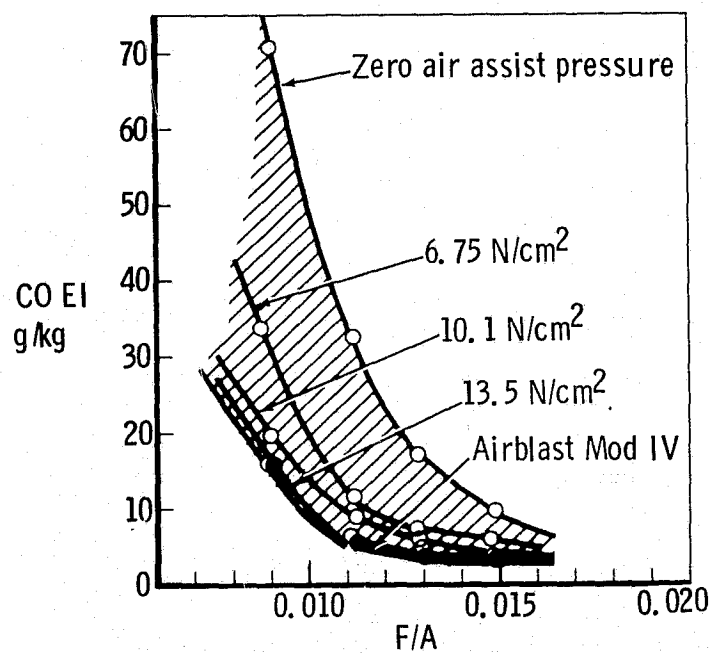
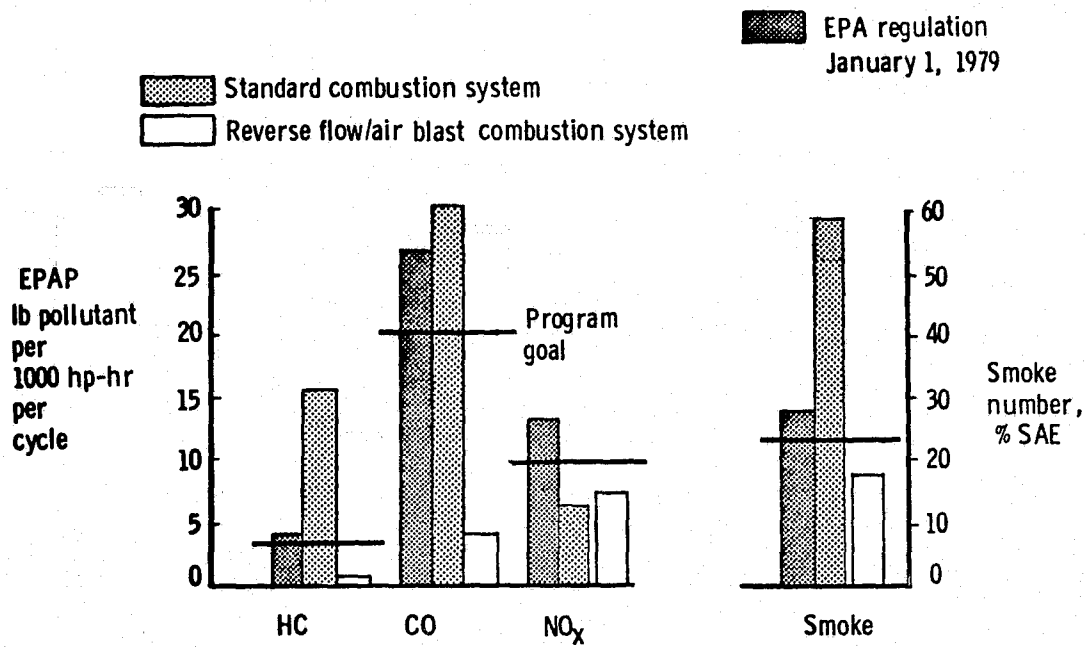


Figure 6-5. Effect of air assist fuel nozzle air pressure on Mod III idle emissions.



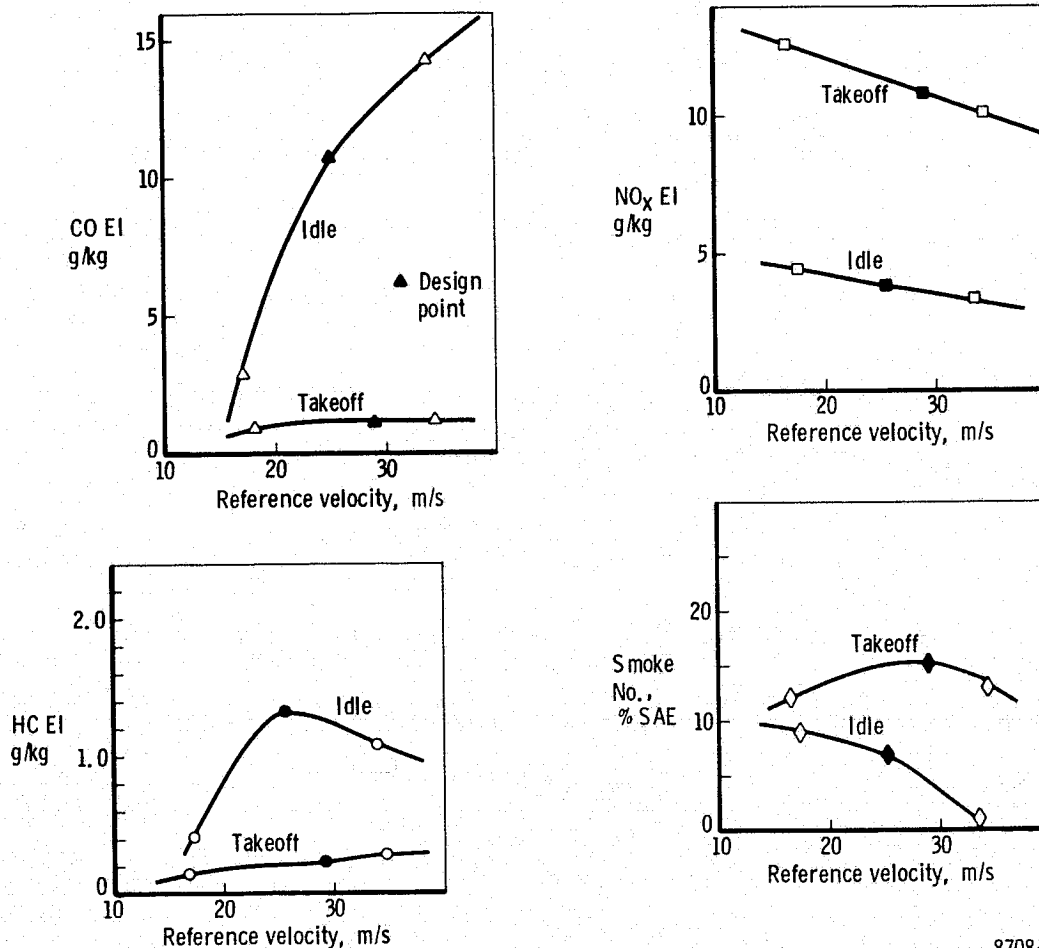
8708-21

Figure 6-6. Results of combustion rig tests of Mod IV design reverse flow system.

Parametric Tests

During all test series, the effects of changes in fuel flow at both idle and takeoff conditions were evaluated. Trends in HC and CO emissions at idle with changes in fuel flow are typified by the curves shown in Figure 6-5. Oxides of nitrogen emissions, not shown, increased slightly with increasing fuel flow.

Variations in combustor reference velocity, and in inlet temperature and pressure were also evaluated on Mod II, III and IV. Figures 6-7 and 6-8 are typical. They show how the variations in reference velocity and inlet temperature effected the emissions from the Mod II design. Pressure changes had little apparent effect on emissions and therefore were not shown.



8708-25

Figure 6-7. Mod II parametric test, effect of liner velocity on emissions.

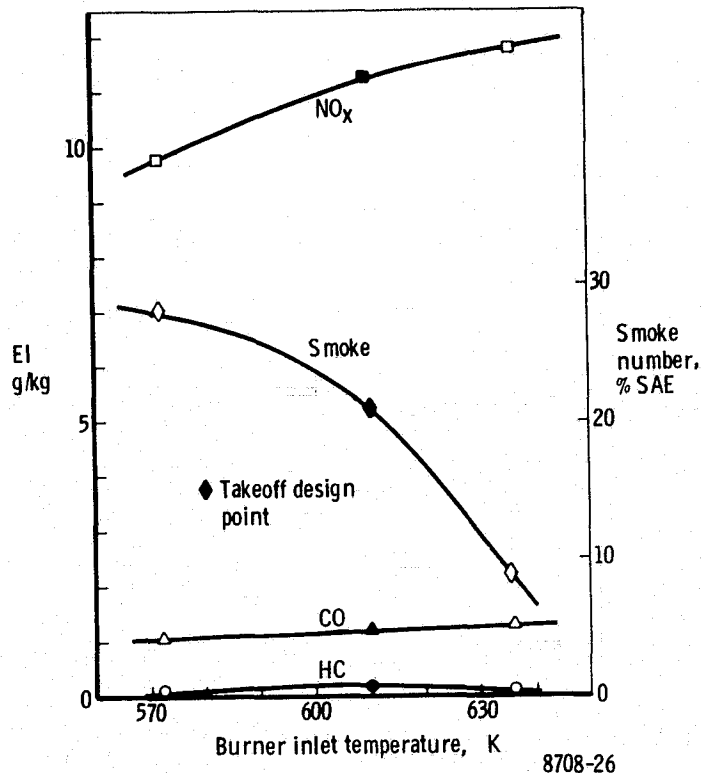


Figure 6-8. Mod II parametric test, effect of inlet temperature on emissions.

Combustor Wall Temperatures

Combustor wall temperatures were measured continuously during the testing at four locations on the external surface which were predicted to run hot. These locations were numbered as follows:

1. The uncooled section between the forward and aft acting part of the second reversing baffle
2. Just forward of the second cooling corrugation
3. The liner to transition butt weld
4. Aft on the underneath side of the transition

The locations of the skin temperature thermocouples are shown in Figure 6-9.

Results of the skin temperature measurements were consistent throughout the entire test series. They were highest at takeoff and lowest at idle. At

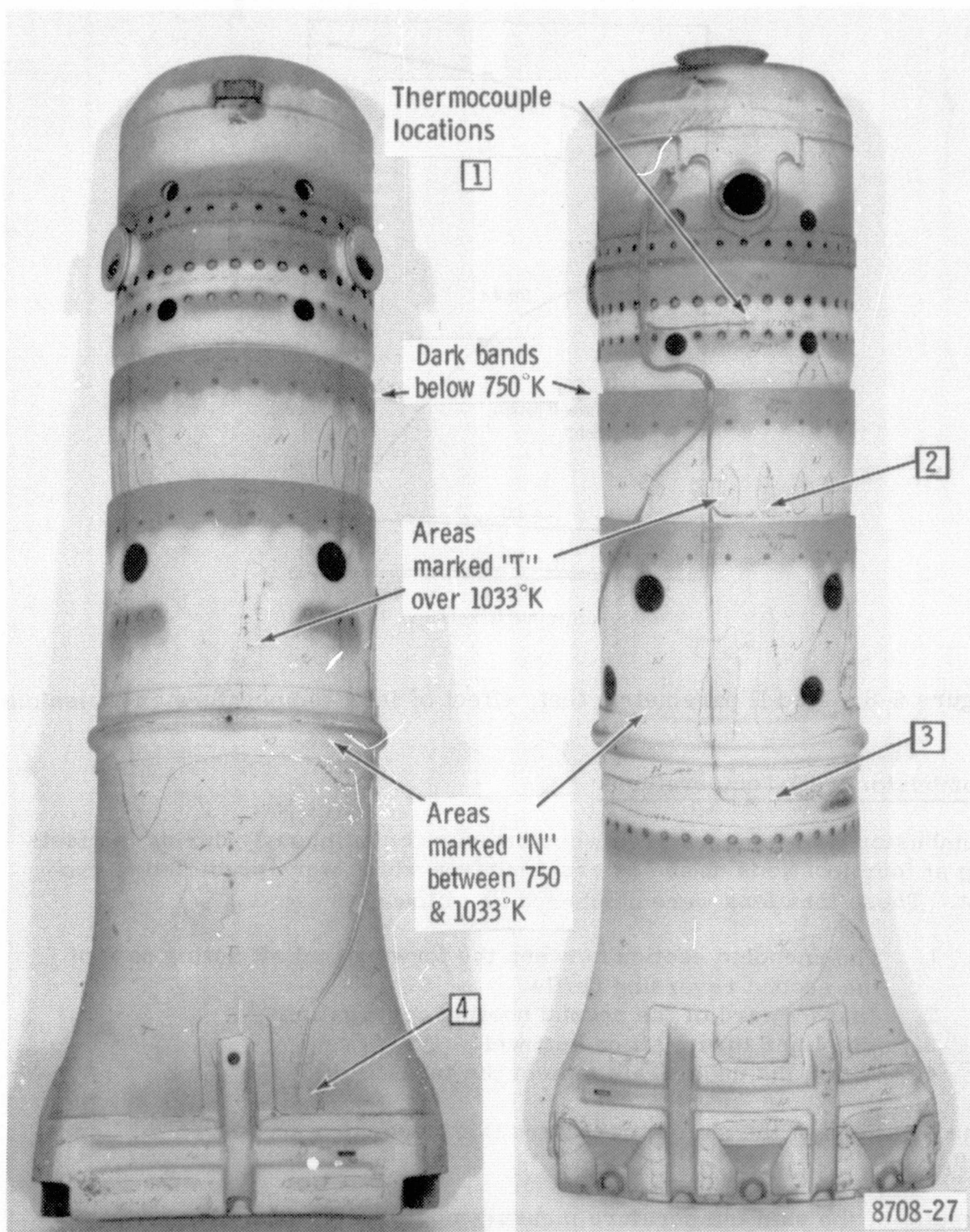


Figure 6-9. Thermal paint markings, Mod IV combustor.

takeoff the lowest temperatures were located at the baffle, No. 1 location, and proceeding aft they became progressively higher. The highest temperatures therefore were observed at the transition, No. 4 location. These are given in summary Table 6-V.

TABLE 6-V. REVERSE FLOW COMBUSTION SYSTEM, TAKEOFF DESIGN POINT PERFORMANCE SUMMARY				
Configuration	Maximum skin temp (transition) (K)	Combustor outlet temp pattern $\left(\frac{T_{\max} - T_{\text{avg}}}{T_{\text{avg}} - T_{\text{inlet}}}\right)$	Combustor pressure loss (%)	Combustor efficiency (%)
Production	*	0.18	5.12	99.87
Baseline	1134	0.19	5.17	99.87
Mod I	1138	0.17	5.18	99.86
Mod II	1132	0.15	5.64	99.88
Mod III	1154	0.18	5.73	99.88
Mod IV	1152	0.11	5.19	99.90
Mod II Repeat	1142	0.15	5.31	99.89
*Thermocouple failure				

Mod IV testing also included running the combustion liner with the outer skin painted with temperature sensitive paint. After the run, the color patterns in the paint were analyzed and the isotherms marked on the liner. Figure 6-9 shows the color bands and isotherm markings.

Outlet Temperature Pattern

The combustor outlet temperature pattern was measured by a 28-thermocouple matrix, and from this pattern factor was computed. Combustor outlet temperature pattern factors at takeoff are shown in Summary Table 6-V. All configurations produced acceptable pattern factors.

Altitude Ignition Performance

The reverse flow Mod IV configuration was tested for stability by measuring the lean-blowout fuel flow for several flow and altitude pressure conditions at ambient inlet temperature. The results are presented in Figure 6-10 in the form of blowout fuel/air ratio versus reaction rate parameter, θ .

where $\theta = \frac{P^{1.75} A_r D e^{T/b}}{W_a}$

- P = combustor inlet pressure, Pa
 A_r = combustor reference area, m^2
 D = combustor diameter, m
 T = inlet temperature, K
 b = 300 for stoichiometric primary zone
 W_a = combustor airflow, kg/s
 e = natural logarithm base

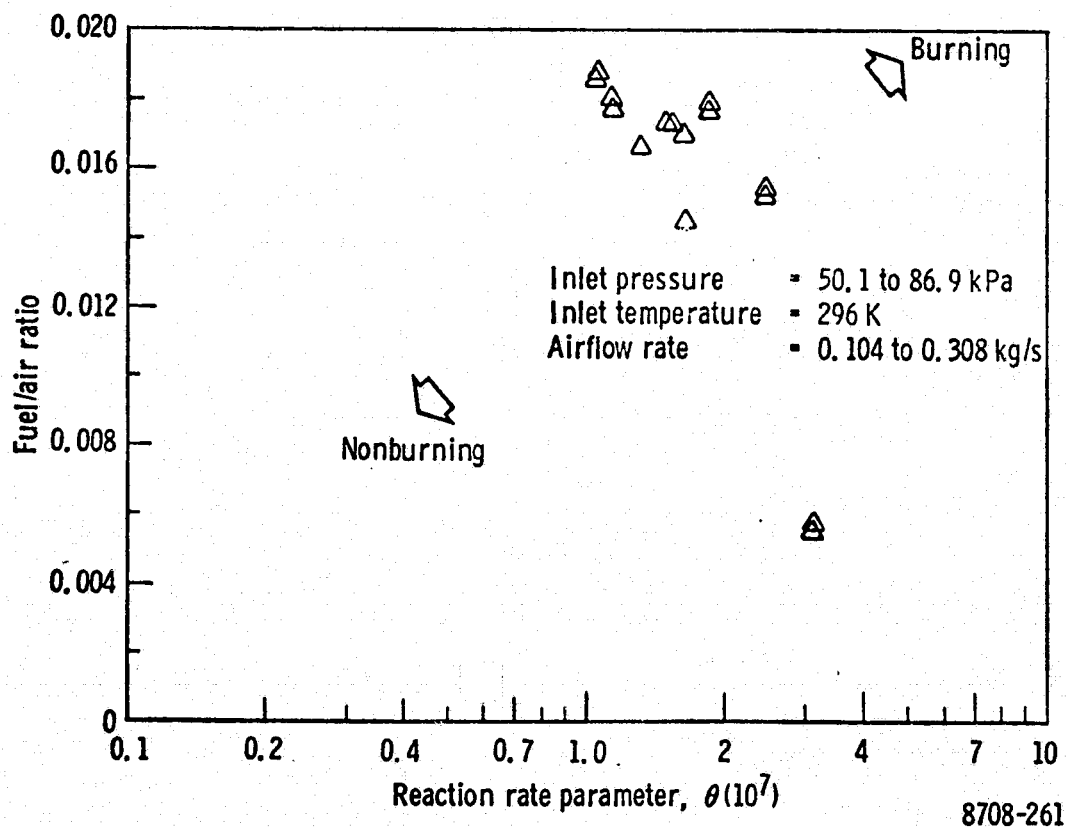


Figure 6-10. Reverse flow Mod IV combustor lean-blowout results.

The combustion stability data are limited to the testing of one configuration of each combustor type. The improvement of stability is beyond the scope of this program.

PRECHAMBER

Extensive testing was accomplished to survey various combinations of variable geometry setting. The results of the optimized geometry settings are presented herein. The emissions are computed for the EPA-LTO cycle. These results are expressed as EPA Parameter Values, and they are compared to program goals and to the production liner emissions in Table 6-VI.

TABLE 6-VI. PRECHAMBER COMBUSTOR EMISSION RESULTS

	Total hydrocarbons lb/1000 hp-hr/cycle	Carbon monoxide lb/1000 hp-hr/cycle	Oxides of nitrogen lb/1000 hp-hr/cycle	Maximum SAE smoke No.
EPA Limits—Class P2	4.9	26.8	12.9	29
Program goals				
75% of Class P2	3.7	20.1	9.7	22
Production liner	15.0	31.5	6.2	55
Prechamber baseline (extrapolated results)	1.58	3.99	6.10	1
Prechamber Mod I	2.27	21.67	6.53	52
Prechamber Mod II	0.85	37.49	6.40	29
Prechamber Mod III	0.39	2.05	8.50	1
Prechamber Mod IV	0.27	4.83	7.93	1
Prechamber Mod V	0.20	4.71	6.39	5

The measured pressure drop of each prechamber configuration for each of the EPA-LTO cycle points is compared to the measured pressure drop for the production liner in Table 6-VII.

TABLE 6-VII. PRECHAMBER COMBUSTOR
PRESSURE LOSS* (%)

	Idle	Approach	Climbout	Takeoff
Production Liner	4.91	6.49	5.76	5.12
Prechamber Baseline	6.33	8.05	-	-
Prechamber Mod I	4.84	6.51	4.08	4.08
Prechamber Mod II	5.14	7.40	5.14	4.81
Prechamber Mod III	6.05	8.24	5.21	5.34
Prechamber Mod IV	7.02	8.95	6.23	6.24
Prechamber Mod V	8.38	11.23	8.49	7.30

*Includes diffuser loss

The combustion efficiency calculated from exhaust gas analysis is compared for the prechamber configurations and the production liner in Table 6-VIII.

The measured pattern factor for the prechamber combustors and the production liner is compared in Table 6-IX.

TABLE 6-VIII. MEASURED PRECHAMBER COMBUSTION EFFICIENCY (%)				
	Idle	Approach	Climbout	Takeoff
Production Liner	97.4	99.7	99.8	99.9
Prechamber Baseline	99.9	99.3	-	-
Prechamber Mod I	99.2	99.4	99.9	99.9
Prechamber Mod II	98.0	99.3	99.9	99.9
Prechamber Mod III	99.9	99.9	99.9	99.9
Prechamber Mod IV	99.9	99.5	99.9	99.9
Prechamber Mod V	99.9	99.7	99.9	99.9

TABLE 6-IX. PRECHAMBER COMBUSTORS MEASURED PATTERN FACTOR, $\frac{T_{\max} - T_{\text{avg}}}{T_{\text{avg}} - T_{\text{in}}}$				
	Idle	Approach	Climbout	Takeoff
Production Liner	0.15	0.16	0.20	0.18
Prechamber Baseline	0.14	0.18	-	-
Prechamber Mod I	0.13	0.11	0.11	0.11
Prechamber Mod II	0.19	0.18	0.14	0.10
Prechamber Mod III	0.16	0.13	0.15	0.14
Prechamber Mod IV	0.11	0.12	0.13	0.12
Prechamber Mod V	0.16	0.16	0.16	0.17

The stability of idle emissions at a range of F/A ratios for the short prechamber configurations is presented in Figures 6-11 through 6-14. The effect of F/A ratio on the emission of the short prechamber liners at

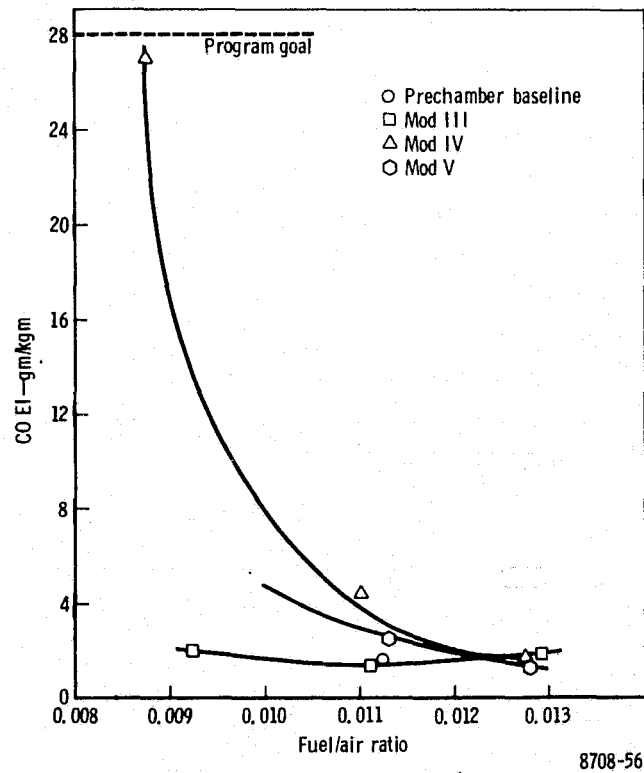


Figure 6-11. Short prechamber combustors—CO emissions at idle.

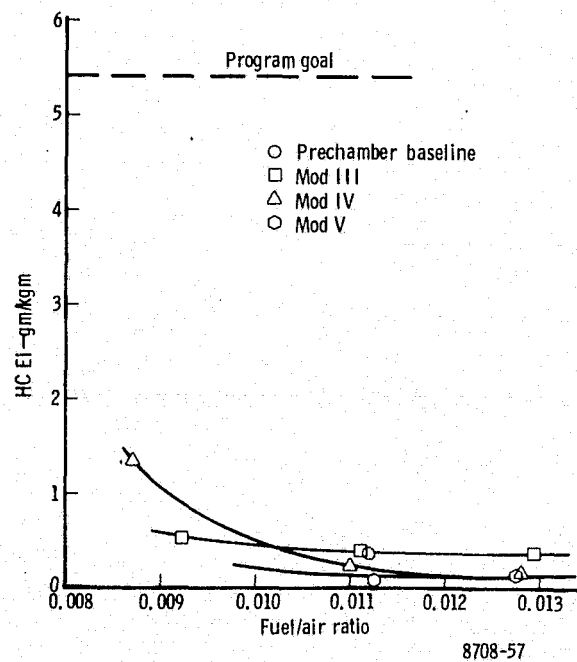


Figure 6-12. Short prechamber combustors—HC emissions at idle.

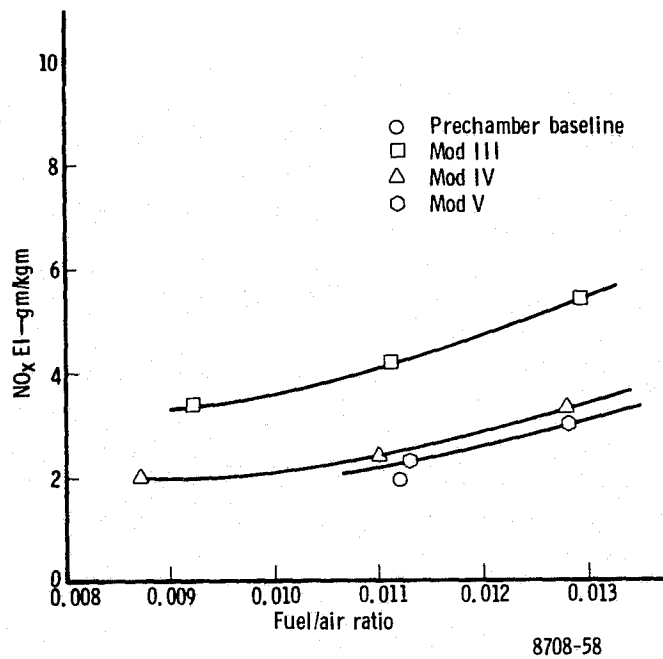


Figure 6-13. Short prechamber combustors—NO_x emissions at idle.

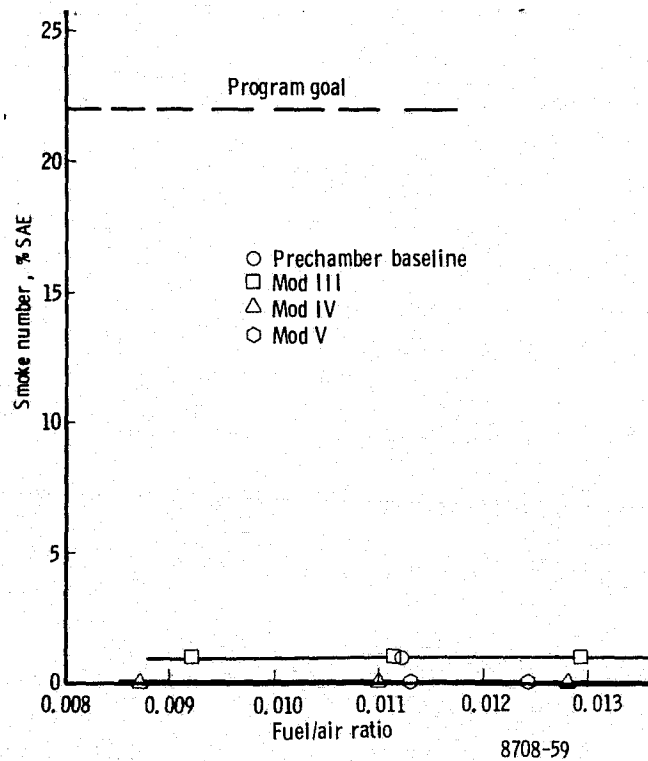


Figure 6-14. Short prechamber combustors—Smoke emissions at idle.

T.O. flow conditions is shown in Figures 6-15 through 6-18. An inadvertent rig shutdown, after idle data were taken for the Prechamber Baseline, caused the fuel nozzle to remain for a period of time, unpurged of fuel, at high burner inlet temperature. This caused the fuel nozzle valve to stick and limited max fuel flow from the nozzle at 29.5 kg/hr (65 lb/hr). The remainder of the fuel was injected as wall film. This was an off design condition and a small fuel leak was also found in the wall film feed line external to the burner. Therefore, the Baseline Prechamber takeoff data are not presented.

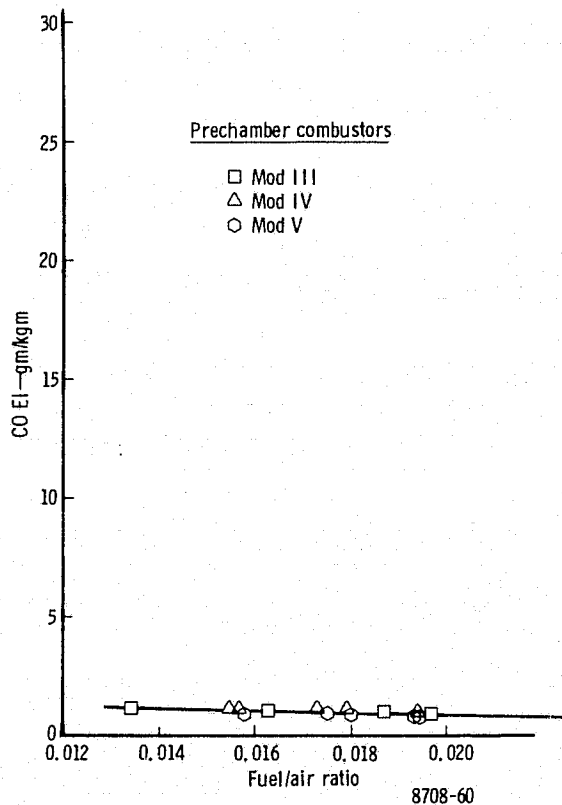


Figure 6-15. Short prechamber combustors—CO emissions at takeoff.

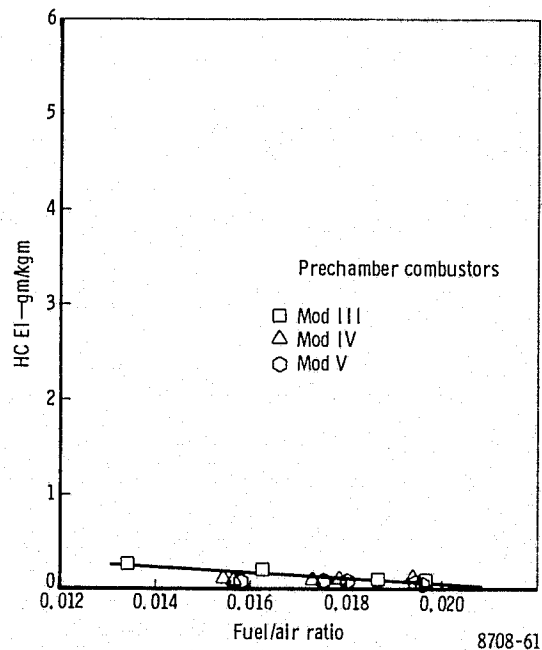
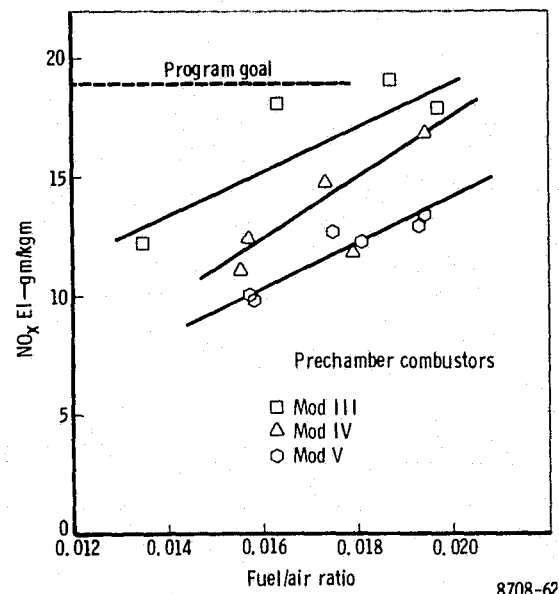
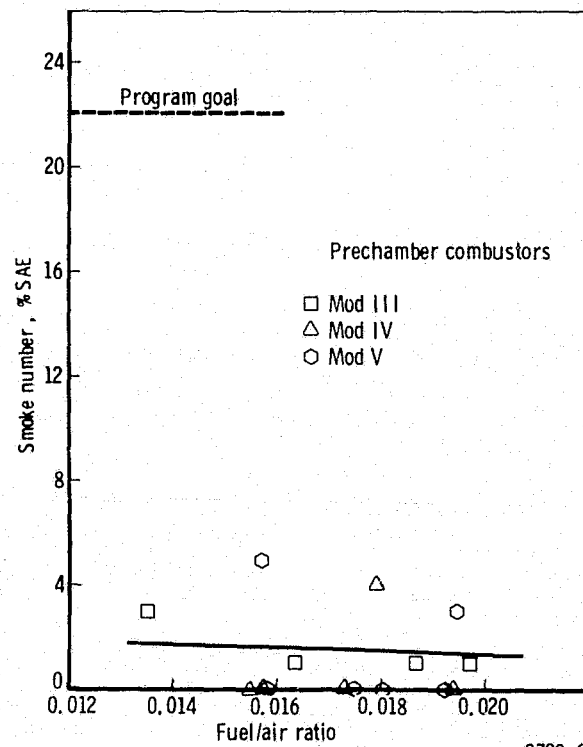


Figure 6-16. Short prechamber combustors—HC emissions at takeoff.



8708-62

Figure 6-17. Short prechamber combustors— NO_x emissions at takeoff.



8708-63

Figure 6-18. Short prechamber combustors—smoke emissions at takeoff.

The sensitivity of the idle emissions of the long prechamber configurations are shown in Figures 6-19 through 6-26. The emissions for a reference velocity parametric point are also included. The velocity parametric was achieved by reducing the burner inlet airflow while maintaining the other inlet conditions. The purpose of the velocity parametric was to simulate a longer residence time that would be obtained with a longer prechamber. Emissions data for takeoff flow conditions for Mods I and II are presented in Figures 6-27 through 6-34 vs F/A ratio.

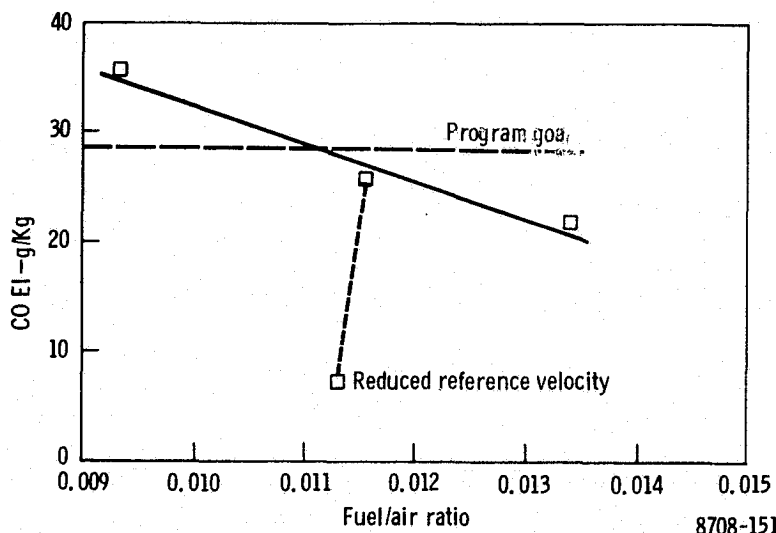


Figure 6-19. Prechamber Mod I—CO emissions at idle.

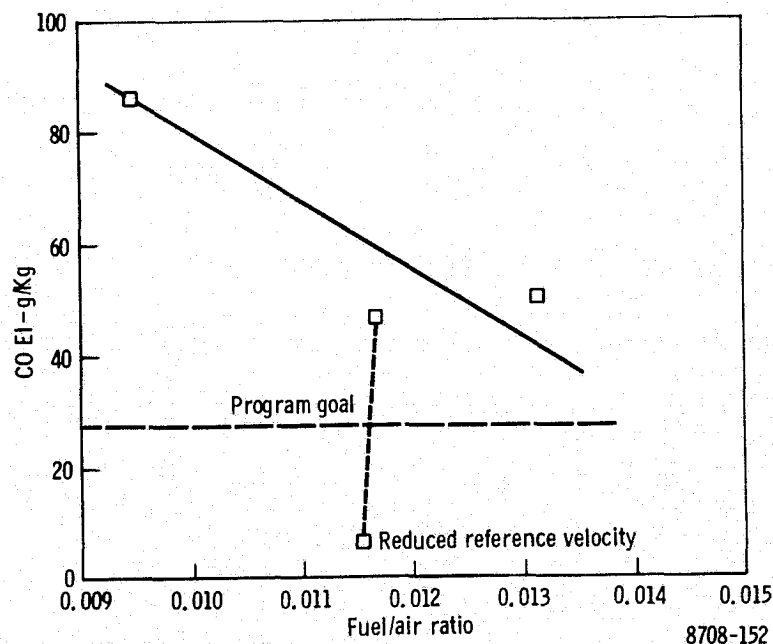


Figure 6-20. Prechamber Mod II—CO emissions at idle.

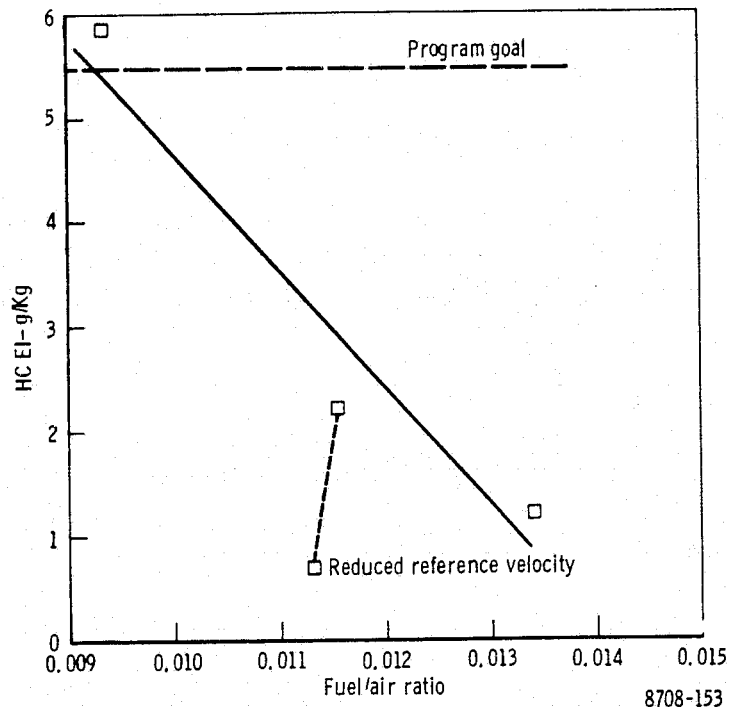


Figure 6-21. Prechamber Mod I—HC emission at idle.

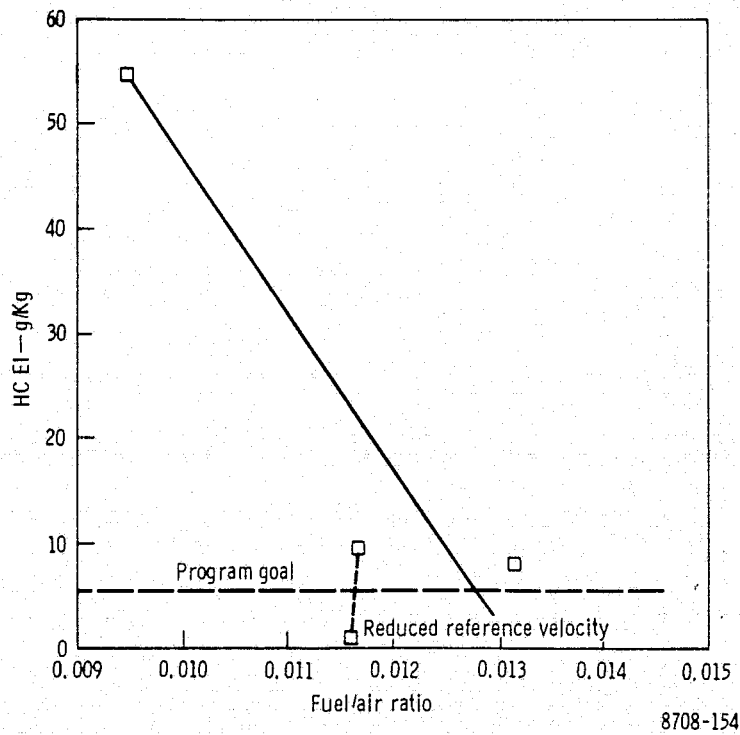


Figure 6-22. Prechamber Mod II—HC emissions at idle.

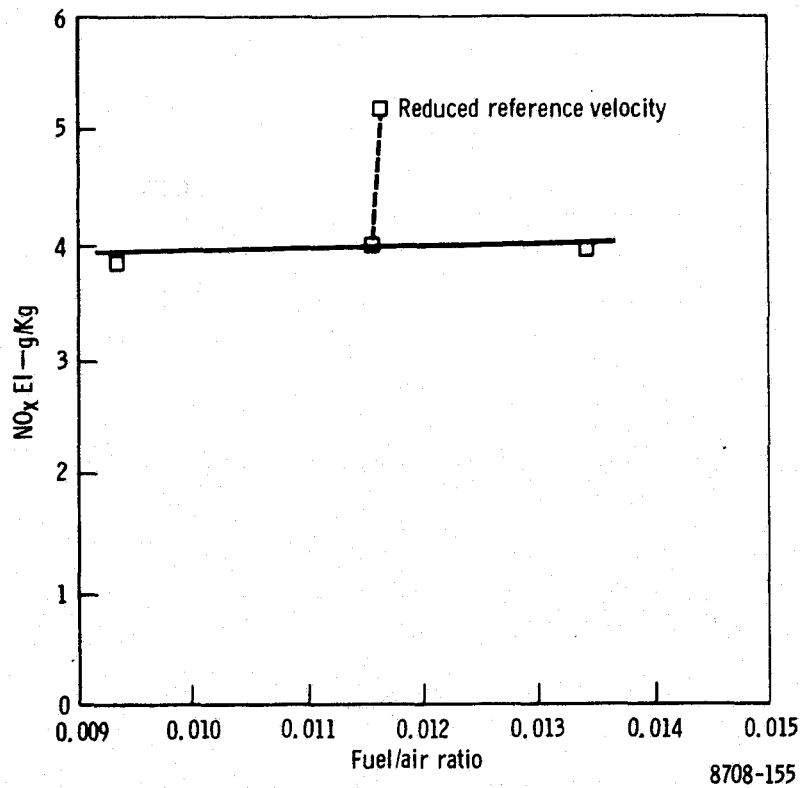


Figure 6-23. Prechamber Mod I-NO_x emissions at idle.

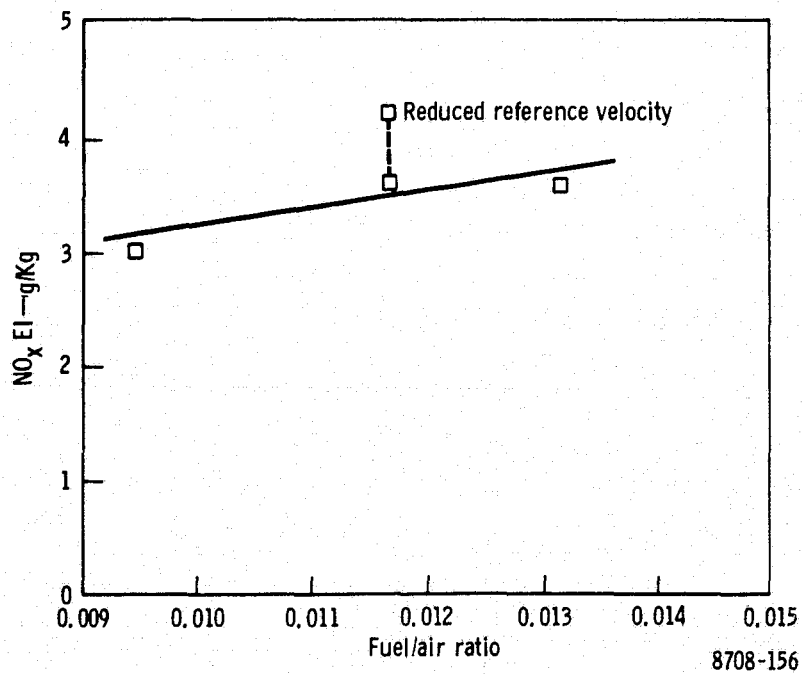


Figure 6-24. Prechamber Mod II-NO_x emissions at idle.

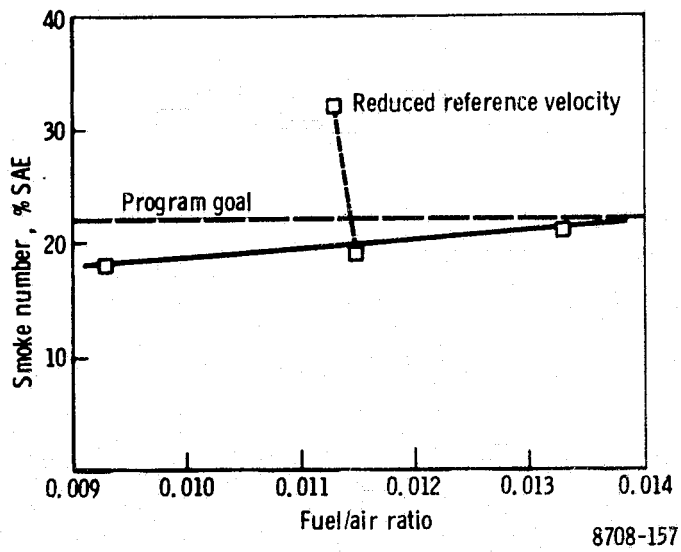


Figure 6-25. Prechamber Mod I—smoke emissions at idle.

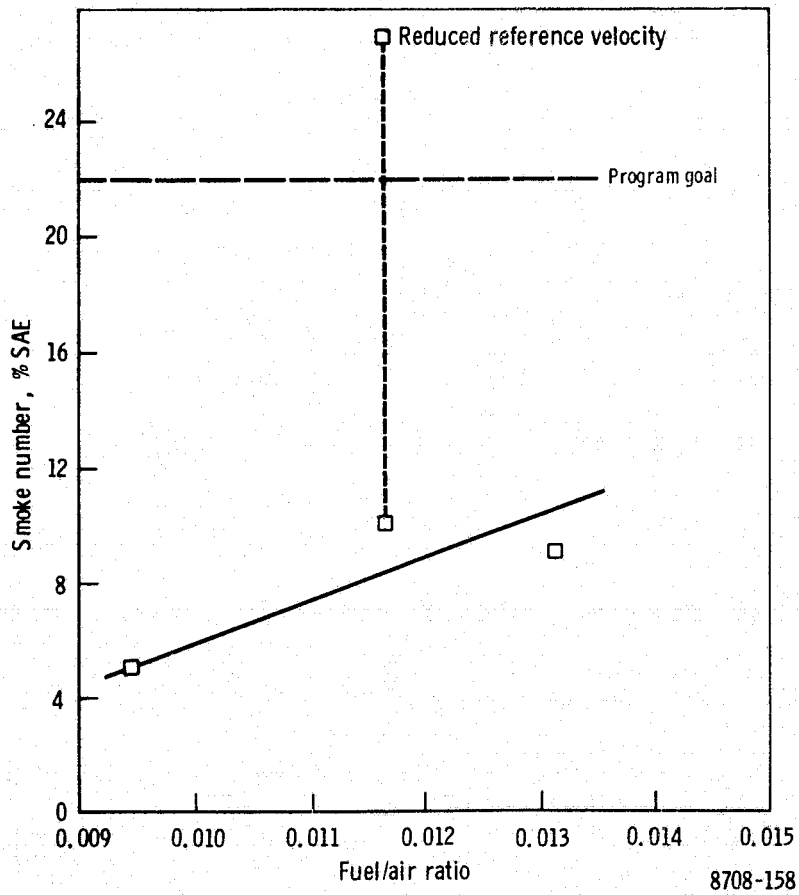


Figure 6-26. Prechamber Mod II—smoke emissions at idle.

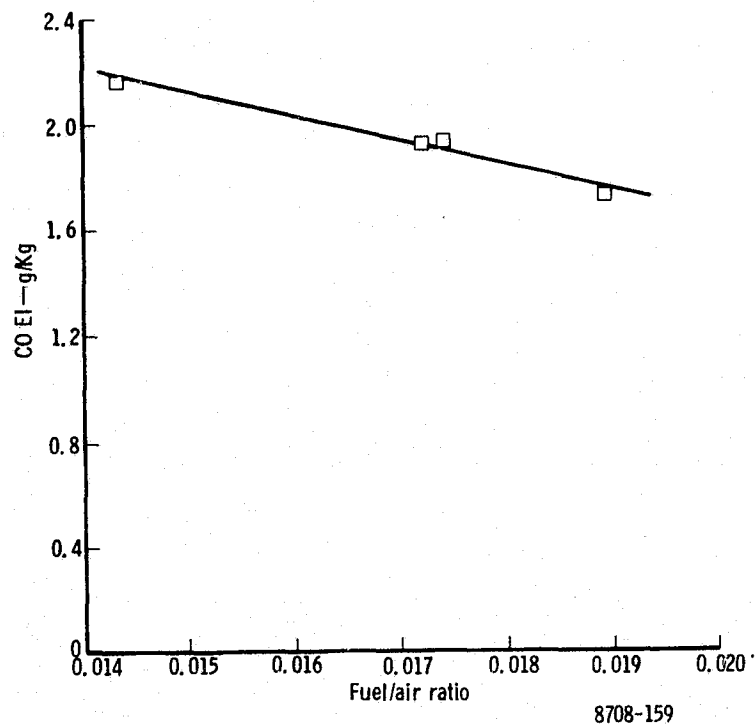


Figure 6-27. Prechamber Mod I—CO emissions at takeoff.

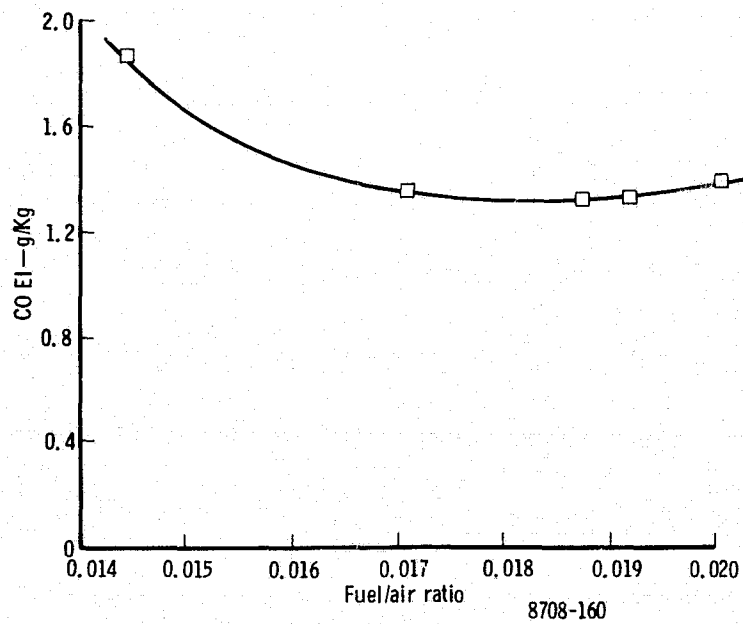


Figure 6-28. Prechamber Mod II—CO emissions at takeoff.

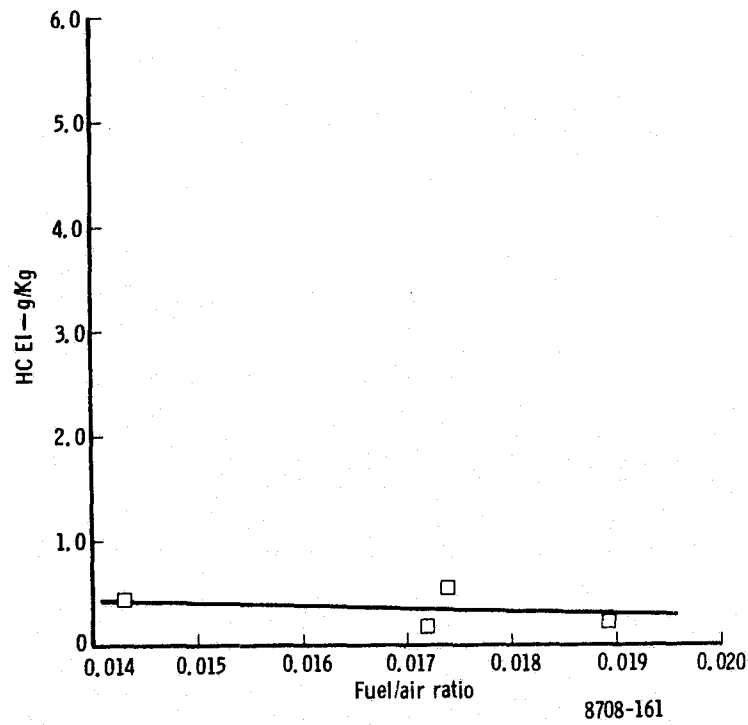


Figure 6-29. Prechamber Mod I—HC emissions at takeoff.

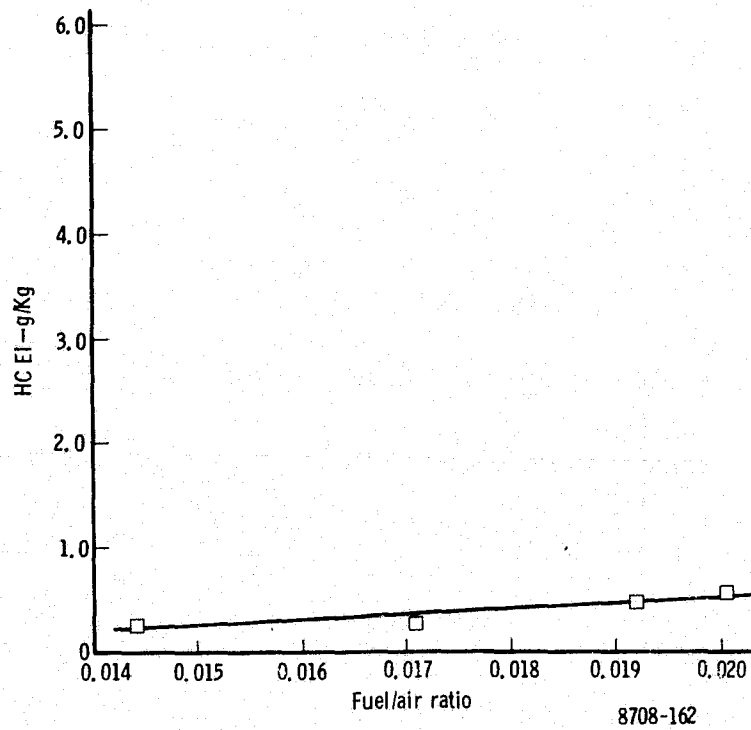


Figure 6-30. Prechamber Mod II—HC emissions at takeoff.

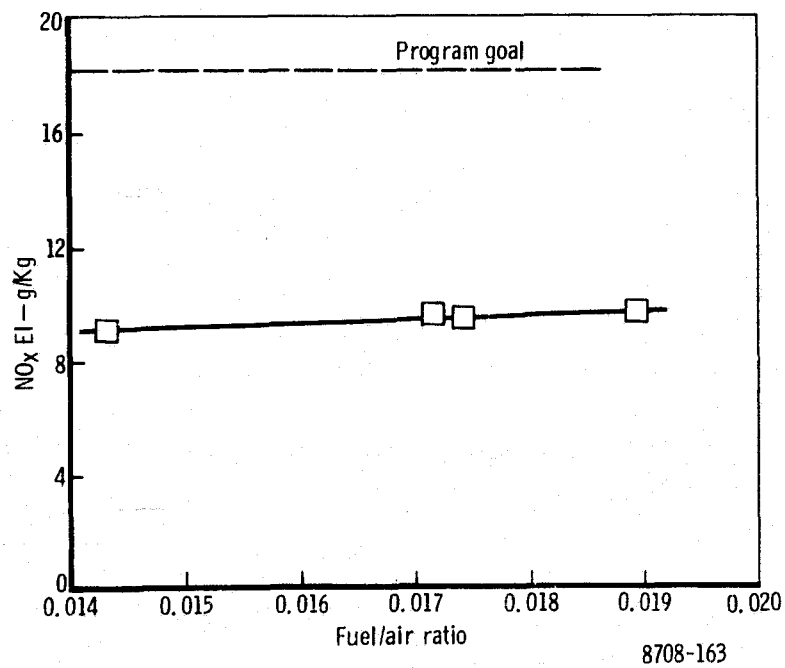


Figure 6-31. Prechamber Mod I—NO_x emissions at takeoff.

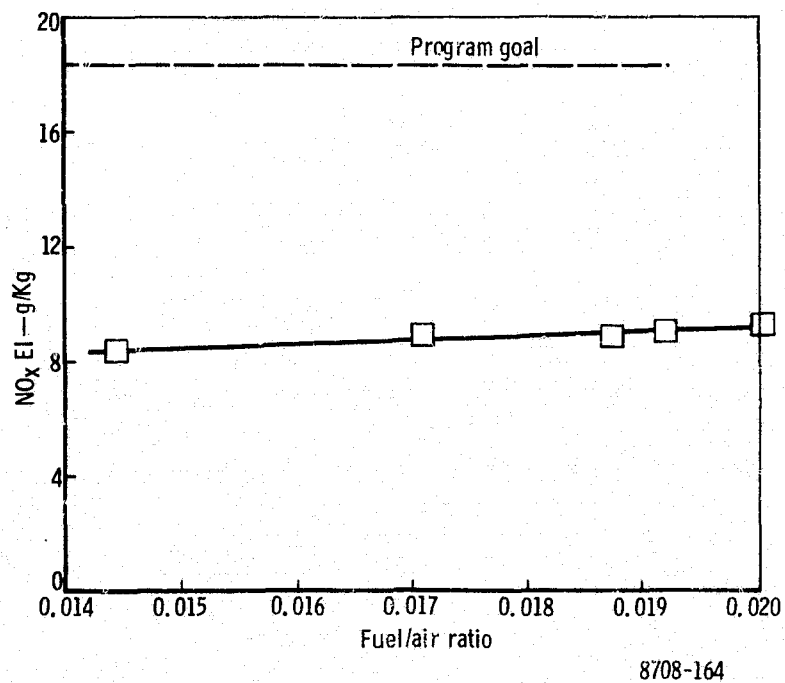


Figure 6-32. Prechamber Mod II—NO_x emissions at takeoff.

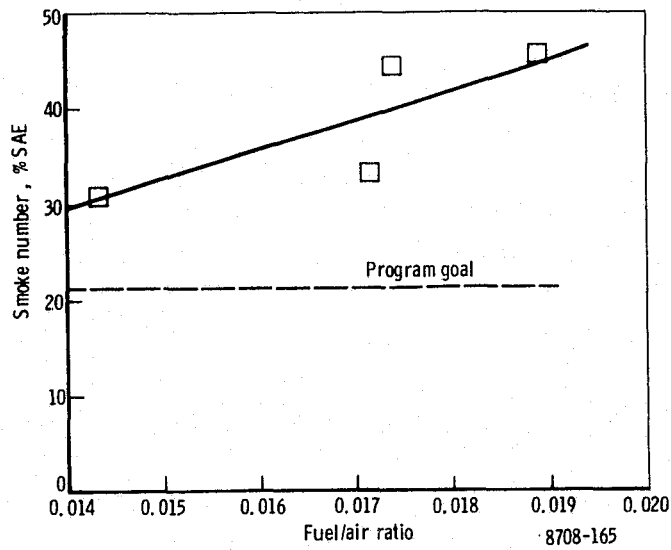


Figure 6-33. Prechamber Mod I—smoke emissions at takeoff.

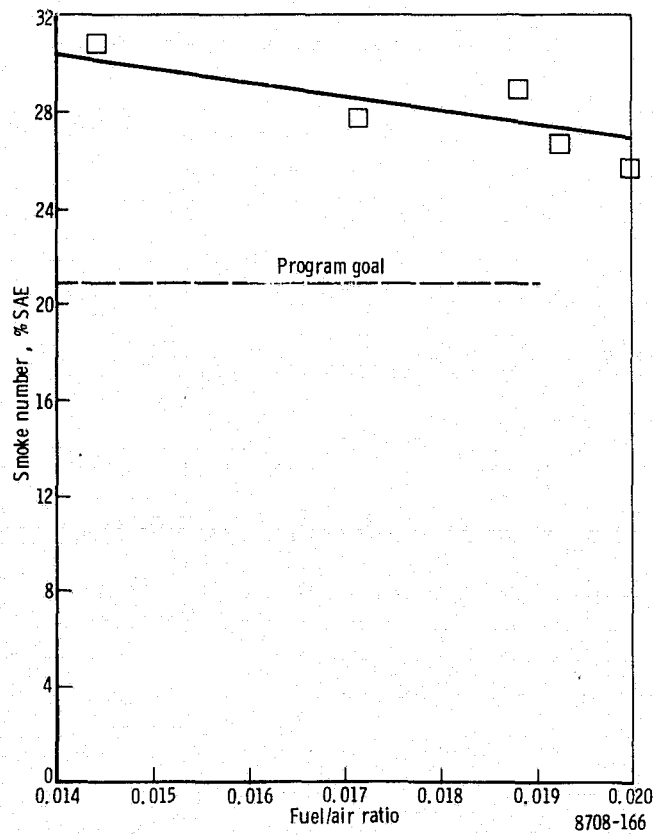


Figure 6-34. Prechamber Mod II—smoke emissions at takeoff.

During the Baseline Prechamber test, a thermocouple between the forward and reverse cooling air baffles (Figure 6-35) measured a temperature of 1205 K at 0.0135 F/A. A substantial redesign would have been required to reduce these temperatures to a level that would provide durability in commercial service. A major redesign, in turn, would have had a severe impact on the program from schedule as well as cost considerations. Therefore, a series of small effusion holes were put in the hot area as a short-term fix to facilitate testing. Figure 6-36 shows the Baseline Prechamber which was run without the cooling holes, and Figure 6-37 shows the Prechamber Mod III with the effusion cooling holes. Although this fix permitted the completion of all testing, thermal paint results from Prechamber Mod V (Figures 6-38 and 6-39) indicate that this area as well as the liner wall in the vicinity of the intermediate holes needs further development of skin cooling.

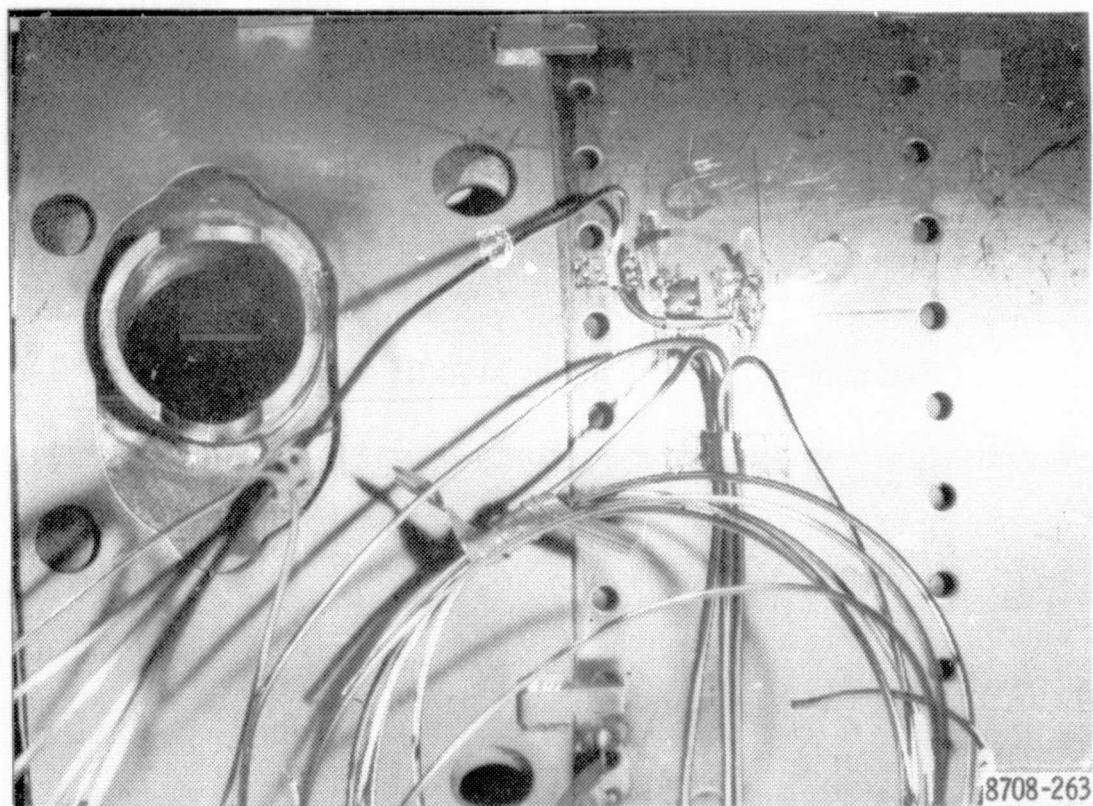


Figure 6-35. Baseline Prechamber combustor—hot spot thermocouple location.

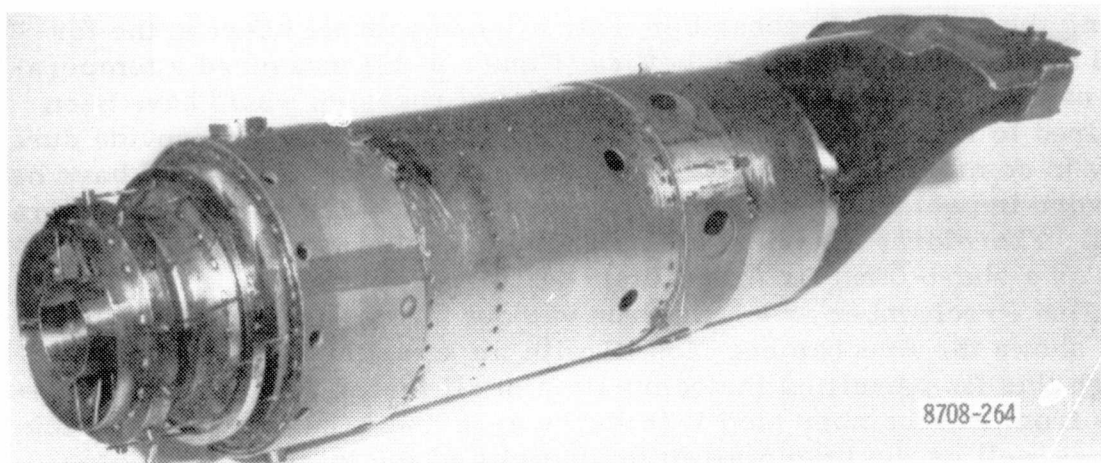


Figure 6-36. Baseline Prechamber combustor.

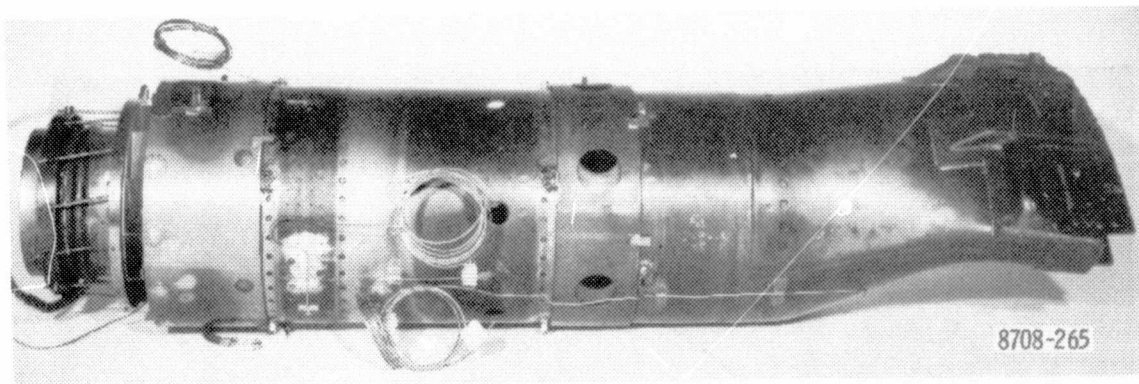


Figure 6-37. Prechamber Mod III combustor.

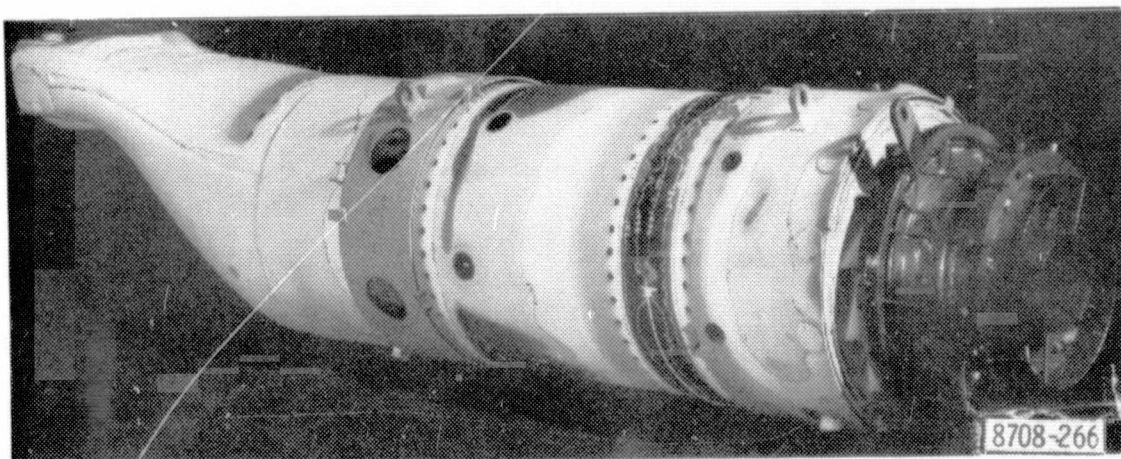


Figure 6-38. Prechamber Mod V—thermal paint results (left side).

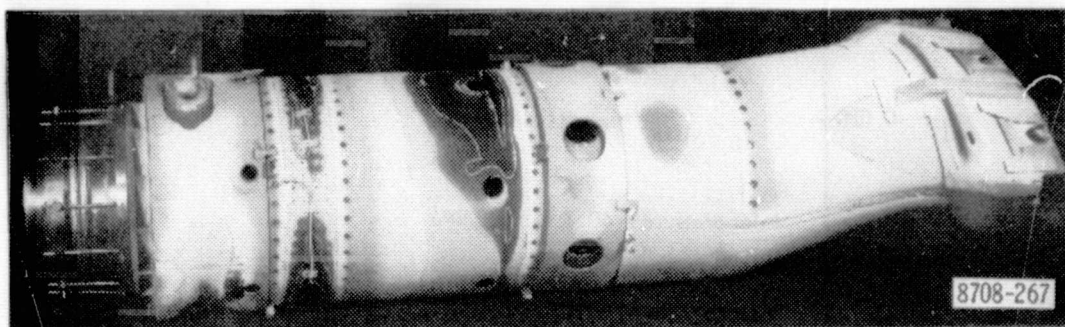


Figure 6-39. Prechamber Mod V—thermal paint results (right side).

The Prechamber Mod V design was tested for altitude ignition potential. Lean-blowout fuel/air ratio was measured at different altitude pressure levels and airflow rates. At an early test point, combustion was stable at approximately 3.6 kg/hr (8 lb/hr) fuel flow. Unfortunately, the fuel nozzle was not designed for this low flow rate. Subsequent analysis indicated that the poor fuel atomization at low fuel flows resulted in local burning of the combustor wall in the bottom position under the primary zone variable geometry band. Because of this poor fuel nozzle performance, at or near 83 K (150°F) ΔT altitude relight conditions, and because of the physical damage to the liner, the results of this portion of the testing were not conclusive.

These data are not indicative of combustion liner performance but, rather, of the limitations of the fuel nozzle which was used. Further development of the fuel nozzle to operate at this condition would be required to determine the true liner performance at this condition.

The data points from this testing are plotted in Figure 6-40.

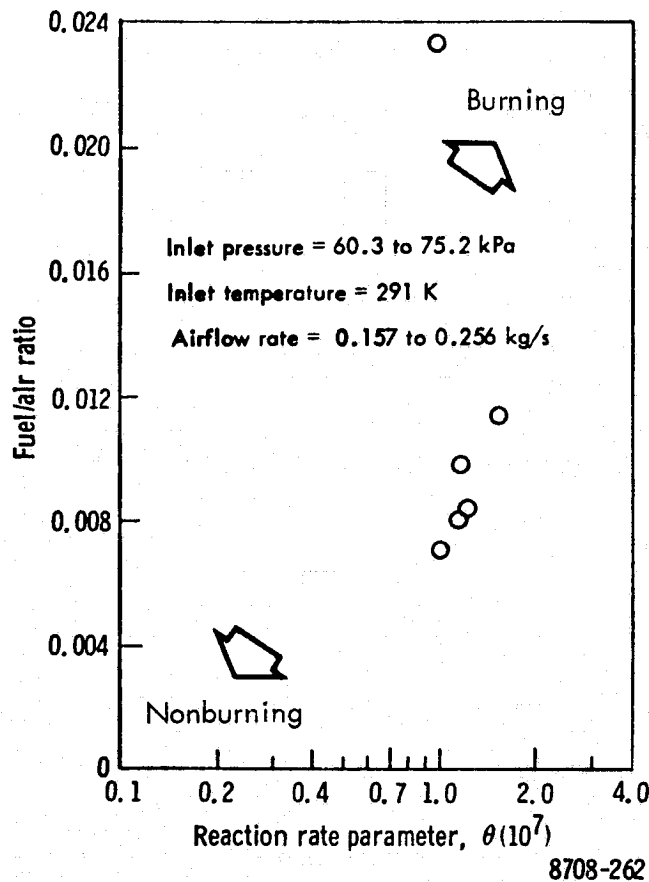


Figure 6-40. Prechamber combustor low-pressure blowout results.

STAGED FUEL COMBUSTOR

EPA Parameter (EPAP) Results

A large amount of data (145 data points) was obtained in tests of the staged fuel combustor. Emissions testing was accomplished at the four basic engine operating conditions of the LTO cycle, idle, approach, climbout, and takeoff. Parametric data were also obtained for fuel/air ratio, and combustor reference velocity. The staged fuel combustors were capable of being operated at various pilot-to-main fuel splits, and with various airflow splits as determined by the variable geometry (VG) settings. Data were obtained for only a limited number of VG settings and pilot-to-main fuel splits to indicate emission trends. This emission mapping was by no

means completed because of the large number of variables involved. The staged fuel configurations for which EPAP values were obtained are summarized in Table 6-X. The baseline combustor and Mods I through IV employed the original combustor design but with various pilot fuel injectors. The Mod V and VI configurations employed a new combustor design with an airblast pilot fuel injector. All EPA parameter (EPAP) values were computed based upon fixed-geometry data. The fuel flow split was allowed to vary to obtain low EPAP values.

TABLE 6-X. STAGED FUEL COMBUSTOR CONFIGURATIONS				
Build No.	Nomenclature	Combustor description	Pilot fuel injector P/N	No. of data pts
1	Baseline	Original Design	Std Dual Orifice	22
2	Mod I	Original Design	Air Assist	35
	Mod II	Original Design	Air Assist	
3	Mod III	Original Design	Airblast	48
	Mod IV	Original Design	Airblast	
4	Mod V	Modified Design	Airblast	40
	Mod VI	Modified Design	Airblast	
Total				145

The fixed geometry definitions for the EPAP computations are summarized in Table 6-XI. The fuel staging schedule for the EPAP configurations is summarized in Table 6-XII for the four duty cycle conditions. The low power points were always run with 100% pilot fuel. The climbout and takeoff conditions were generally tested with both pilot and main zones fueled. Main fuel flow ranged from 100% (no pilot flow) to about 50%. The fuel split at high power was generally selected for low NO_x emission.

The EPAP results are summarized in Table 6-XIII and Figure 6-41.

The EPA limits, program goals, and the production liner emissions are also shown for comparison.

For every basic configuration tested, a geometry and fuel scheduling mode was found that met the emission goals with considerable margin. In general CO, HC, and smoke were greatly reduced, and NO_x increased a small amount. A large emissions improvement was achieved relative to the production liner with the initial staged fuel design. Improvements were made with each successive staged fuel test. Mod V was the best overall with HC and smoke reductions of about 88% and a NO_x increase of 14% which is still 44% below EPA limits.

TABLE 6-XI. FIXED GEOMETRY DEFINITIONS				
Configuration	Build No.	Dilution		Prechamber VG
		Zone VG % Closed	Primary Zone VG	
Baseline	1	0	*	†
Mod I	2	0	*	†
Mod II	2	20	*	†
Mod III	3	0	*	†
Mod IV	3	40	*	†
Mod V	4	80	Open	Open
Mod VI	4	50	Open	Open
*Primary zone holes were fixed open in Builds 1 through 3. †Prechamber VG radial swirler did not exist in Builds 1 through 3.				

TABLE 6-XII. FUEL STAGING					
	Build No.	Idle	Fuel Schedule, % Pilot Chamber Fuel*		
			Approach	Climbout	Takeoff
Baseline	1	100	100	15	13
Mod I	2	100	100	31	0
Mod II	2	100	100	31	0
Mod III	3	100	100	12	10
Mod IV	3	100	100	12	11
Mod V	4	100	100	51	51
Mod VI	4	100	100	51	51
*Balance is supplied to the main combustion chamber					

The staged fuel combustor emissions for each configuration as defined in Table 6-XI and each power mode are summarized and compared with those of the production combustor in Table 6-XIV. Large CO and HC reductions were accomplished, especially at idle. Combustion efficiency (gas analysis) was never below 99.5%. Smoke was generally reduced to low values.

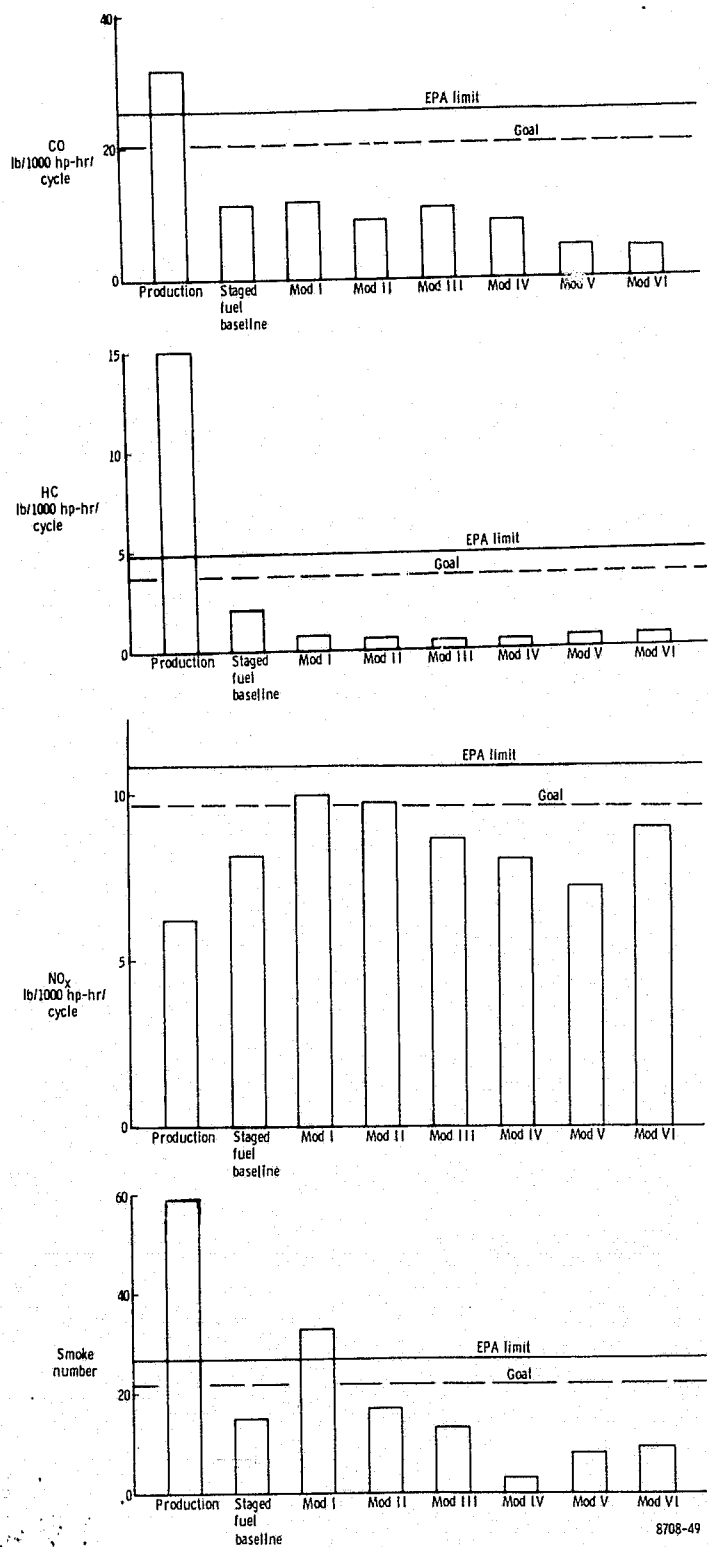


Figure 6-41. Staged fuel EPAP results.

ORIGINAL PAGE IS
OF POOR QUALITY

TABLE 6-XIII. EPAP RESULTS

	Total hydrocarbons lb/1000 hp-hr/cycle	Carbon monoxide lb/1000 hp-hr/cycle	Oxides of nitrogen lb/1000 hp-hr/cycle	Max smoke (% SAE)
EPA limits				
Class P2	4.9	26.8	12.9	29
Program goals				
75% Class P2	3.7	20.1	9.7	22
Production liner	15.0	31.5	6.3	59
Staged fuel baseline	1.9	11.3	8.1	15
Staged fuel Mod I	0.7	11.7	10.0	33
Staged fuel Mod II	0.6	9.2	9.7	17
Staged fuel Mod III	0.4	10.6	8.6	13
Staged fuel Mod IV	0.4	8.4	8.1	3
Staged fuel Mod V	0.6	5.7	7.2	8
Staged fuel Mod VI	0.6	4.3	9.0	9

NO_x generally increased. However, the best configuration (Mod V) accomplished significant NO_x reductions at all power levels except idle. The NO_x emission for this combustor was almost constant over the entire power range.

Parametric Emission Results

Emission data were obtained for the following parameters:

- Effect of fuel-air ratio at given duty cycle conditions
- Effect of fuel flow split (pilot to main combustion zone)
- Effect of combustor reference velocity
- Effect of pilot fuel injector type
- Effect of variable geometry setting

The emission data maps were generally not complete because of the large number of variables involved. Consequently, the optimum operating modes (VG position, fuel scheduling) for each basic combustor configuration were probably not identified.

Parametric Idle Performance Results

The highest CO, and HC emissions were generally at idle conditions due to the low pressure, and low fuel/air ratio. The production liner idle CO and HC contribution was approximately 95% of the total. Figures 6-42 and 6-43 show parametric idle results for the baseline combustor with an airblast pilot fuel injector. Figure 6-42 shows the effect of idle fuel/air ratio variations. Minimum CO occurs at a somewhat lower fuel/air ratio

**TABLE 6-XIV. STAGED FUEL COMBUSTOR EMISSION
INDEX SUMMARY***

Configuration	Percent pilot fuel	CO	EI (g/kg) HC	NO _x	Combustion efficiency	Smoke No. (% SAE)
Idle						
Production liner	---	42.90	17.63	3.74	97.38	45
Staged fuel baseline	100	16.68	1.403	6.47	99.47	15
Mod I	100	15.40	0.260	5.38	99.59	27
Mod II	100	11.76	0.353	5.29	99.66	17
Mod III	100	12.91	0.293	4.98	99.64	13
Mod IV	100	10.17	0.233	4.58	99.71	3
Mod V	100	5.85 [†]	0.360 [†]	5.15 [†]	99.80 [†]	1 [†]
Mod VI	100	4.81	0.431	6.52	99.80	1
Approach						
Production liner	---	5.10	1.96	7.49	99.67	59
Staged fuel baseline	100	2.68	0.894	6.97	99.81	9
Mod I	100	3.03	1.40	11.36	99.71	33
Mod II	100	2.38	0.926	10.39	99.78	11
Mod III	100	2.89	0.490	11.43	99.81	7
Mod IV	100	1.92	0.518	9.17	99.84	2
Mod V	100	1.67	0.58 [‡]	6.88	99.72	8
Mod VI	100	1.83	0.58 [‡]	9.77	99.76	9
Climb						
Production liner	---	2.06	0.889	9.22	99.81	38
Staged fuel baseline	15	1.88	0.522	8.61	99.86	1
Mod I	31	1.54	0.281	13.37	99.85	5
Mod II	31	1.36	0.271	13.59	99.86	5
Mod III	12	2.82	0.746	8.34	99.81	2
Mod IV	12	2.37	0.600	9.12	99.83	0
Mod V	51	4.26	0.404	6.48	99.82	5
Mod VI	51	1.40	0.331	9.48	99.88	3
Takeoff						
Production liner	---	2.04	0.279	8.88	99.87	37
Staged fuel baseline	13	1.57	0.502	8.37	99.87	4
Mod I	0	2.03	0.279	8.51	99.88	10
Mod II	0	1.77	0.222	8.57	99.89	1
Mod III	10	2.11	0.141	8.57	99.88	5
Mod IV	11	1.69	0.139	9.25	99.89	0
Mod V	51	1.49	0.212	7.35	99.90	4
Mod VI	51	1.11	0.213	10.83	99.89	1

*Combustion rig data. Values may differ slightly from EI values computed for duty cycle emission analysis.

[†] Emission data interpolated between two VG settings.

[‡] Estimated HC emissions; no data available because of sample line HC "hang-up" from previous readings.

than the 0.0113 idle value. Smoke begins to increase rapidly at fuel/air ratios greater than idle. Figure 6-43 shows the effect of dilution hole variable geometry position at idle. This again shows a CO reduction as the pilot zone is leaned by closing the dilution holes. Smoke is also reduced in this case. Figure 6-44 shows the effect of fuel staging at idle. As expected, the CO and HC increased significantly as fuel is added to the main zone at constant overall fuel/air ratio of 0.0113. Significant NO_x and smoke reduction occur as combustion is leaned. Figure 6-45 shows

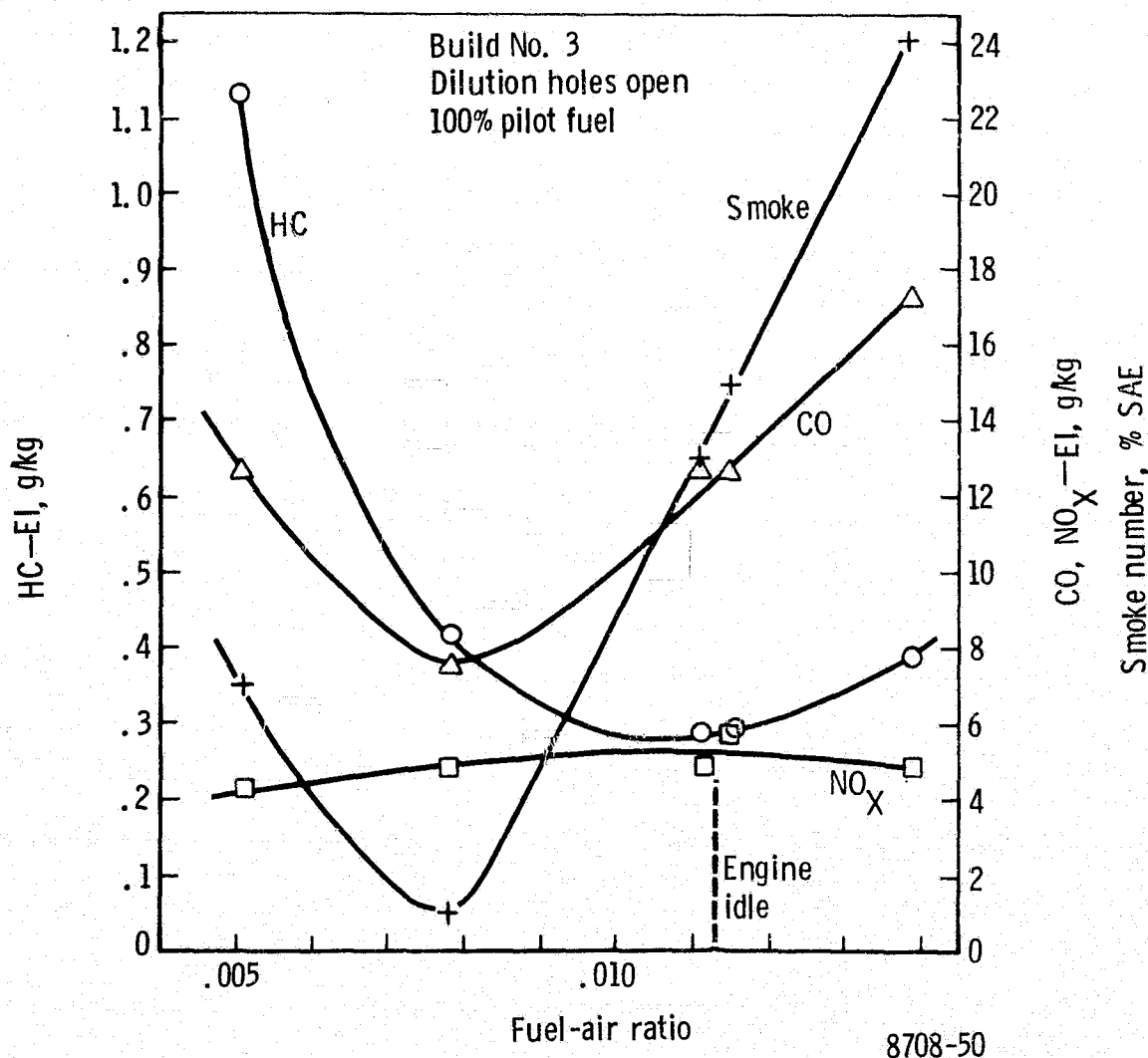


Figure 6-42. Effect of fuel/air ratio on idle emissions.

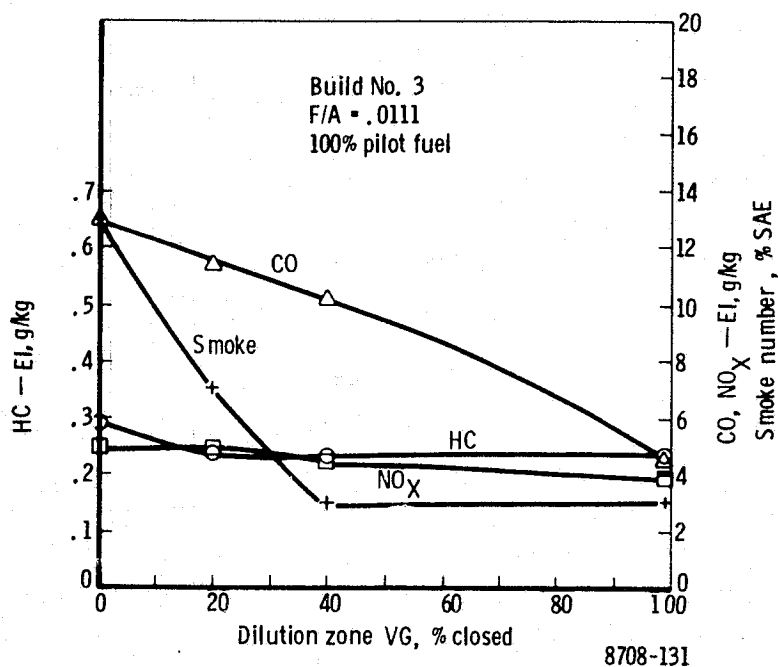


Figure 6-43. Effect of variable geometry setting on idle emissions.

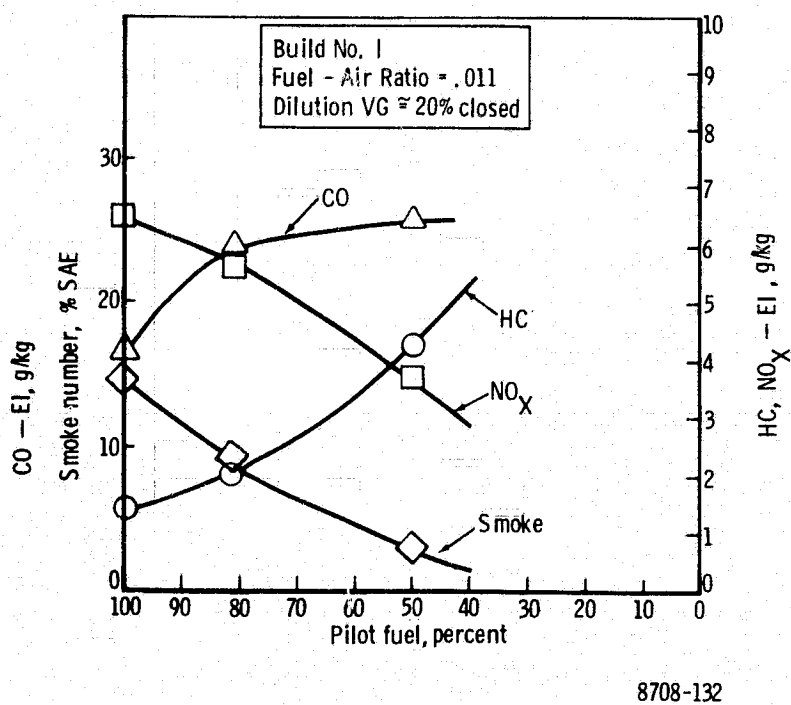


Figure 6-44. Effect of fuel staging on idle emissions.

the effect of combustor reference velocity on emissions (original combustor design with the air assist fuel injector with 135×10^3 Pa differential pressure). A large CO reduction was noted for reduced combustion loading. Based on these idle results, the Mods V and VI pilot zone equivalence ratio was reduced and the pilot zone volume was increased to reduce idle CO emission.

Parametric Pilot Fuel Injector Results

Three pilot zone fuel injectors were tested in conjunction with the original staged fuel combustor design; standard pressure atomizer, air assist and airblast. The principal emission variations occurred at idle, as expected. HC emission results at idle for the three fuel injectors are shown in Figure 6-46 as a function of fuel/air ratio.

A very large HC emission reduction was demonstrated with the air assist and airblast injectors relative to the standard pressure atomizer, especially at low fuel/air ratio. At high fuel/air ratio, all injectors gave low HC. This HC reduction is attributed to the improved fuel atomization and

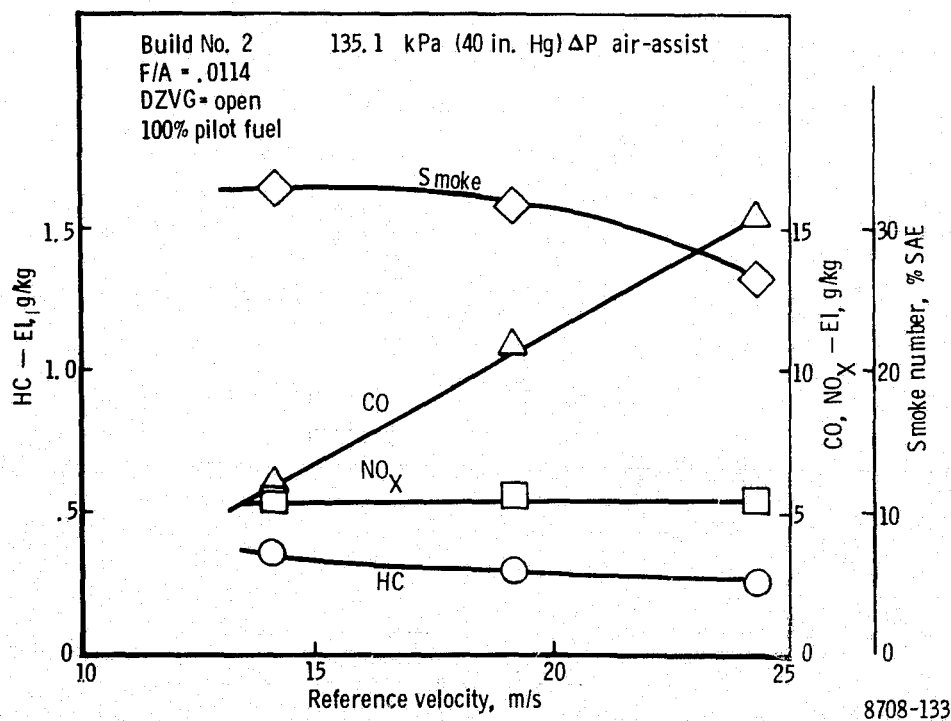


Figure 6-45. Effect of reference velocity on idle emissions.

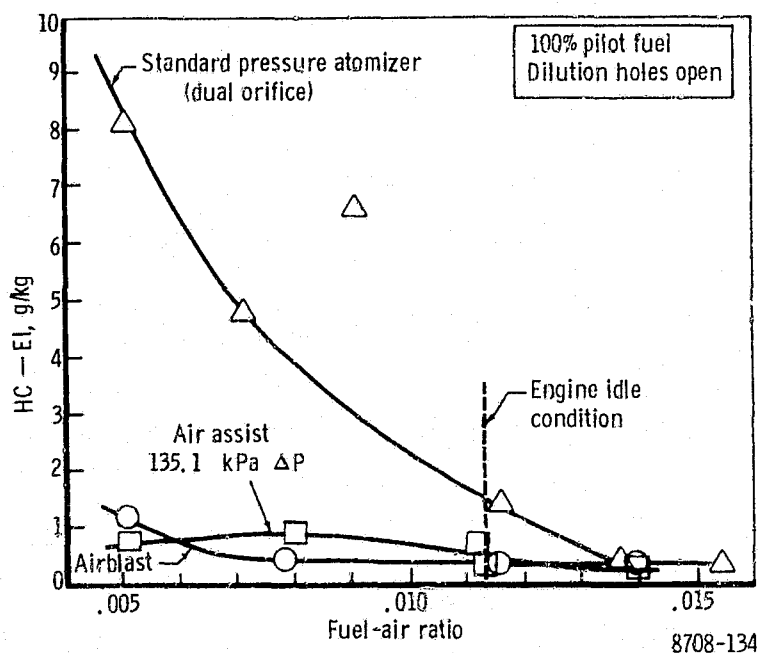


Figure 6-46. Effect of pilot fuel injector on idle HC emissions.

preparation obtained with the aerating systems. The CO results shown in Figure 6-47 were similar to those for HC. The air assist injector provided the lowest CO at very low fuel/air ratio. At engine idle all three nozzles had similar performance. Idle smoke results are shown in Figure 6-48 as a function of fuel/air ratio. The standard pressure atomizer produced the highest smoke at very high fuel/air ratio. At T56 idle, the airblast and dual orifice injectors had the same smoke emissions and were superior to the air assist nozzle. At very low fuel/air ratios, all three systems had similar performance. Smoke performance at high pressure shown in Figure 6-49, is also important since peak smoke is generally emitted at high power. The purpose of Figure 6-49 is to illustrate the sensitivity of pilot fuel nozzle selection on smoke emission because the combustor was not designed to run at 100% pilot fuel at high power conditions. Data for the standard pressure atomizing nozzle was obtained at the approach condition which is approximately the same pressure, temperature, and airflow as takeoff. Smoke increased with fuel/air ratio for all systems with the standard nozzle having the best

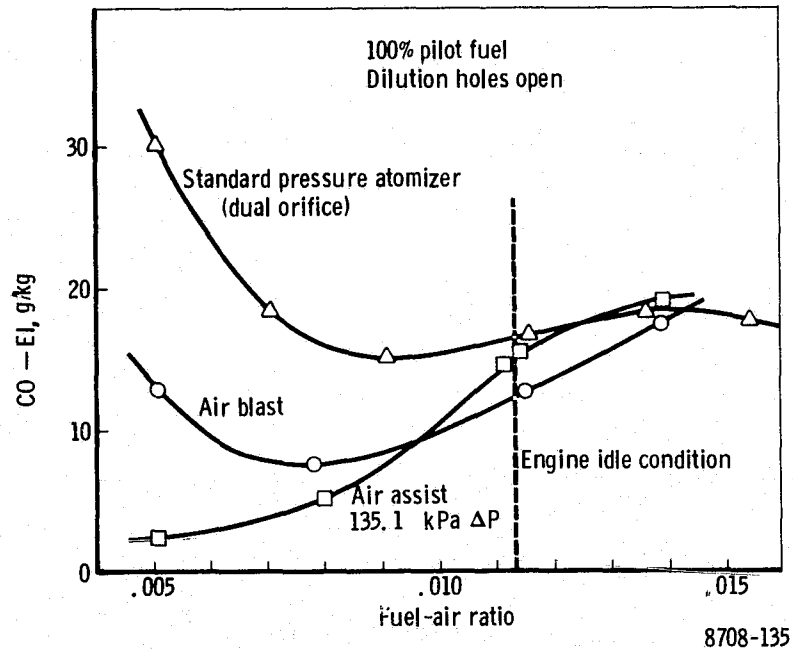


Figure 6-47. Effect of pilot fuel injector on idle CO emissions.

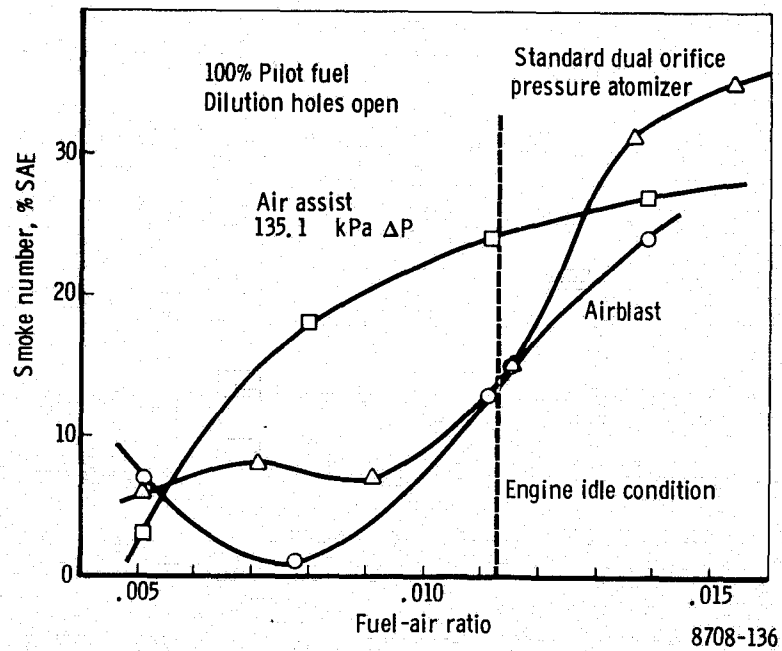


Figure 6-48. Effect of pilot fuel injector on idle smoke emissions.

C-2

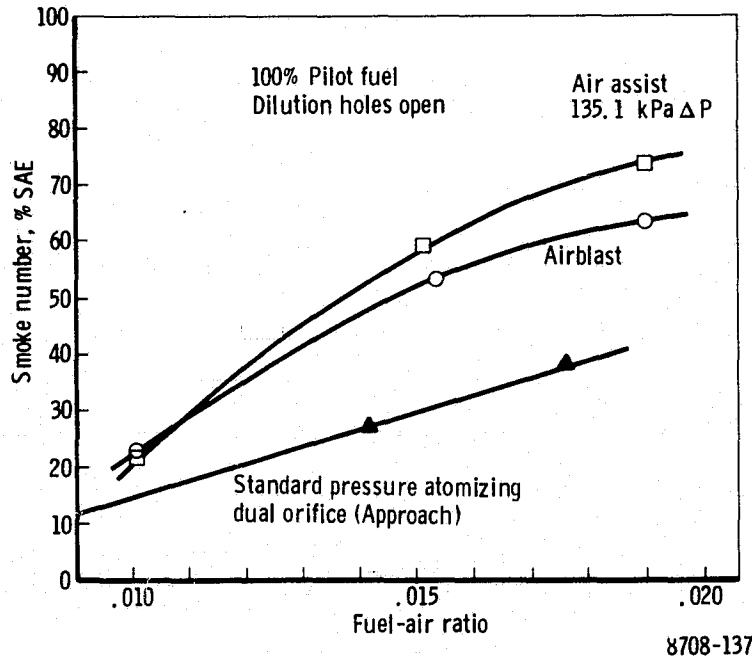


Figure 6-49. Effect of pilot fuel injector on takeoff smoke emission.

performance. This is evidently a result of the fuel injector/pilot pre-chamber swirler integration. The standard nozzle spray angle was well matched to the pilot prechamber geometry to obtain good fuel/air mixing at the prechamber exit. Even the standard fuel injector smoke was higher than desired at high fuel/air ratio, however, due to the high combustor pilot zone equivalence ratio. NO_x results for the three nozzles at idle are shown in Figure 6-50. The standard pressure atomizing nozzle generally produced the highest NO_x . Differences between the three injectors were not very large, however. Based on these results, the airblast nozzle was selected for the final (Mod V, VI) test, primarily for its idle CO, and HC advantages.

Parametric Takeoff Performance Results

At the takeoff condition, CO and HC are generally low, and NO_x and smoke are the most important emissions. As previously discussed, NO_x reduction was not required in this program. Takeoff emissions for the baseline staged fuel combustor and airblast fuel nozzle are shown in Figure 6-51

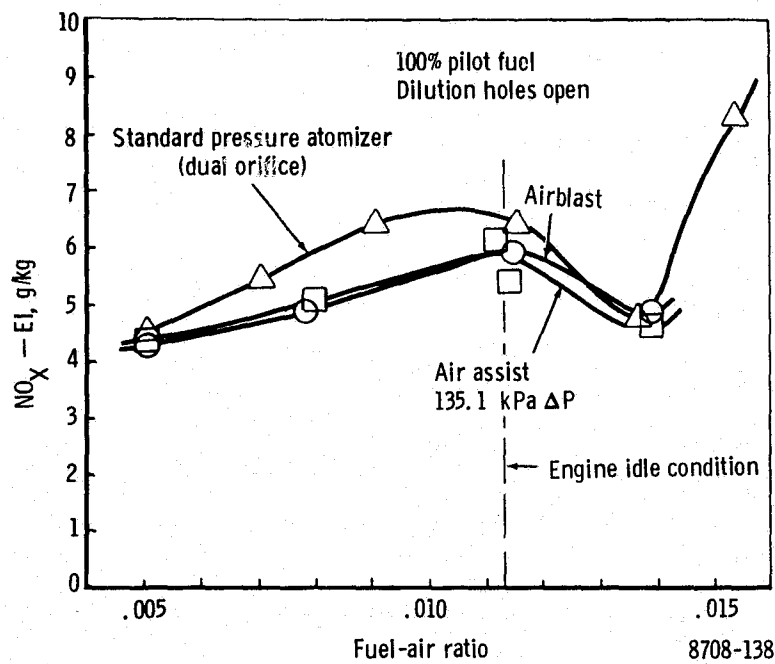


Figure 6-50. Effect of pilot fuel injector on idle NO_x emissions.

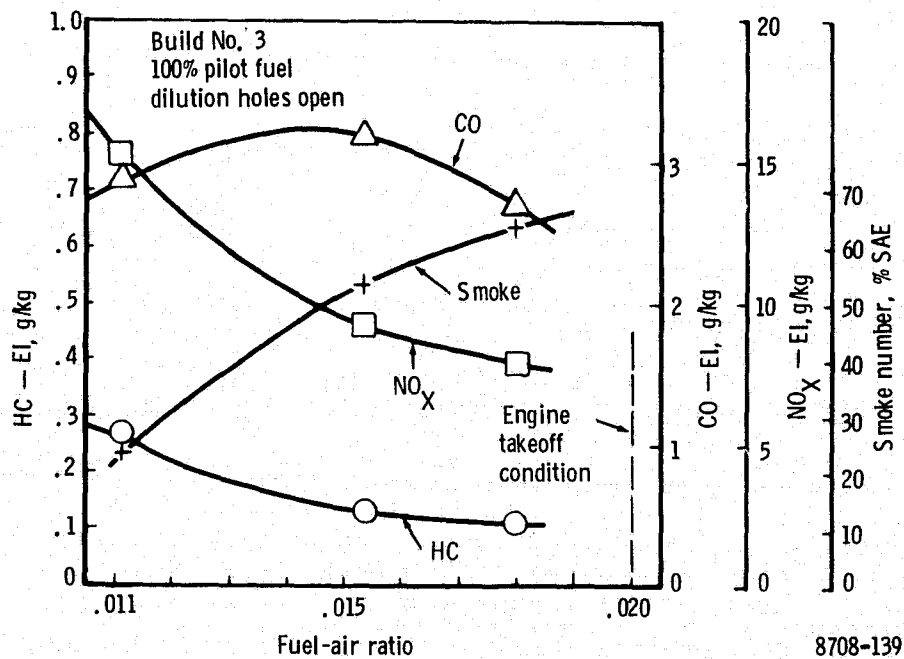


Figure 6-51. Effect of fuel/air ratio on takeoff emissions (100% pilot fuel).

for a range of fuel/air ratios and 100% pilot zone fuel. These results show that smoke rapidly increases to very high values as fuel/air ratio increases, approaching takeoff (0.020). NO_x emission decreases with increased fuel/air ratio. This is a consequence of the low airflow and pilot zone equivalence ratio exceeding stoichiometric at fairly low overall fuel/air ratio. Increased fuel/air ratio beyond this point causes a NO_x reduction because the reaction zone temperature and free oxygen concentration are reduced. Figure 6-52 shows takeoff emissions for a range of fuel/air ratio and 0% pilot fuel (i.e., all fuel enters the main combustion zone). The smoke emissions in this operating mode were very low for the complete range, evidently a result of the superior main zone fuel preparation and mixing. The main zone operating range tends to be low F/A limited by the rapidly increasing CO and HC as the fuel/air ratio decreases below about 0.011. NO_x emissions peak at a fuel/air ratio of 0.012. This is expected based on the high initial main zone equivalence ratio ($\phi = 0.8$) at this condition. NO_x reductions from this maximum are achieved by leaner or richer operation. Figure 6-53 shows the effect of fuel staging at takeoff conditions with slightly reduced fuel/air ratio. The results again are consistent with the stoichiometry of the zones. With 100% pilot fuel, the pilot zone is quite rich at this fuel/air ratio so that smoke emission is high, and NO_x is low. As main fuel is added, smoke emission is reduced and exhaust smoke is very low all the way to 0% pilot fuel

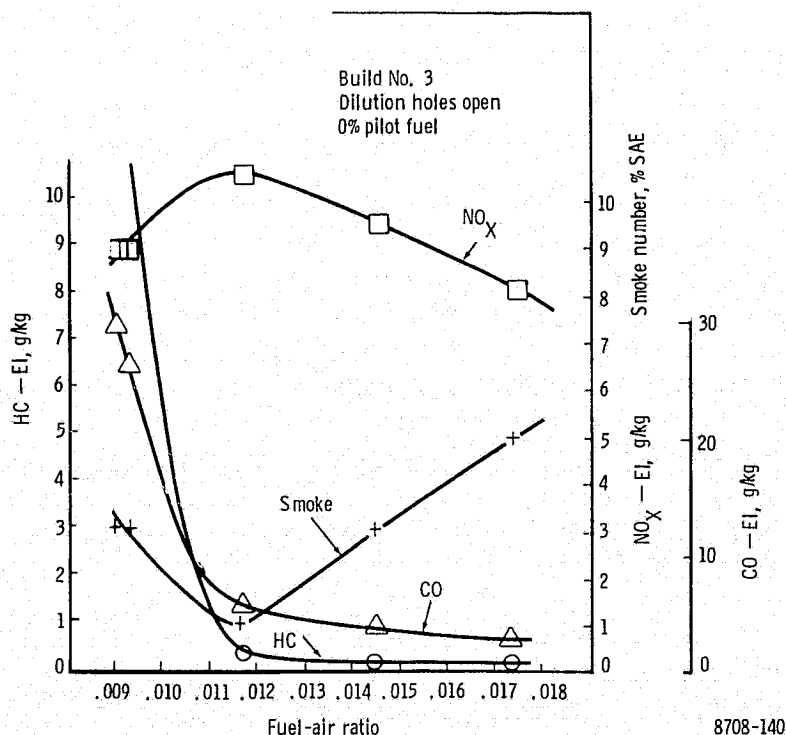


Figure 6-52. Effect of fuel/air ration on takeoff emissions (0% pilot fuel).

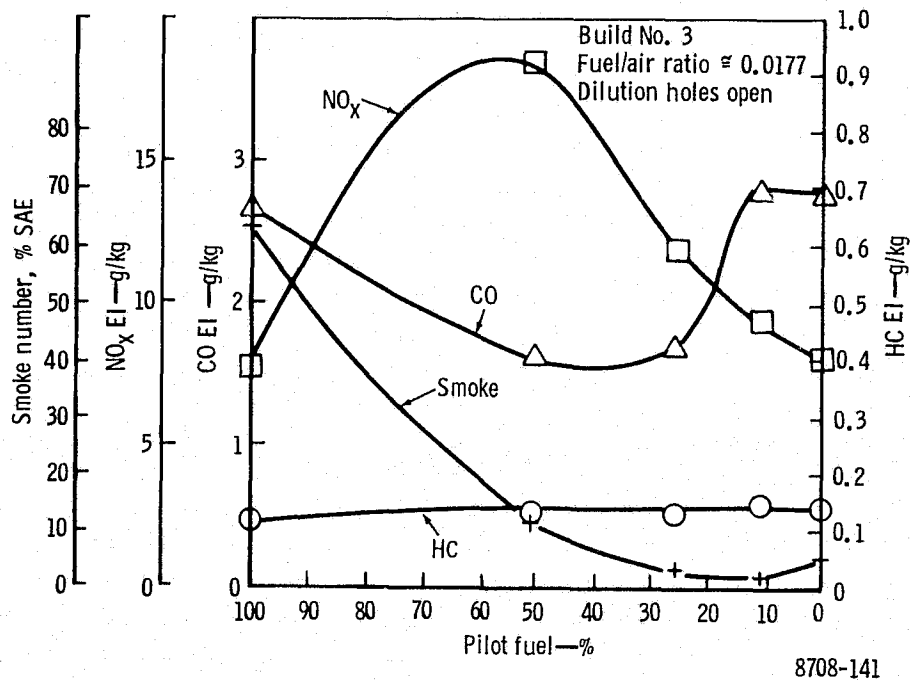


Figure 6-53. Effect of fuel staging on takeoff emissions (Build 3).

(100% main) because of the excellent main zone mixing characteristics. The pilot zone equivalence ratio decreases towards stoichiometric as main fuel is added so that NO_x increases as pilot fuel is decreased by staging. At about 50% pilot fuel, both zones are slightly lean and NO_x is a maximum. Further pilot fuel reductions lean the pilot zone, and increase the main zone equivalence ratio from the point of maximum NO_x formation so that NO_x is again reduced. NO_x emission was almost identical for 100% and 0% pilot fuel splits. Based on these NO_x and smoke results, fuel splits of 10% pilot fuel were selected for the original design EPAP test. Figure 6-54 shows the effect of dilution hole area for this fueling mode. As the dilution zone is closed, additional main zone airflow changes the initial main zone equivalence ratio from very rich towards stoichiometric so that NO_x increases. These NO_x characteristics are summarized in Figure 6-55 as a function of fuel/air ratio and fueling mode.

The Mod V/VI design pilot and main zone equivalence ratios were reduced to allow very lean operation in both zones at high fuel/air ratio with 50% pilot-main fueling, and dilution VG settings near closed. These changes

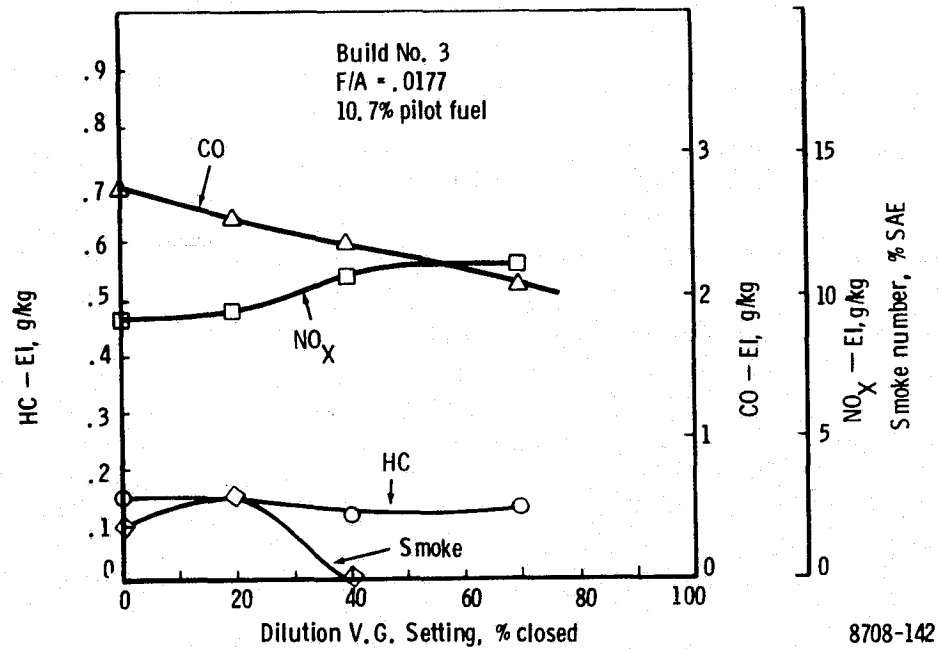


Figure 6-54. Effect of variable geometry setting on takeoff emissions.

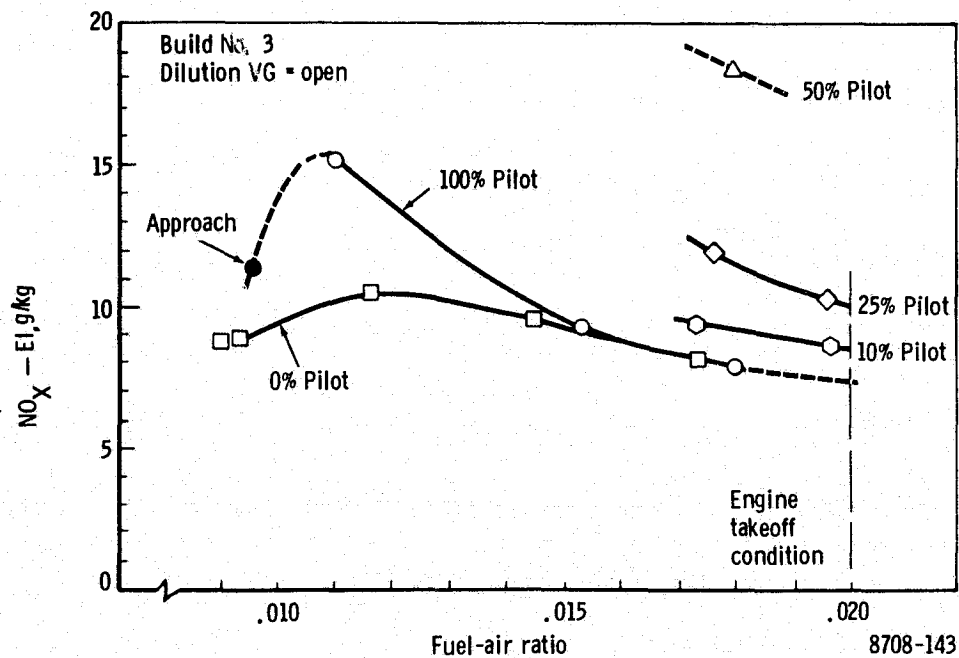


Figure 6-55. NO_x characteristics for Build three (takeoff).

were made to reduce CO at idle and NO_x at high power by operating very lean. Takeoff emission results for 100% pilot fuel are shown in Figure 6-56 for parametric fuel/air ratio. An effectively rich pilot zone is again evident with decreasing NO_x and increasing smoke with increasing fuel/air ratio. The effect of fuel staging at high fuel/air ratios is shown in Figure 6-57. CO and NO_x trends are again consistent with combustion zone stoichiometry. High CO is obtained from a small amount of main zone fueling due to the low initial main equivalence ratio. NO_x initially increases as pilot fuel is reduced and the pilot zone equivalence ratio approaches stoichiometric. NO_x reduction occurs with further pilot fuel reductions as both zones become somewhat lean. A large smoke reduction is also obtained as main fuel is added. The effect of dilution zone VG is shown in Figure 6-58 for 50% pilot fueling. The lean reaction zones are further leaned by dilution zone VG closure and a large NO_x reduction is obtained. With full dilution hole closure, NO_x at 0.018 fuel/air ratio was 55% below the standard aircraft combustor. With 80% dilution VG closure, a 45% NO_x reduction over the standard combustor was obtained. The complete operating range was tested with this dilution VG setting by means of the flexibility inherent in the fuel staged design. Combustion at low power conditions was stable with 100% pilot zone fuel. NO_x results are summarized in Figure 6-59 at takeoff conditions for various fuel/air ratios, dilution VG positions, and fueling schedules.

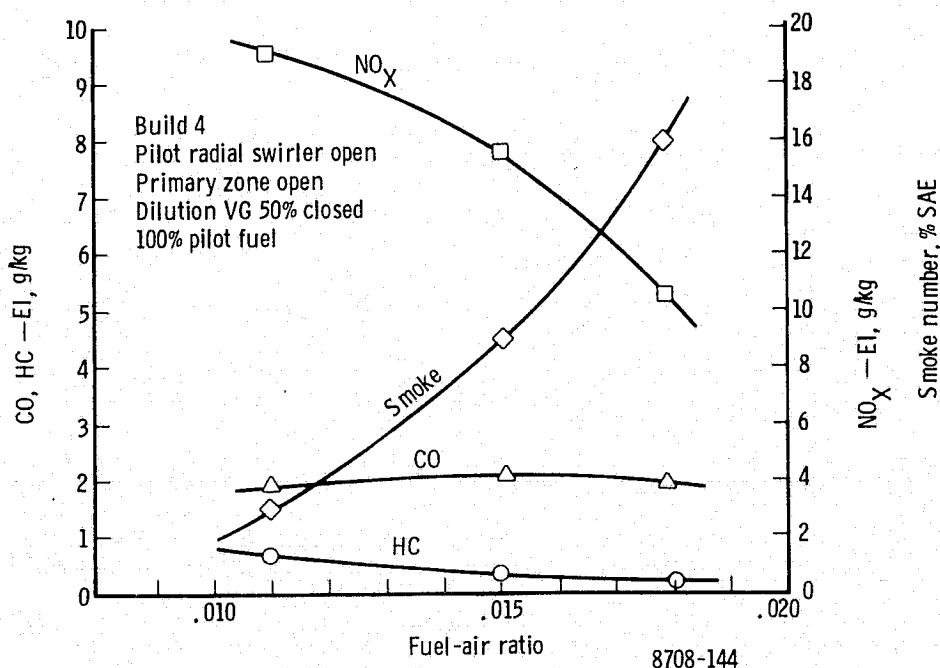


Figure 6-56. Effect of fuel/air ratio on takeoff emissions (100% pilot fuel)

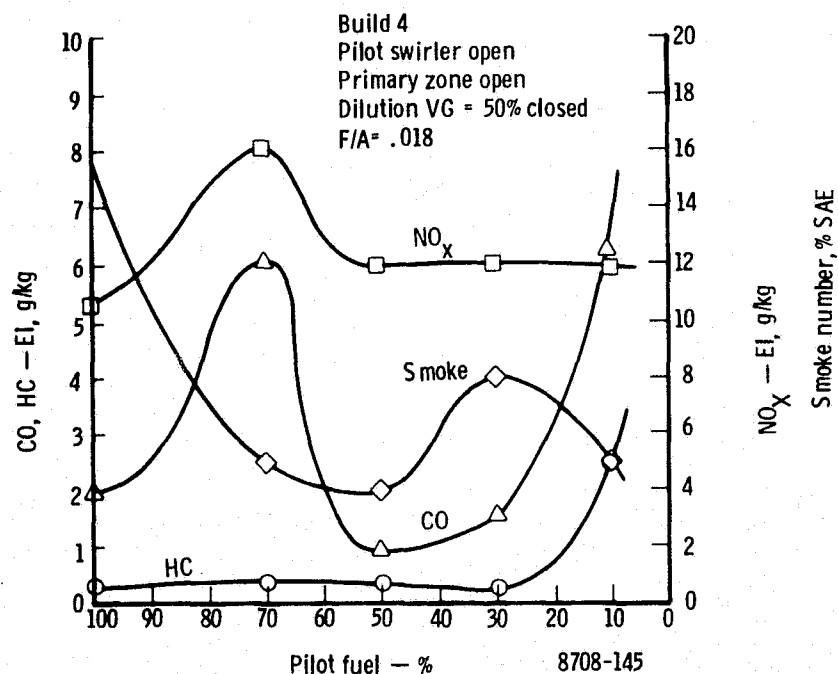


Figure 6-57. Effect of fuel staging on takeoff emissions (Build 4).

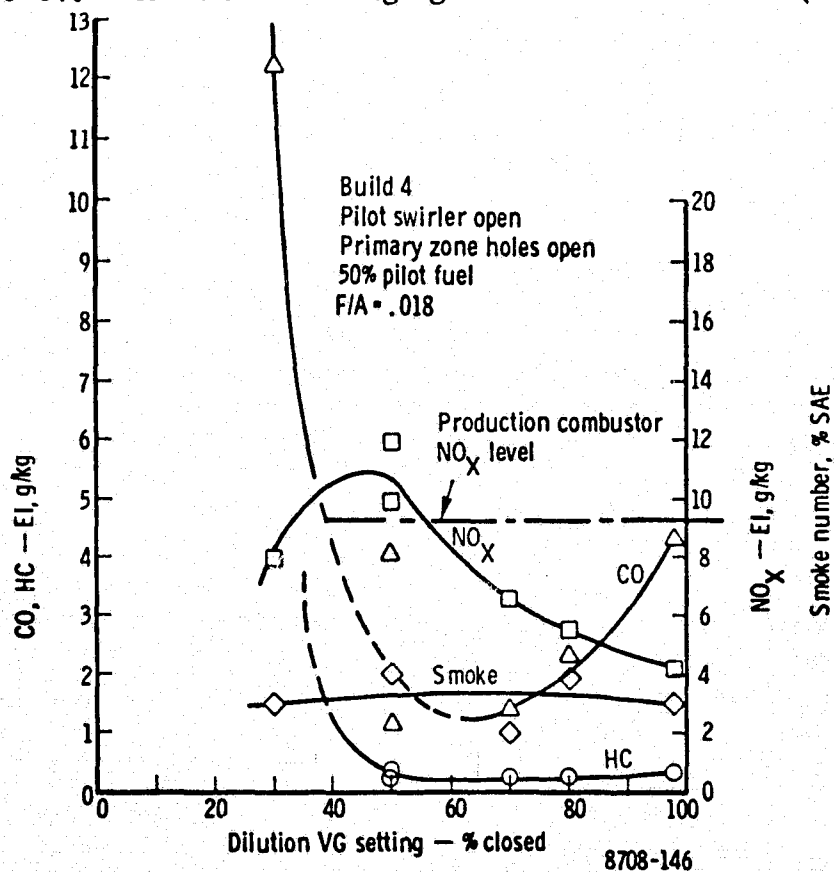


Figure 6-58. Effect of variable geometry setting on takeoff emissions (Build 4).

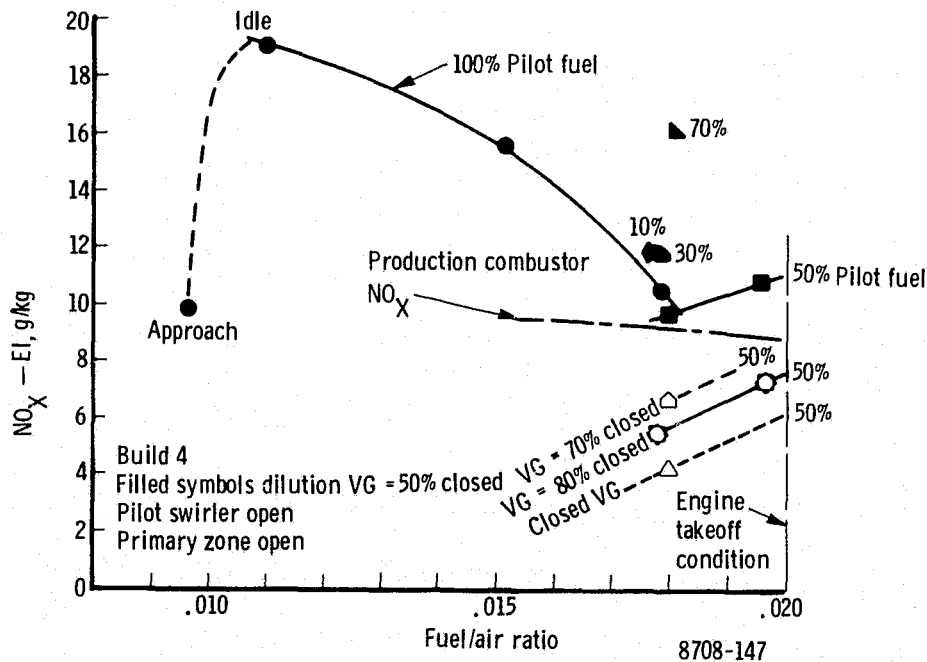


Figure 6-59. NO_x characteristics for Build 4.

Exhaust Temperature Pattern Factor

Typical pattern factor (PF) results are shown in Figure 6-60. The PF was a function of dilution VG setting. PF increased with reduced dilution air flow. Mods V and VI performance were an improvement over the original design especially at very closed dilution VG settings. Staged fuel PF performance was also an improvement over the standard combustor for a large DZVG range.

Combustor Pressure Loss

The combustion system pressure loss (including diffuser) is shown in Figure 6-61. This loss was measured from the engine compressor discharge pressure measurement plane and includes combustor plus a large fraction of diffuser loss. The pressure loss was a strong function of dilution VG setting. Over a large DZVG range the pressure loss was less than for the production combustor.

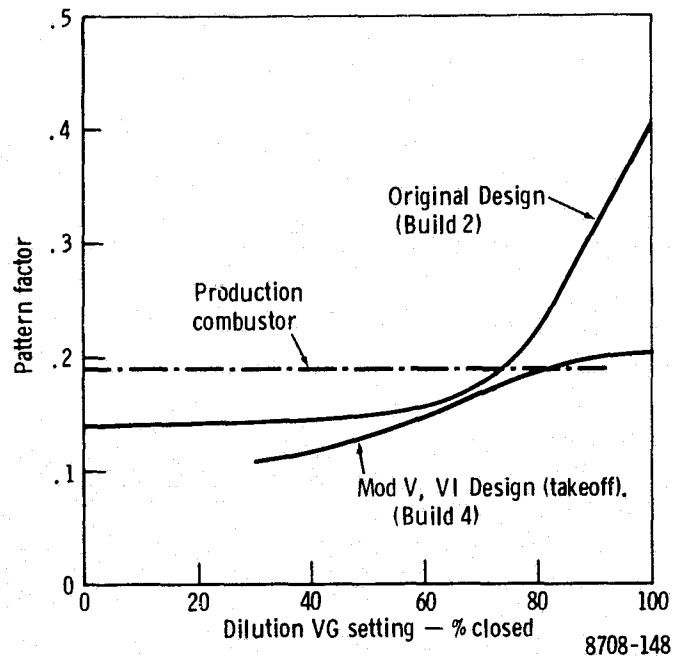


Figure 6-60. Staged fuel combustor pattern factor.

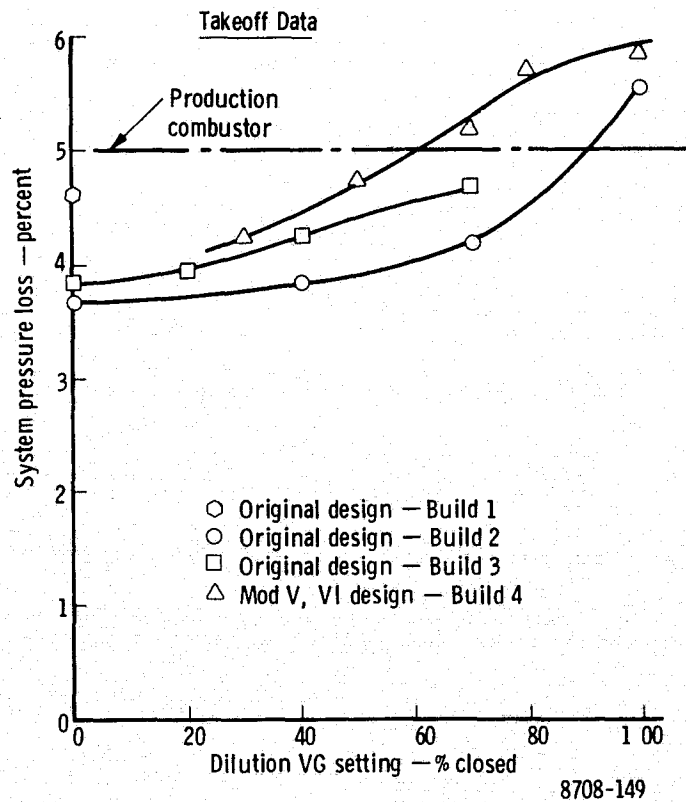


Figure 6-61. Staged fuel combustor pressure loss.

Altitude Ignition Performance

Low pressure stability testing was accomplished on the Mod V/VI design to assess altitude ignition potential. Lean-blowout fuel/air ratio was measured at several altitude pressure levels and several airflow rates. With further development, ignition could be accomplished at a somewhat higher fuel/air ratio than the lean blowout value. Stability results are shown in Figure 6-62. Blowout fuel/air ratio is presented as a function of reaction rate parameter θ .

θ is a fundamental chemical reaction rate parameter used to correlate combustion performance such as efficiency. Figure 6-62 shows improved blowout performance as combustion conditions improve (increased θ). Improved performance may be possible by using a pilot orifice in the pilot fuel injector.

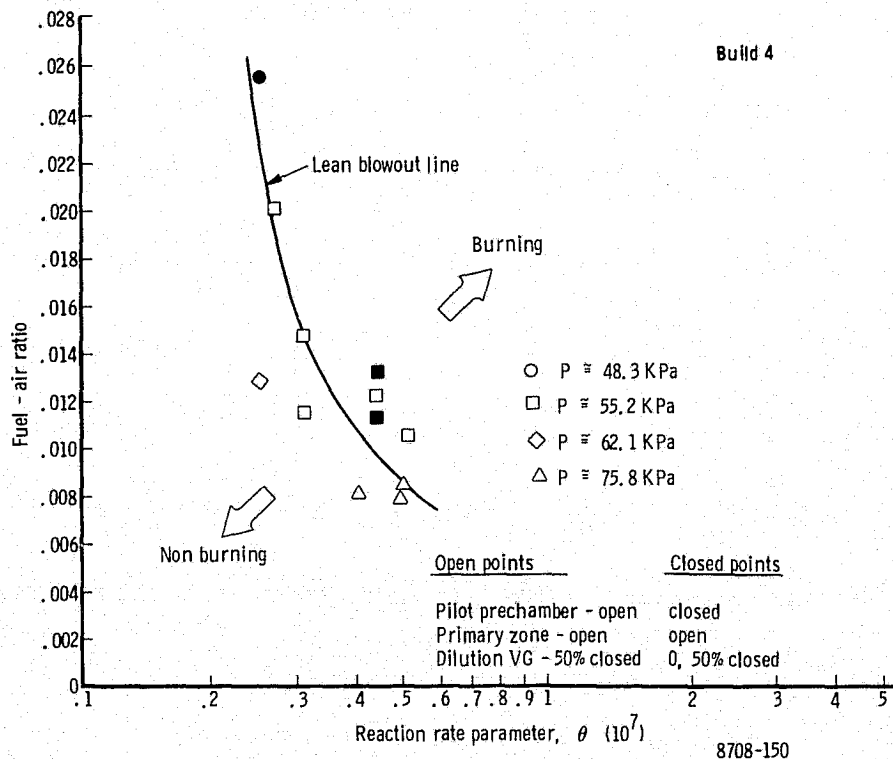


Figure 6-62. Staged fuel combustor low pressure blow out results.

Durability Performance

The staged fuel combustors were instrumented for wall temperature measurement on each of the main zone prechambers to monitor for preignition/flashback. Thermocouples were also attached to the inner wall of the film-convection cooling section, and on the combustor transition. Over the very wide range of fuel splits and VG settings no preignition was encountered and wall temperatures were sufficiently low for good durability potential. Figure 6-63 shows the skin temperature patterns, as indicated by thermal paint. The necked-down section between pilot and main combustion zones was generally the hottest area. No damage occurred on any of the emission runs. A small area in the film-cooled region of the pilot-to-main chamber transition was burned during altitude testing. Altitude testing involved many blowouts with potential accumulation of fuel. The burned area occurred near the liner bottom and could have been the result of an accumulation of raw fuel. This problem could be solved by extending the convectively cooled region and reducing the film-cooled length.

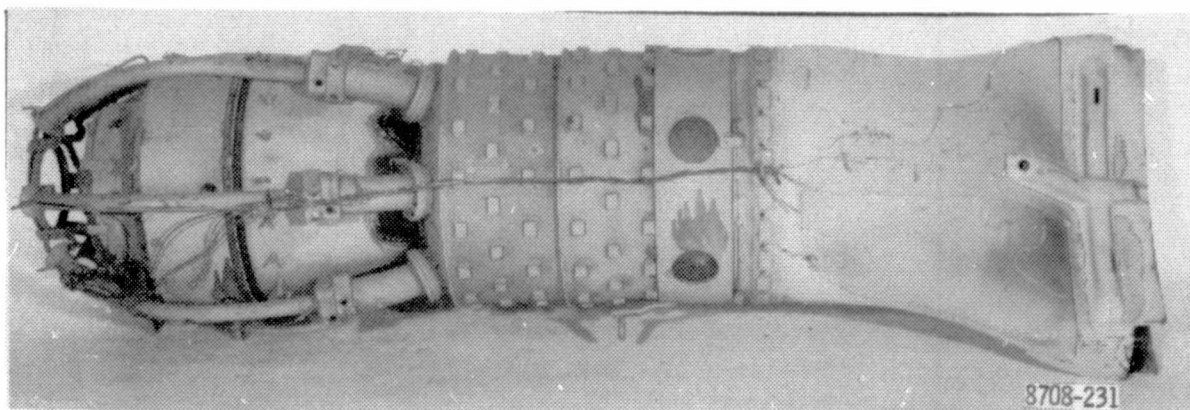


Figure 6-63. Typical staged fuel combustor temperature pattern.

VII. DISCUSSION OF RESULTS

PRODUCTION LINER

Prior to this program the 501-D22A combustion system emissions were measured with a probe located in the engine exhaust pipe. These engine data compare favorably with the rig data described herein for HC, CO and NO_x over the entire fuel air range from approach to takeoff. The smoke data are reasonably close at idle and approach, within $\pm 5\%$. However, the comparison of rig and engine data at the high fuel-air conditions of climb-out and takeoff shows the difference to be $\pm 20\%$ from the average of the two sets of data.

The fuel-air ratio was varied from nominal by -20% and $+15\%$ at idle. Only the hydrocarbon emission responded to these changes in fuel-air ratio.

The data shown in Figure 7-1 indicate a rapid decrease in hydrocarbons with increasing fuel-air ratio. Similar tests at takeoff in which fuel-air ratio was decreased by 10% and 20% from nominal gave no emission reduction.

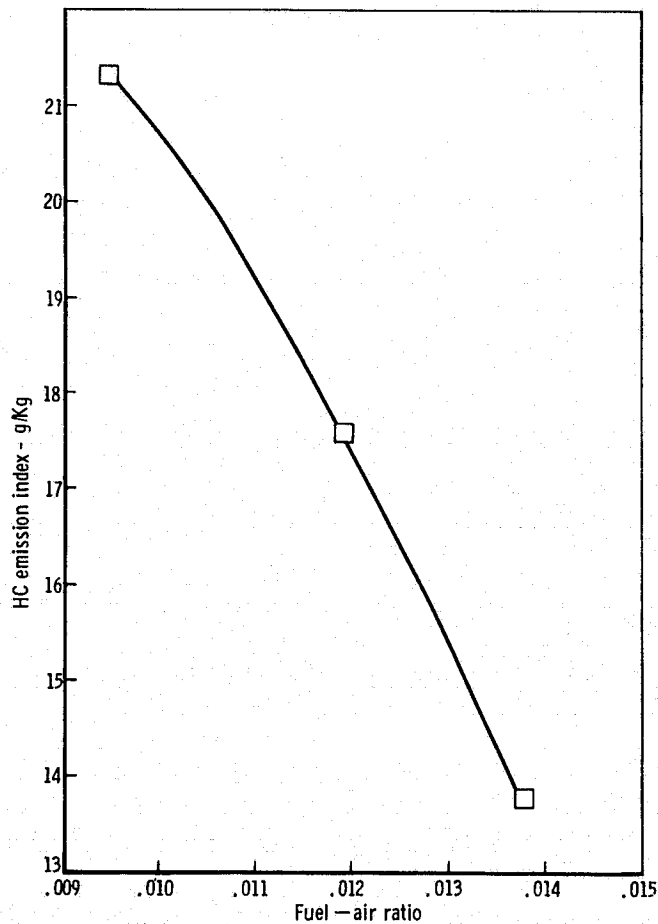
Measured pressure loss of the combustion system was 4.7% to 6.3% which is consistent with engine data. Pattern factor ranged from 0.15 to 0.20. This is also reasonable for the 501-D22A combustor. These values of pressure loss and pattern factor are the combustor performance values against which the low emission designs are compared.

REVERSE FLOW

The design-development changes made in the reverse flow 501-K industrial engine combustion system successfully reduced hydrocarbon and carbon monoxide emissions to a level below the program goals. In the reverse flow system smoke and oxides of nitrogen were already below the required levels. During the experimental program changes in primary zone equivalence ratio, and in the methods of injecting fuel were investigated. The effects of both types of changes in reducing idle exhaust emissions were noteworthy.

Primary Zone Equivalence Ratio

The design changes which increased the equivalence ratio of the primary zone were previously described in Section III of this report, "Description of Designs". In these changes the airflow into the primary zone was decreased by 20 percent. As a result the unburned fractions in the exhaust



8708-86

Figure 7-1. Hydrocarbon emissions at idle conditions.

(HC and CO) were reduced markedly at idle, and the oxides of nitrogen production at idle were slightly increased. The reduction of unburned material in the exhaust is shown in Figure 7-2 in which "combustion inefficiency" ($100-\eta$) at 10,000 RPM inlet conditions is plotted against primary zone equivalence ratio. At the taxi-idle mode (fuel air ratio of 0.011) the inefficiency was reduced from 2.3% for the industrial system to less than 0.5%, as summarized as follows:

Test Configuration	"Combustion Inefficiency" ($100-\eta$, %)
Baseline	0.36
Mod I	0.17
Mod II	0.43
Mod III	0.25
Mod IV	0.16

An additional, more subtle change was made in the primary zone equivalence ratio by increasing the airflow into the second air reversing baffle by 19%. This small change was made in Mod II, and reduced the overall primary zone equivalence ratio by 2%. It did not make a major change in the combustion efficiency (Baseline compared with Mod II, and Mod I compared with Mod IV). However, due to this change HC and CO idle emissions were "traded-off". Figure 7-3 shows this trade-off, where increasing the baffle airflow reduced hydrocarbons but increased carbon monoxide. Oxides of nitrogen at idle did not change significantly. It is thought that the reason for this trade-off is that increasing second reversing baffle air flow increased the available oxygen near the end of the reaction zone.

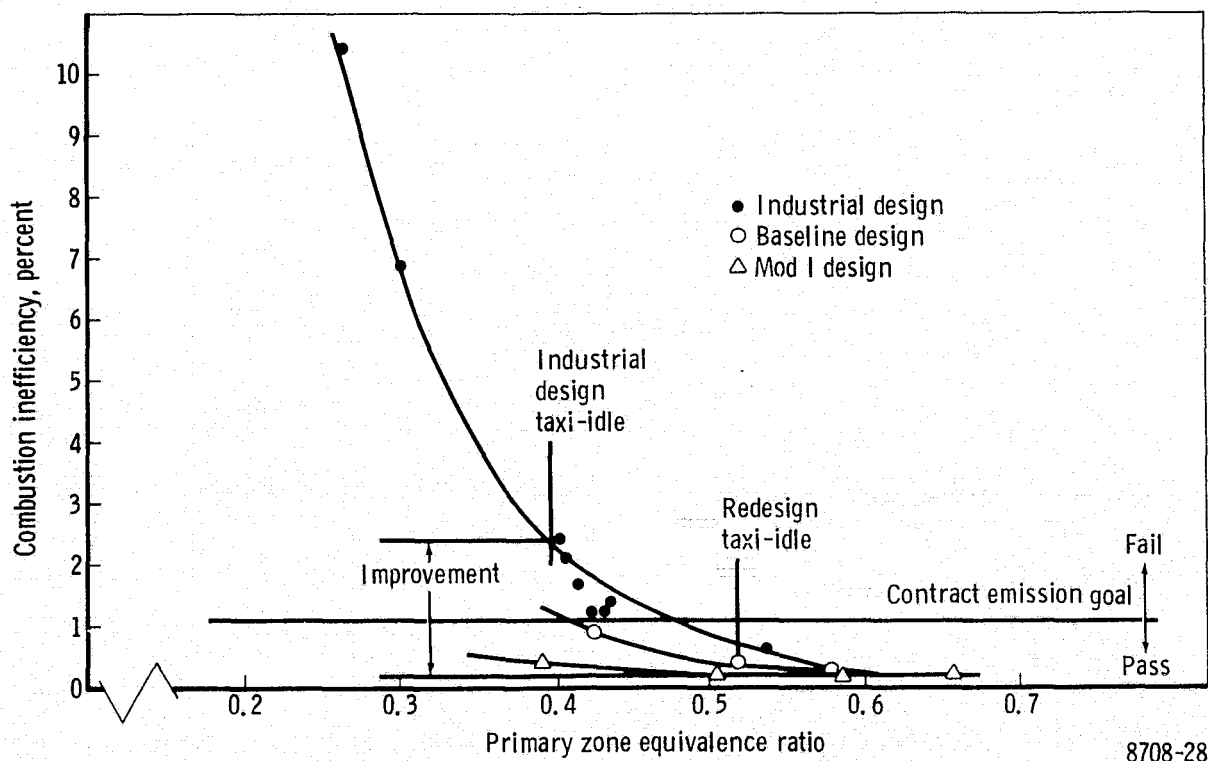


Figure 7-2. Improvement in combustion efficiency from redesign of primary zone to increase equivalence ratio.

This, in turn, increased the oxidation of hydrocarbons to CO. The increased quantity of CO was not reacted, but to the contrary, was less completely burned because of a local reduction of temperature (increased flow) at the end of the reaction zone.

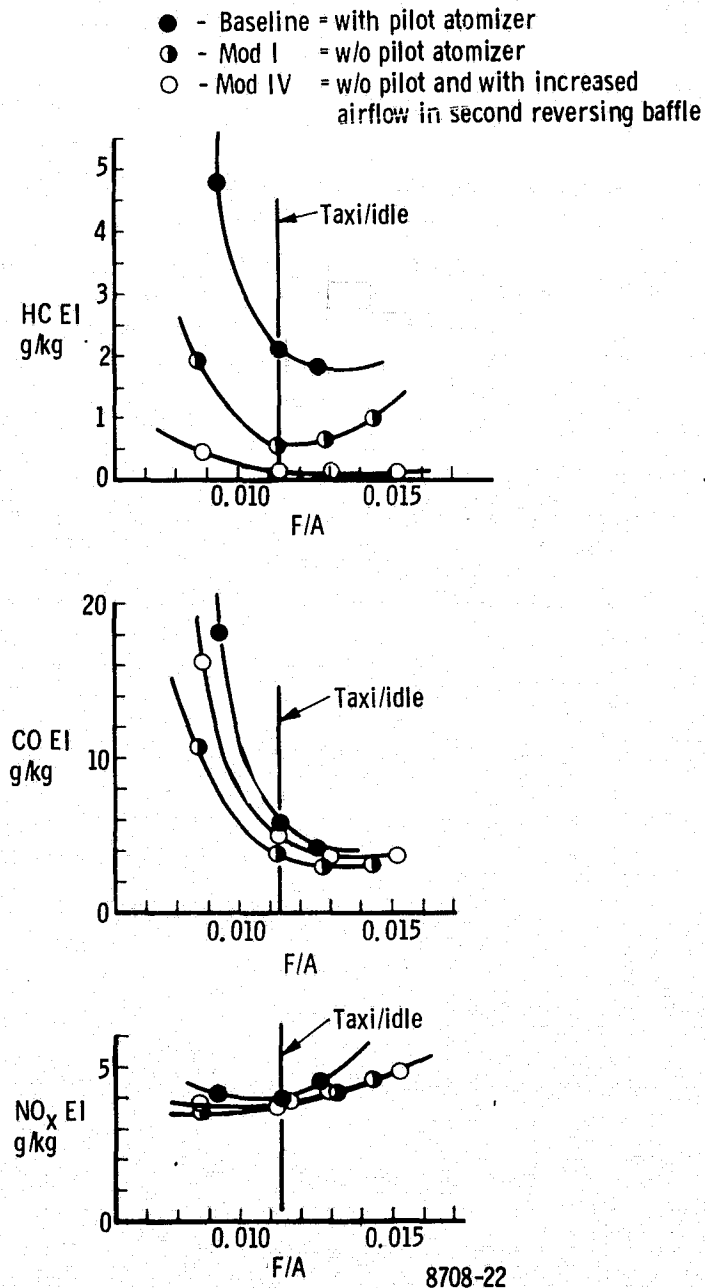


Figure 7-3. Comparison of emissions at idle showing effect of pilot fuel flow and increased airflow into second reversing baffle.

Fuel Nozzle Changes

The effects of fuel nozzle changes on idle emissions and on smoke production at high power were marked. The initial reverse flow configuration, baseline, carried over the industrial design fuel nozzle. This nozzle has an airblast main flow and a pressure atomizing pilot. At starting, the pilot is the only flow, at idle its flow is about 40% of the total, and at takeoff about 20%, the balance coming from the airblast main. The change in emissions when the pilot flow was eliminated is shown in Figure 7-3. In this figure emissions index at idle conditions is plotted at various fuel/air ratios. During the baseline running both the pressure pilot and airblast main were operating, while Mods I and IV were run on airblast alone. When the pressure atomizing pilot was eliminated, the HC EI dropped from 2.1 to 0.54 and CO EI from 5.8 to 3.9. NO_x EI did not show a measurable increase. The trade-off between HC and CO caused by increasing second reversing baffle air flow is also shown in Figure 7-3 in the differences between Mod I and Mod IV emissions. This trade-off was discussed previously.

The effect of fuel nozzle changes on idle emissions was even more pronounced during the Mod III tests. In the Mod III configuration, the airblast fuel nozzle was replaced by an air assist nozzle. In this design, high pressure air is supplied to the nozzle from an external source, to improve fuel atomization at the low fuel flows found in idle operation. Without external air pressure the nozzle acts like the main flow nozzle used in the production combustion system. It has a flow number of 24. Prior to testing, the effect of external air pressure on spray quality was determined qualitatively by observation of the spray on a flow bench. The results of these observations were used to establish air pressures for the Mod III tests. At a fuel flow of 12.6 g/sec, the observed characteristics were as follows:

Zero air pressure:	Conical sheet - no fuel breakup
6.75 N/cm ² :	First observed break-up
13.5 N/cm ² :	Extremely fine atomization (like airblast).

The Mod III emissions reflect the above changes in fuel preparation. Figure 7-4 shows the test results for different fuel nozzle air pressures and fuel flows at idle conditions. Improvement in fuel atomization made a marked reduction in emissions of HC and CO. Smoke number was reduced from 7 to 3 by this change. Oxides of nitrogen, however, were increased from an EI of 3.7 to 4.2, g/kg of fuel. While the CO emissions from the best air assist run were as low as those produced by an airblast fuel injector, hydrocarbon emissions were higher by a factor of 3.

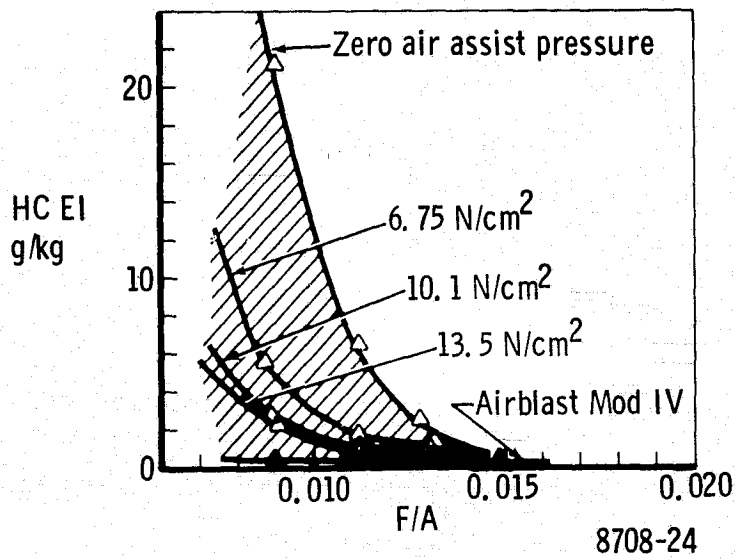
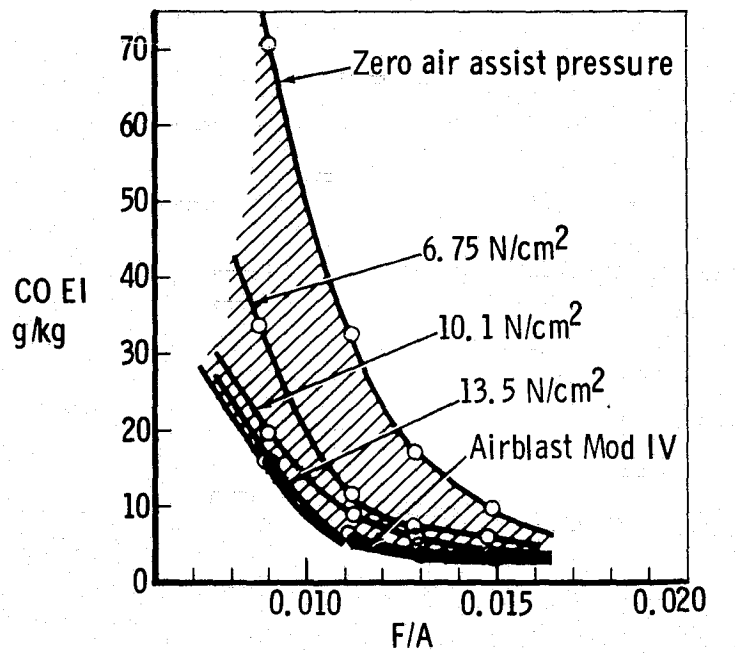


Figure 7-4. Effect of air assist fuel nozzle air pressure on Mod III idle emissions.

The emissions produced at the other three modes of operation were also significantly related to fuel preparation. Table 7-I shows emissions index at zero fuel nozzle air assist, and 13.5 N/cm² for each of the four modes of the LTO cycle. The smoke produced in the Approach, Climb and Takeoff modes was above the program goal of SN = 22. Table 7-I also shows that with zero air assist, HC and CO exceed the taxi/idle mode levels (HCEI = 5.4 and COEI = 27.9) which would prevent this configuration from meeting the program goals.

The above results confirm the important role the airblast fuel nozzle plays in reducing emissions both at idle operation and at power (approach through takeoff).

TABLE 7-I. EFFECT OF AIR ASSIST FUEL NOZZLE PERFORMANCE ON MOD III EMISSIONS.					
LTO Cycle Mode	Air Assist Pressure (N/cm ²)	Emission Index (g/kg)			Maximum Smoke
		HC	CO	NO _x	
Taxi/Idle	0	[6.50]	[32.3]	3.70	7.0
	13.5	0.80	6.73	4.23	3.0
Approach	0	1.32	5.42	6.44	[27]
	13.5	0.95	3.26	6.12	[29]
Climb	0	0.48	1.24	10.7	[23]
	13.5	0.39	1.18	10.8	[25]
Takeoff	0	0.30	1.15	10.4	[26]
	13.5	0.34	1.15	10.8	[26]
[] Exceeds Program Goals.					

Combustor Wall Temperatures

Combustor wall temperatures were analytically predicted prior to experimental test, and measured by thermocouples and temperature sensitive paint during the test program. Table 7-II compares wall temperatures obtained by these three methods. As this Table shows, agreement among methods was only fair, there being better agreement between the predicted

TABLE 7-II. COMBUSTION LINER WALL TEMPERATURES, K

Location on outer wall	Predicted analytically	Measured	
		Thermocouple Mod IV	Thermal Paint MOD IV
1. 2nd reversing baffle	1187	933	Over 1033
2. Ahead of 2nd corrugation	1023	949**	750 - 1033
3. Transition butt weld	1037	1064	Over 1033
4. Underneath transition aft	*	1152	Over 1033
* Not analyzed.			
** From Mod II tests; Mod IV thermocouple failed during test.			

values and the thermal paint than with the thermocouple data. However, the skin temperature analysis served its purpose in that it correctly predicted that there would be no unacceptable liner wall temperatures during the testing.

Outlet Temperature Pattern

There were no adverse burner outlet temperature patterns obtained during Reverse Flow testing. The values of pattern factor at takeoff power were approximately equal to that recorded during testing of the production 501-D22 liner and fuel nozzle. These pattern factors are given in Table 6-V, Section VI of this report.

PRECHAMBER

The two basic prechamber designs, the short prechamber and the long prechamber produced substantially different results and they had substantial differences in their combustion characteristics. Therefore, each of these will be discussed separately.

Short Prechamber (Baseline Prechamber, Mod III, IV and V)

Internal Combustor Flow

The results of a flow visualization study on an evacuation rig are shown in Figure 7-5. There were several indications during hot combustor tests that supported these findings. The hot combustion gases impinged on the wall causing very high skin temperatures in the area of impingement. Thermocouples on the dome and on the forward portion of the main chamber showed substantially different wall temperatures depending on the proportion of fuel delivered by the wall film fuel system at a fixed overall F/A ratio. The fuel nozzle appeared to primarily fuel the center recirculation zone, while the wall film appeared to fuel the outer recirculation zone. At one point, there was a short lag from the time when the wall fuel was turned on until ignition was indicated by BOT and skin thermocouples. Thermocouples on the prechamber did not indicate any combustion in the prechamber at any time. There was also no evidence of combustion in the prechamber on inspection of any of the short prechamber configurations. All of these facts confirm that burning did not take place in the prechamber.

Wall Film Fuel System

After the run of Prechamber Mod III, slight damage was found on the exterior of the combustor. This damage was traced to a leak in the feed line to the wall film system. This leak was caused by a defect which existed

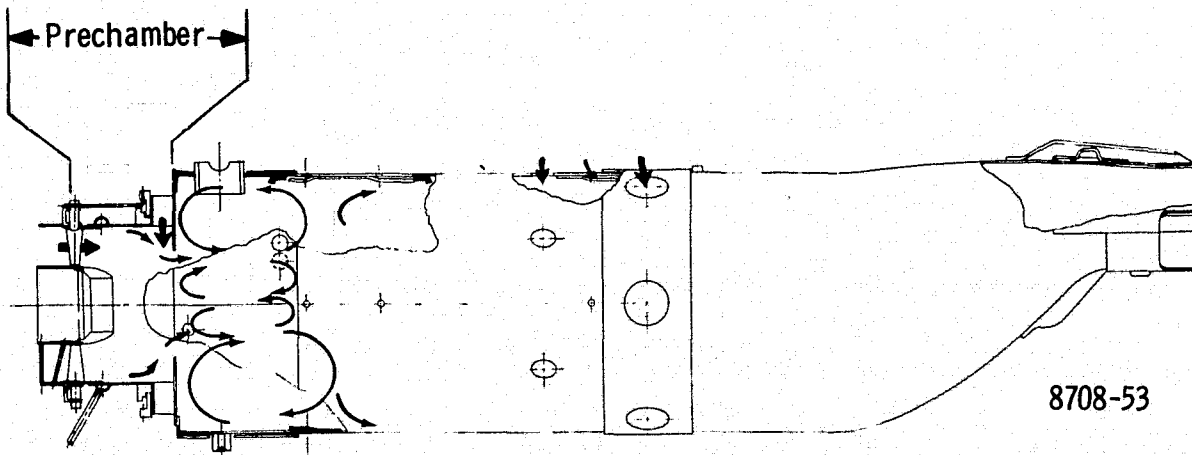


Figure 7-5. Flow visualization, short-prechamber combustor.

prior to the baseline run. Therefore, all of the wall film fuel data on the Baseline Prechamber and Mod III, cannot be considered completely valid, because the amount of fuel released external to the combustor is unknown. However, all of the data with only fuel nozzle feed was unaffected by this leak.

The trend from Mod III and the verification from Mods IV and V, indicate that a small improvement in NO_x emissions is achievable by using some proportion of wall film fuel at power. At the same time, there is little change in CO, HC or smoke emission levels.

Pressure Atomizer Pilot in Fuel Nozzle

The pressure atomizer pilot was used in three configurations. The Baseline, Mod IV and V. The data indicate that there is little difference in emissions with the pilot on or off at the same overall F/A ratio. The pressure atomizer pilot was also used in Mod V for altitude relight stability testing. The flow number of the pressure atomizer nozzle used for this testing was too high for the required 83 K temperature rise at altitude relight conditions. A very coarse spray was produced, and there was not sufficient airflow available to atomize the droplets. A lower flow number pilot atomizer would probably produce considerably more altitude relight stability.

Variable Geometry

The variable geometry provided a wide range of combustor configurations to be surveyed in a very short period of time. It also provided a measure of the sensitivity of the emissions to hole sizes and locations and swirler angle. Continued development with a fixed geometry combustor at the optimized configuration would be required to verify and final tune the emissions, temperature pattern, and durability.

Liner Wall Cooling

Although the impingement of air on the wall was observed during flow visualization, the extent that this would affect the skin temperature in a very local area was not anticipated. The thermal analysis predicted a maximum temperature of 1207 K (1714°F) in this area at max power. Thermocouples were placed in this area in the Baseline Prechamber test and they measured unacceptably high temperatures well below T.O. power. A substantial redesign would be required to reduce these temperatures to

a level that would provide durability in commercial service. A major redesign would have had a severe impact on the program from both schedule and cost considerations. Therefore, a series of small effusion holes were put in the hot area as a short term fix to facilitate testing. This fix did allow the completion of all testing, however, thermal paint results from Mod V indicate that this area and the liner wall in the vicinity of the intermediate holes need further development in skin cooling.

BOT Traverse Quality

T.O. F/A was not run on the Baseline Prechamber. The traverse was very good on the other short prechamber mods:

<u>Mod</u>	<u>Pattern Factor (at T.O. F/A)</u>
III	0.14
IV	0.12
V	0.17

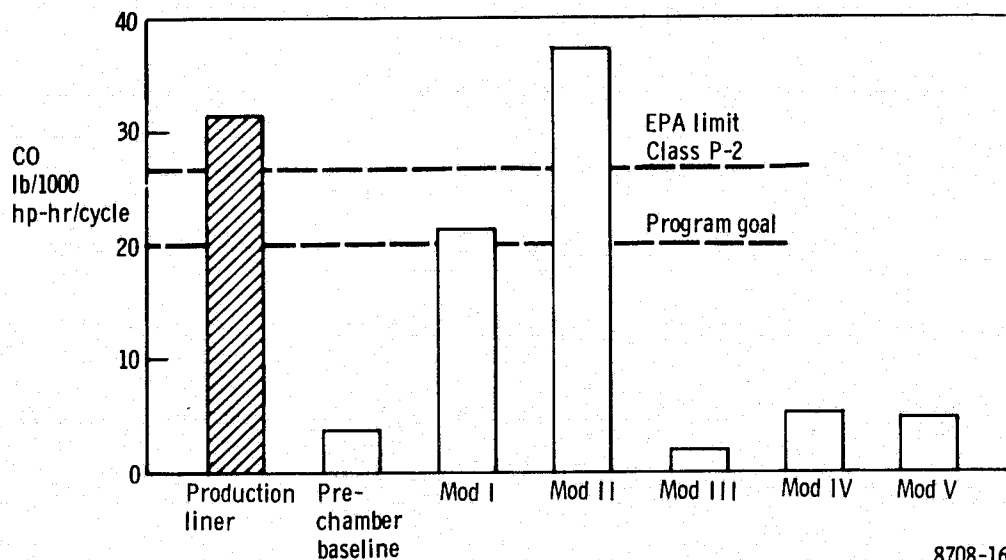
No effort was made to tune or develop the dilution zone for optimum temperature traverse during this program. A development program would probably improve the traverse even more.

CO Emissions

The EPA parameters for CO emissions for all of the prechamber mods are shown in Figure 7-6. The projected Baseline Prechamber results and complete results for Mod III, IV, and V, are all well within the program goals and considerably below the production liner emissions. The fuel from the fuel nozzle seems to penetrate the central recirculation zone first, and then as fuel flow increases, the excess fuel goes to the outer recirculation zone. This provides for a rich, well mixed combustion zone at idle with sufficient length downstream to provide enough residence time to consume the CO before the dilution air is introduced. When the VG was set to position the primary holes in the forward position, the primary air penetrated into the central combustion zone, quenched the reaction, and produced very high CO emissions. Therefore, in all of the short prechamber Mods, the primary holes are positioned in their aft location.

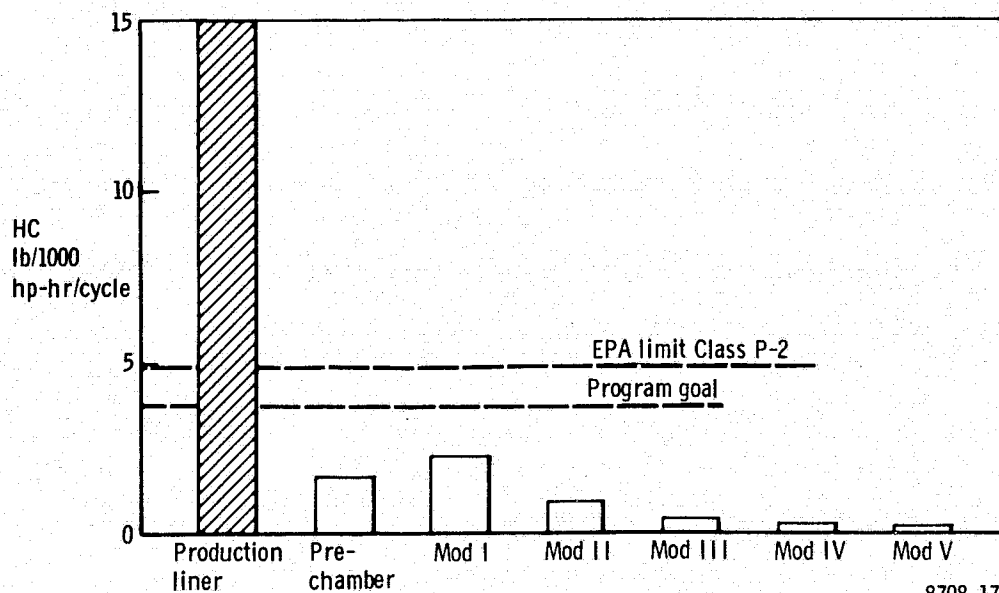
HC Emissions

The EPA parameters for HC emissions for all of the prechamber mods are shown in Figure 7-7. Like the CO emissions, the HC emissions for the short prechamber mods are all well within the program goals and considerably below the level of the production liner. For the most part, the same factors which reduce CO emissions also reduce the HC emissions. Therefore, the optimization of geometry for CO emissions also produces extremely low HC emissions.



8708-169

Figure 7-6. EPA parameter—CO emissions—prechamber combustors.



8708-170

Figure 7-7. EPA parameter—HC emissions—prechamber combustors.

NO_x Emissions

The EPA parameters for NO_x emissions for all of the prechamber mods are shown in Figure 7-8. The Prechamber Baseline NO_x emissions include results projected from questionable data. Therefore, the Mod III results must be used in preference to the baseline. The Mods III, IV and V, NO_x emissions were all well within the program goals, although they were slightly higher than the production liner NO_x emissions. A limited amount of testing was conducted with fuel staging using the wall film fuel system. Fuel staging generally produced slightly lower NO_x emissions at high power. This is due to both the partial prevaporization of filming the fuel on the prechamber wall and to the separate combustion zones of the two fuel systems. Additional testing to determine optimum fuel splits, and to achieve more prevaporization by moving the wall film fuel system further forward would reduce the NO_x emissions. However, because all of the configurations produced results within the program goals, the additional complexity of a secondary fuel system is not warranted. The results presented in Figure 7-8 for Mods III, IV, and V do not include wall film fuel injection.

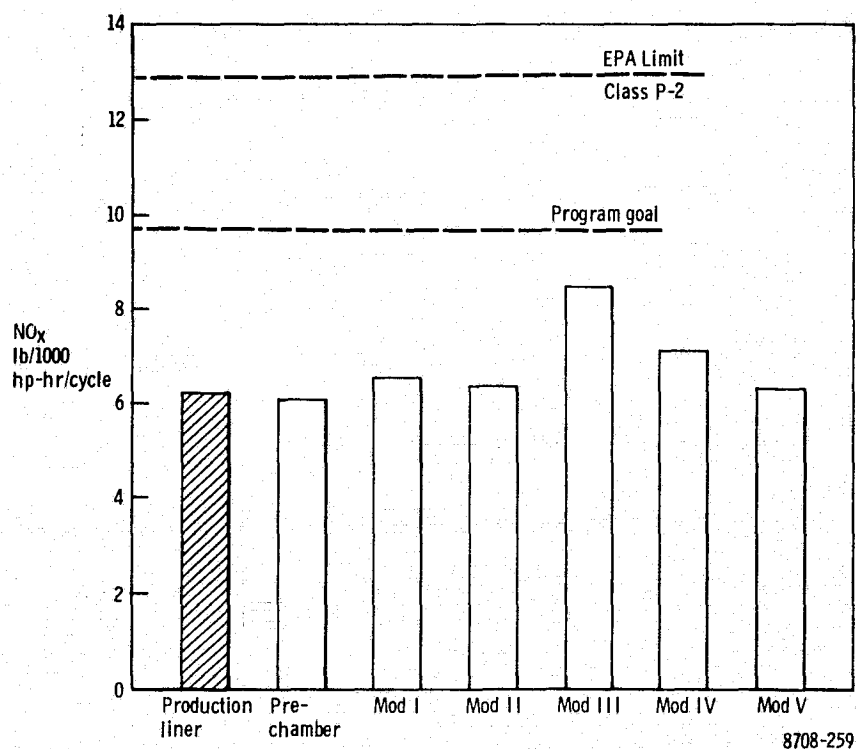


Figure 7-8. EPA parameter—NO_x emissions—prechamber combustors.

Smoke

The maximum smoke number in any of the program test points for all of the prechamber configurations are compared graphically against the production liner in Figure 7-9. The amount of smoke produced is primarily a function of the atomization and mixing of the fuel with the air prior to combustion. The combination of the airblast fuel nozzle, axial and radial swirler, and trip, provided enough mixing so that smoke was almost non-existent in the short prechamber configurations.

Long Prechamber (Prechamber Mods I and II)

Internal Combustor Flow

The results of a flow visualization study on an evacuation rig are shown in Figure 7-10. The flow in the main chamber was very similar to the flow in the main chamber of the short prechamber configuration (Figure 7-5). There was an indication of a small recirculation at the ID of the axial swirler. This may have acted as a flame holder for the prechamber.

Wall Film Fuel System

The wall film fuel system is an integral part of this design. The fuel nozzle is designed to fuel the prechamber, and the wall system is designed to fuel the main chamber. This provides considerable control over the fuel/air ratio in each zone. The fuel nozzle was used exclusively at idle, and

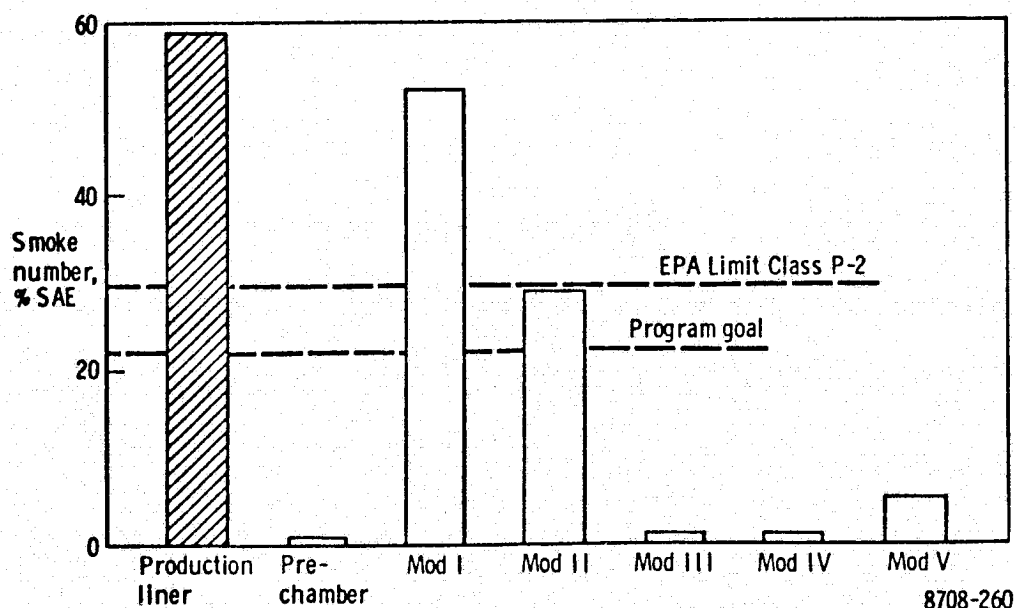


Figure 7-9. Max smoke number for LTO cycle—prechamber combustors

the wall fuel system was turned on at higher power so that both systems would operate together. The fuel proportion of the two systems could then be varied to change the equivalence ratio of the two combustion zones.

Pressure Atomizer Pilot In Fuel Nozzle

Because the fuel is burned in the prechamber in this configuration, prior to the radial swirler and trip, adequate atomization and mixing were more difficult to achieve than in the short prechamber. The pressure atomizer pilot was tried at idle for Mods I and II. CO, HC, and smoke emission all increased substantially with this system. Therefore, the pressure atomizer pilot was shut off by an external valve. Only data with this pilot off is included in the emission results.

Variable Geometry

The size of the dilution holes in these configurations was controlled by variable geometry. Smaller dilution holes produced more pressure drop along with higher velocities in the prechamber resulting in shorter residence time. Larger dilution holes produced lower velocity and longer residence time, along with less pressure drop resulting in reduced fuel/air mixing effectiveness.

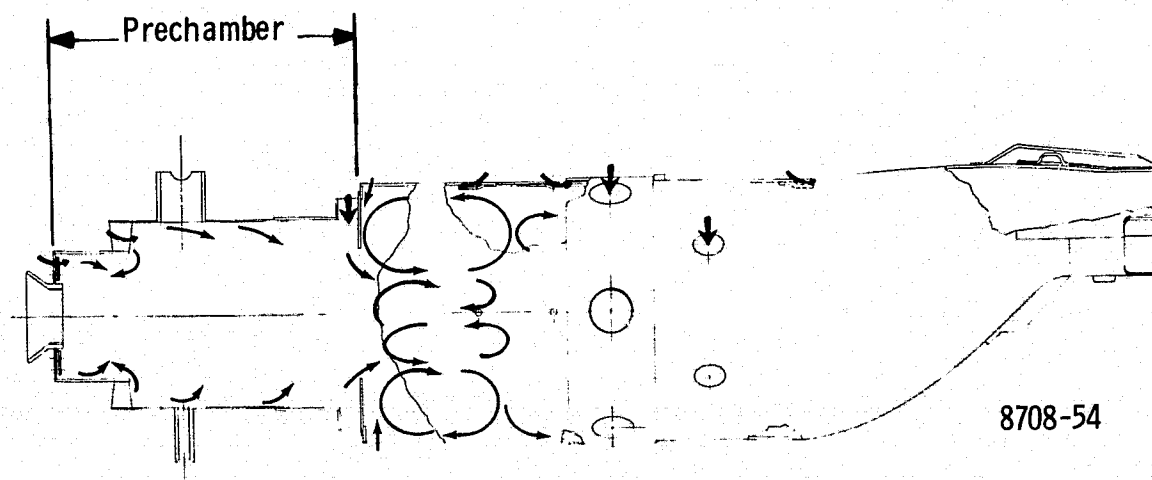


Figure 7-10. Flow visualization, long-prechamber combustor.

Liner Wall Cooling

The similarity in combustor air flow shown by the flow visualization studies warned that the long prechamber would have the same skin cooling problem experienced by the Baseline Prechamber due to impingement of hot gases. A series of small film cooling holes were placed in suspected hot area, prior to running, as a short term solution to facilitate testing.

No wall cooling was used in the prechamber portion of the combustor. The axial swirler served the combined functions of fuel mixing, providing combustion air, and wall cooling. Thermocouples on the prechamber wall showed no problems with skin temperature in this area.

BOT Traverse Quality

The traverse quality was excellent on both the Mod I and II configurations. The pattern factor at T.O. power for Mod I was 0.11 and for Mod II it was 0.10.

CO Emissions

The EPA parameters for CO emissions are shown in Figure 7-6. The Mod I configuration failed to meet the program goal by a small margin, and the Mod II configuration failed by a larger margin. Operation at idle produces the major contribution to total CO emissions. To determine if longer residence time would reduce the CO emissions, the reference velocity was reduced in Mods I and II by approximately 26%. Figures 7-11 and 7-12 show the substantial reductions that were obtained in CO emissions. A longer residence time can easily be achieved in these designs by increasing the length of the prechamber. This delays the quenching action of the radial swirler.

HC Emissions

Figures 7-13 and 7-14 show that substantial improvement in HC emission is obtained by reducing the reference velocity by 26%. Therefore, an increase in prechamber length would produce a reduction in HC as well as CO.

NO_x Emissions

The EPA parameters for NO_x emissions are shown in Figure 7-8. The total cycle emissions of Mods I and II were slightly above the level of the production liner. Optimization of the proportion of wall-film fuel to nozzle

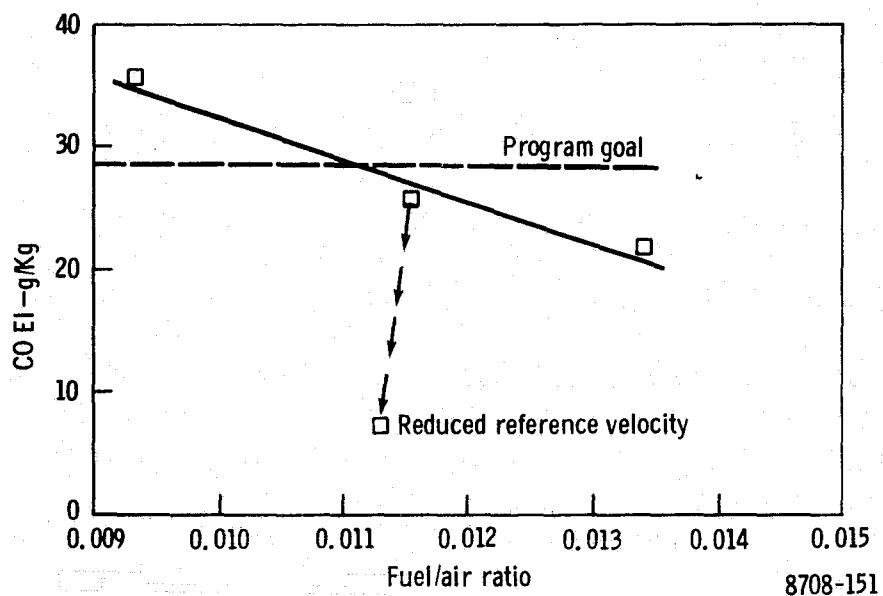


Figure 7-11. Prechamber Mod I—CO emissions at idle.

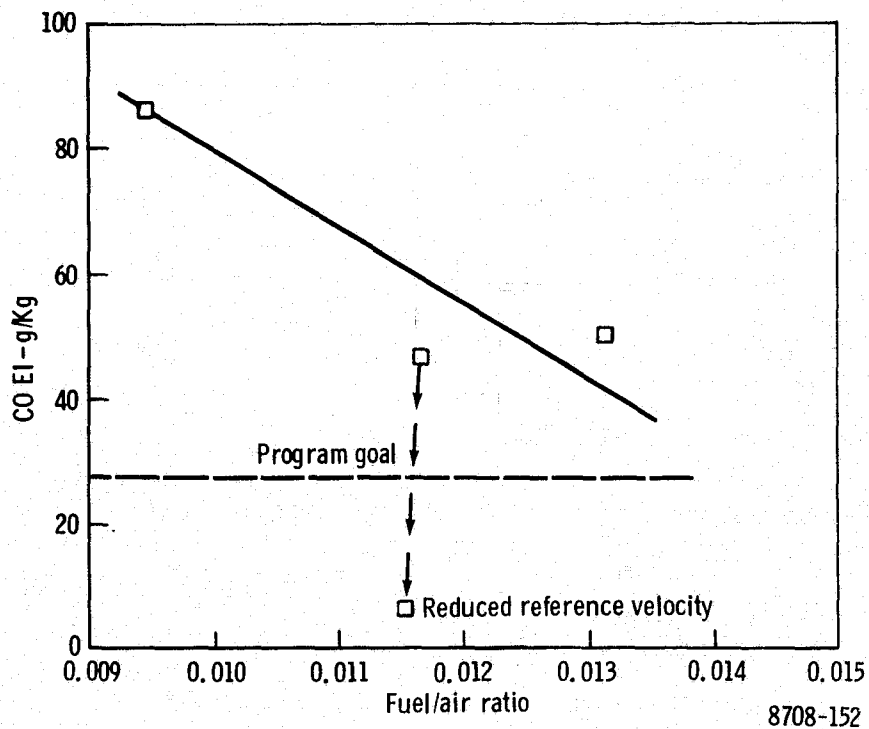


Figure 7-12. Prechamber Mod II—CO emissions at idle.

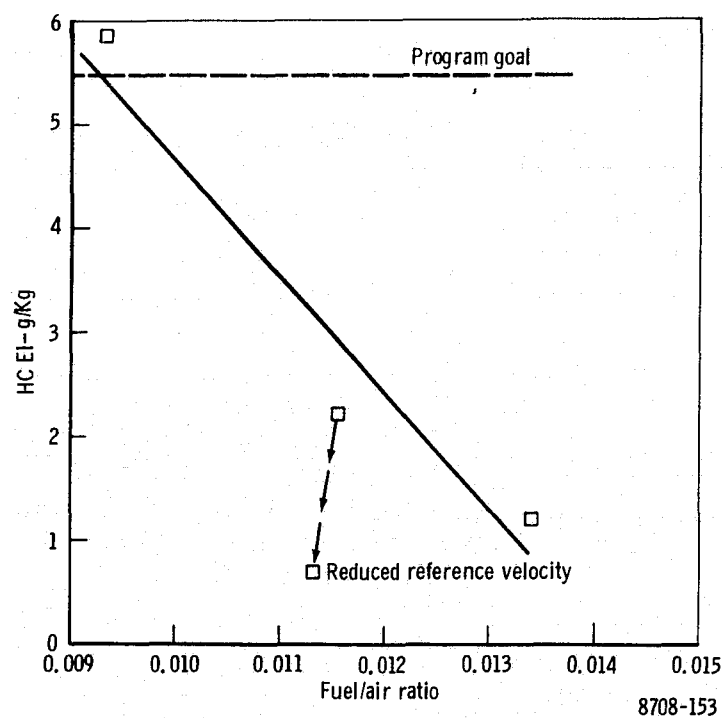


Figure 7-13. Prechamber Mod I—HC Emissions at idle.

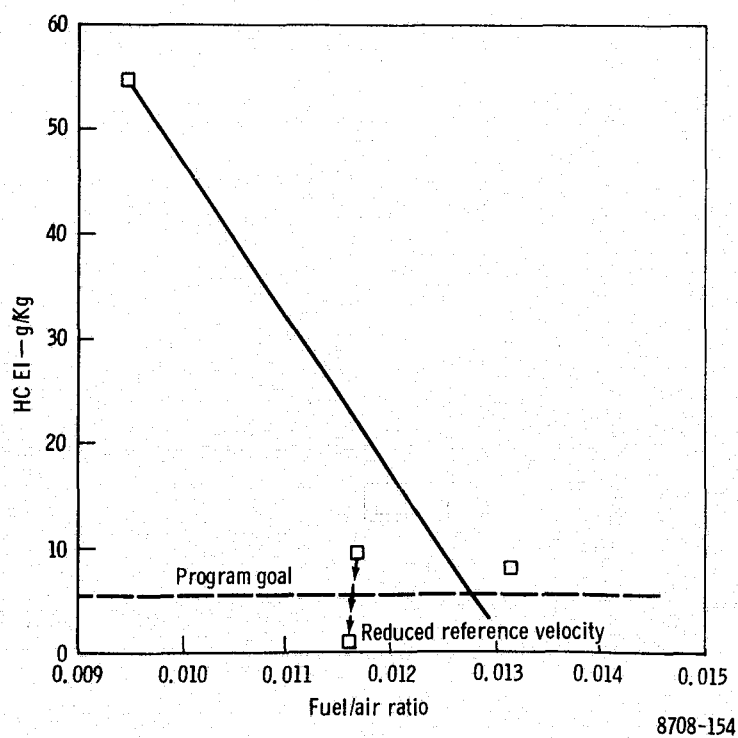


Figure 7-14. Prechamber Mod II—HC emissions at idle.

fuel would probably reduce the NO_x still further. The axial location of the wall-film feed system determines the distance that the fuel must travel along the wall. Relocation of this system towards the forward end of the prechamber would allow for greater prevaporization of the fuel, resulting in still lower NO_x .

Smoke Emissions

The maximum smoke number in any of the program test points for Mods I and II are shown along with the short prechamber configurations in Figure 7-9. Since combustion takes place prior to the radial swirler and trip in the long prechamber, the entire atomization of the fuel must be accomplished by the airblast fuel nozzle and the axial swirler. Liner pressure drop plays a major roll in the atomization process. The Mod. I configuration has a pressure drop about 0.4% less than the production liner. The Mod. II design has a pressure drop about 0.3% greater than the production liner. This difference of about 0.7% in pressure drop considerably lowered the level of smoke in Mod. II. However, more pressure drop or other means of improving the fuel/air mixing would be required to bring the smoke down to an acceptable level.

Figures 7-15 and 7-16 show an increase in smoke level with a reduction in reference velocity. This occurred because the reduction in reference velocity was accompanied by a reduction in pressure drop. The lower reference velocity was used to simulate the longer residence time that would be achieved by increasing the length of the prechamber. If the prechamber were made longer, the residence time in the prechamber would increase reducing the levels of CO and HC, but the pressure drop would not decrease, and no adverse affect on the smoke would be expected.

Optimum Prechamber Configuration

The Prechamber Mod III was higher in NO_x emissions than Mod IV or V. However, the NO_x emissions of Mod III were still well within the program goals. Mod III CO emissions were lower than either Mod IV and V, and the HC and smoke levels of all three of these configurations were extremely low. The pressure drop of Mod III was slightly greater than the production liner. The pressure drop of Mod IV was more than 1% greater than the production liner and the pressure drop of Mod V was more than 2% greater than the production liner. Therefore, even though Mod V produced slightly lower HC and NO_x emissions than Mod III, on the basis of its lower pressure drop, the Mod III configuration is the most promising of the prechamber designs for use as a low emission combustor for the 501-D22A.

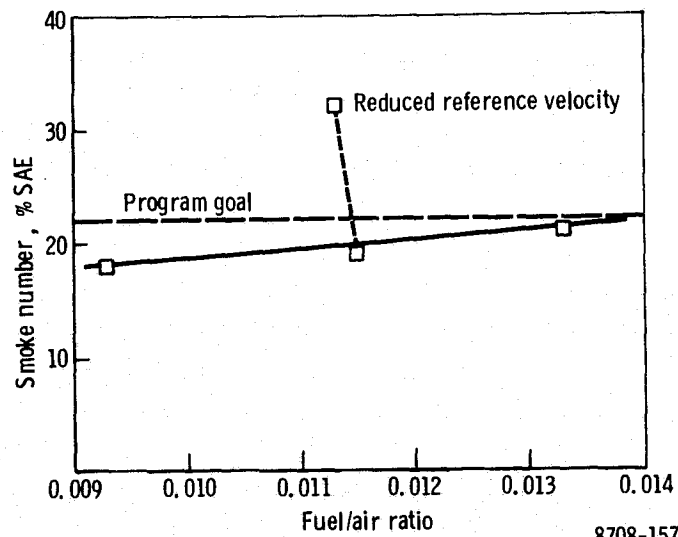


Figure 7-15. Prechamber Mod I—Smoke emissions at idle.

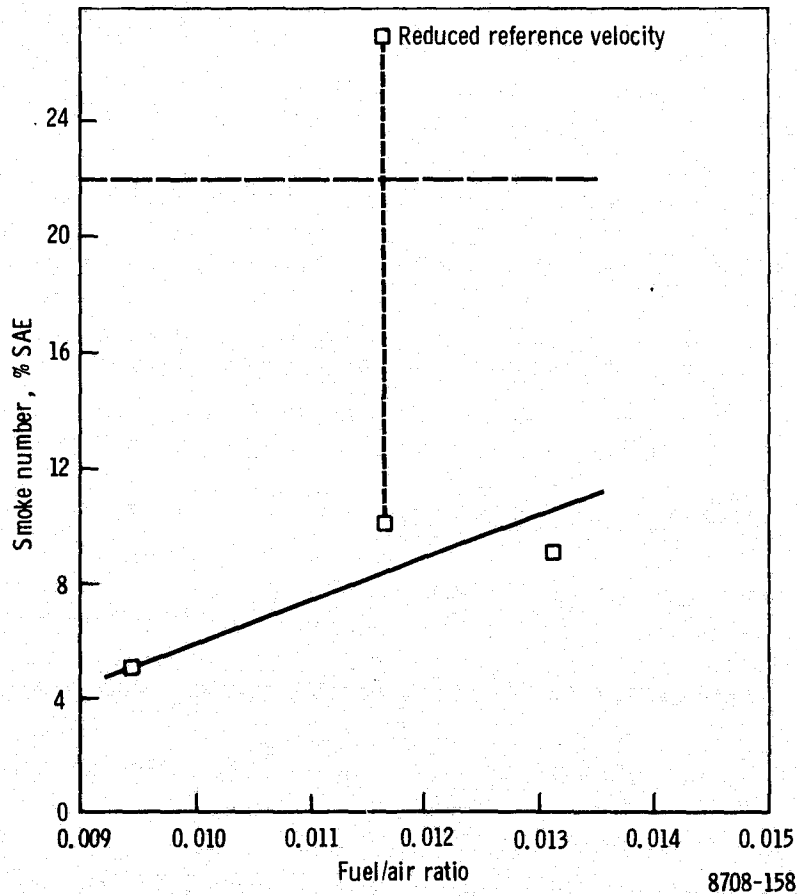


Figure 7-16. Prechamber Mod II—smoke emissions at idle.

STAGED FUEL COMBUSTOR

The staged fuel designs successfully met the program emission goals. The CO and HC reductions required at idle, and large smoke reduction required at high power were accomplished without degrading combustion performance. The pilot zone of the baseline staged fuel design achieved the required idle reductions by means of reduced pilot zone airflow loading, and operation with a slightly lean equivalence ratio. Emission reductions were accomplished even though the pilot zone volume was relatively small. Evaluation of several types of pilot fuel injectors indicated that a significant CO/HC reduction potential exists at idle for airblast or air assist fuel injectors compared to the pressure atomizing type now in use. Further idle CO/HC improvements were made in the second, staged-fuel combustor design (Mods V/VI) by further reducing pilot zone equivalence ratio and increasing pilot zone volume.

When operating with 100% pilot fuel, the pilot zone, as expected, became excessively rich at takeoff conditions, resulting in high smoke emission regardless of the pilot fuel injector type. The addition of main zone fuel always reduced the smoke to very low levels so that the staging concept provided the additional flexibility anticipated from multiple combustion zones. The complete operating range from idle to takeoff was run with constant geometry settings even at the very lean conditions required for NO_x reduction.

Although NO_x reduction was not required, reduced NO_x modes were observed with the staged fuel combustor. The test data indicate that NO_x can be reduced by either running very lean ($\phi \ll 1$), or very rich ($\phi \gg 1$). Maximum NO_x was obtained by running both zones slightly lean ($\phi \approx 0.8$). A very important consideration for a rich burning combustor is the smoke emission. With pilot zone fuel only, the smoke exceeded the goal when sufficiently rich conditions were obtained to reduce NO_x below approximately 9.0 EI at takeoff. With main fuel only, or main fuel and a small amount of pilot fuel, NO_x reductions were attained relative to the production liner, while operating in a rich mode with low smoke. This indicates that the main zone achieved better than conventional fuel/air mixing performance. A single zone low NO_x concept might therefore be based on running rich at takeoff with a fuel/air mixing system similar to that demonstrated on this program. Such a system might be able to achieve sufficiently rich conditions with low smoke levels for very low NO_x at takeoff and high power. Such a system would be expected to also have good stability at idle due to the favorable equivalence ratio. NO_x emissions at low power would be relatively high. However, the inlet pressure and temperature at this condition for most engines tend to limit NO_x formation.

The lowest takeoff condition NO_x level achieved in this program was obtained in the lean combustion mode. At a fuel/air ratio of 0.018 (90% of takeoff), NO_x reduction over the production liner was 40% with a dilution VG setting of 80% closed, and 55% with a fully closed dilution VG setting. At 0.020 fuel/air ratio (takeoff), NO_x reduction was 17%. These results indicate that in this low NO_x regime, NO_x emission is very sensitive to fuel/air ratio. NO_x reductions over the production liner were also accomplished at climbout, and approach power. In spite of these NO_x reductions, the EPAP NO_x emissions were significantly higher than the production liner over the LTO cycle because of the following factors:

- The idle power NO_x contributes approximately 50% to the EPAP total. No significant attempts to reduce idle NO_x were made.
- Since NO_x reduction was not the primary objective, idle, approach, and climbout data were not obtained for the VG setting producing the best takeoff NO_x reductions so that the EPAP could not be evaluated for this promising configuration.

Low NO_x idle data were obtained for the baseline design by staging combustion at idle. Duty cycle emissions in this mode are shown in Table 7-III. This shows that EPAP NO_x was essentially the same as for the production liner, and that all staged fuel baseline emissions met the program goals. These points illustrate that duty cycle NO_x reductions are possible with further development.

The operation of a staged combustor on an engine would probably involve operation on the pilot zone alone to a high power setting. The pilot zone fuel would then be reduced and the main fuel flow established. This transition should occur rapidly for low emissions, and with constant overall fuel flow to maintain power level and engine durability. Large power reductions would involve a reverse sequence. A more sophisticated fuel control system than exists in current engines would be required.

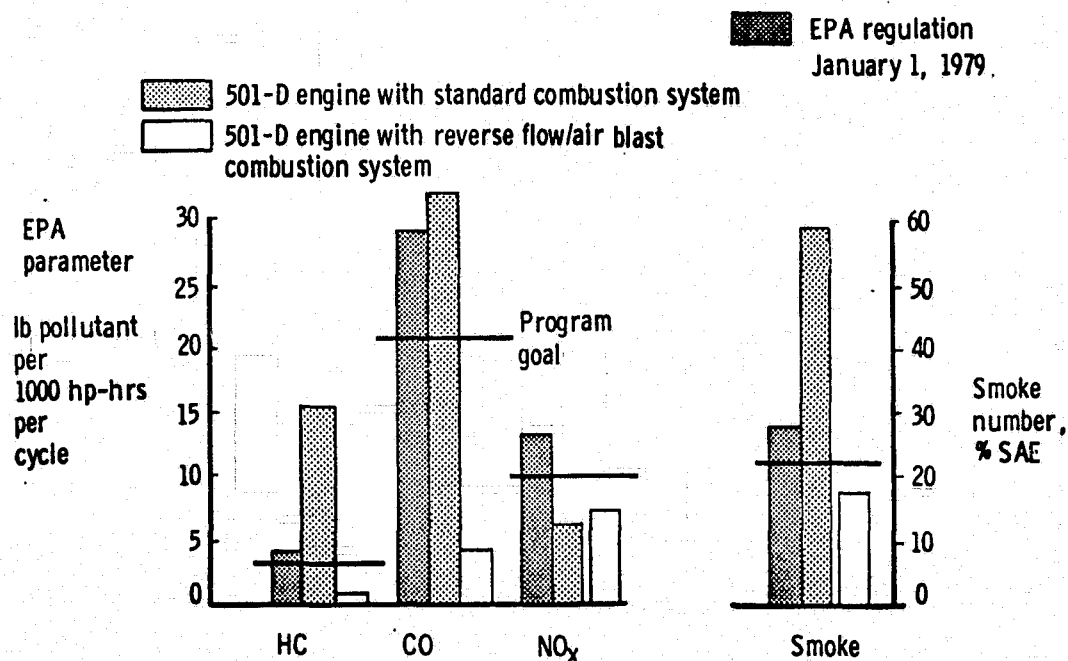
TABLE 7-III. DUTY CYCLE EMISSIONS FOR TEST 1
LOW NO_x OPERATING MODE (lb/1000 hp-hr/cycle).

Component	Production Liner	Test 1 Low NO _x mode	Program Goal
CO	31.5	17.6	20.1
HC	15.0	3.4	3.7
NO _x	6.2	6.4	9.7
Max Smoke (% SAE)	59.0	9.0	22.0

VIII. CONCLUSIONS

The following conclusions are supported by the data presented herein:

1. All three low emission combustor types, reverse flow, prechamber and staged fuel, met the EPA 1979 P2 aircraft regulation. The reverse flow Mod IV is the easiest to incorporate into the engine and the most durable and would require the least cost. Therefore, reverse flow Mod IV is the best candidate for further development into eventual use with the 501-D22A turboprop engine.
2. The reverse flow combustion system met all program goals for emissions by large margins. Emissions from the Mod IV configuration design are shown in Figure 8-1. These emissions are 92% below the HC goals, 77% below the CO, 25% below the NO_x and 23% below the smoke goals established at the beginning of the program.



8708-29

Figure 8-1. Emissions from final design (Mod IV) reverse flow system.

3. The prechamber combustion system met all program goals. Emissions from the Mod III configuration are 89% below the HC goals, 90% below CO, 12% below NO_x and 95% below the smoke goals.
4. The staged fuel combustion system met all program goals. Emissions from the Mod V configuration are 84% below the HC goals, 72% below CO, 26% below NO_x and 64% below the smoke goals. At a fuel/air ratio of 0.018 (90% of takeoff), a NO_x reduction of 55% over the production combustor was demonstrated by reducing the dilution air (leaning the primary zone). Additional EPAP NO_x reductions are most readily accomplished by reducing idle NO_x. The idle point contributes about 50% to the EPAP NO_x LTO cycle value. No main pre-mix tube flashback was encountered over a wide range of fueling modes, operating conditions, and VG settings.
5. The experimental test program demonstrated that enrichening the primary zone made marked improvements in idle emissions. The incorporation of an air assist (external air source) fuel nozzle in place of an airblast nozzle provided acceptable emissions at idle but failed to meet program smoke goals.
6. Large idle CO and HC reductions can be accomplished at some idle conditions by the use of airblast or air assist fuel injection.

IX. REFERENCES

1. Aircraft Exhaust Pollution and its Effect on the U.S. Air Force. W.S. Blazowski and R.E. Henderson. U.S. Air Force Systems Command Report AFAPL-TR-74-64.
2. Pollution Control in Continuous Combustion Engines. A.H. LeFebvre, Professor of Aeronautical Engineering, Cranfield Institute of Technology, Bedford, England. 15th International Combustion Symposium, Tokyo, 1974.
3. Environmental Protection Agency, "Control of Air Pollution from Aircraft and Aircraft Engines," Federal Register Vol. 38, No. 136, Part II, pp 19087-19103, July 17, 1973.